OPTIMIZATION AND CHARACTERIZATION OF MUSCARINIC ACETYLCHOLINE RECEPTOR M_4 POSITIVE ALLOSTERIC MODULATORS

By

Uyen Mai Le

Dissertation

Submitted to the Faculty of the

Graduate School of Vanderbilt University

in partial fulfillment of the requirements

for the degree of

MASTER OF SCIENCE

in

Chemical Physical Biology

December, 2011

Nashville, Tennessee

Approved:

Craig W. Lindsley

P. Jeffrey Conn

Gary A. Sulikowski

ACKNOWLEDGMENTS

The work described in this manuscript would not have been possible without the contributions of many individuals. I would first like to thank my mentor and co-mentor, Craig Lindsley and Jeff Conn, for the opportunity of a lifetime to train under their guidance. I owe the deepest gratitude to everyone in the Lindsley lab, the Conn lab, the Daniels lab, and the Jones lab. I would like to thank Alice Rodriguez, who performed all the in vitro assays, the DMPK group under the guidance of Scott Daniels, who performed all PK characterizations, and Analisa Thompson, who performed the behavioral assay described. I would also like to thank Meredith Noetzel and Karen Gregory in the Conn lab for teaching me everything there is to know about in vitro assays. I would like to thank all past and present members of the Lindsley lab for their support, especially Kyle Emmitte, Mike Wood, and Corey Hopkins, for their guidance and advice. I would like to also thank Kwangho Kim in the Synthesis Core for all the stimulating chemistry discussions and advice over the years. Additionally, I would like to thank Tom Bridges for all the advice and resources he's provided. I would like to thank my family and friends for their continual support. Everyone listed here has been an integral part of my achievements. Lastly, I would like to thank my committee, Craig Lindsley, Jeff Conn, and Gary Sulikoswki for the opportunity to present my research.

TABLE OF CONTENTS

ACKNOWLEDGMENT……ii

Chapter

I. INTRODUCTION

G-Protein coupled receptors……1

Allosteric modulation of GPCRs……3

Muscarinic acetylcholine receptors……6

Therapeutic relevance: schizophrenia……8

II. OPTIMIZATION AND CHARACTERIZATION OF M_4 POSITIVE ALLOSTERIC MODULATORS

Discovery of M_4 PAM VU010010, VU0152099, and VU0152100……18

Optimization of M_4 PAMs……25

Optimization of HTS hit **1**……32

Optimization of VU0152100……48

III. SUMMARY……..73

IV. MATERIALS AND METHODS

Medicinal Chemistry……..81

In vitro pharmacology……81

In vivo pharmacology……84

APPENDIX……...86

REFERENCES……..99

Chapter I

INTRODUCTION

G-protein Coupled Receptors

Acetylcholine (ACh) is a neurotransmitter widely involved in the regulation of many physiological processes and functions. It plays important roles in both the central nervous system (CNS) and peripheral nervous system (PNS). In the periphery, ACh is released in areas such as the neuromuscular junctions, parasympathetic and sympathetic synapses. It is involved in cardiovascular functions, muscle contractions, and many others. In the CNS, acetylcholine is localized in various parts of the brain, and it is responsible for the regulation of functions such as learning, attention, memory, movement, and many others.

Acetylcholine activates two families of ionotropic receptors, the nicotinic and muscarinic cholinergic receptors. Nicotinic acetylcholine receptors (nAChRs) are pentameric ligand-gated ion channels that can be activated by exogenous nicotine.[1] Upon the binding of two acetylcholine molecules, the receptor undergoes conformational changes. These conformational changes trigger the opening of a channel and allow the exchanges of ions such as Ca^{2+} and Na^{+}. Muscarinic acetylcholine receptors (mAChRs) are G-protein coupled receptors (GPCR) that mediate metabotropic signaling of acetylcholine[2]. There exist five different subtypes (M_1- M_5) that are differentially expressed in the periphery and CNS.[2]

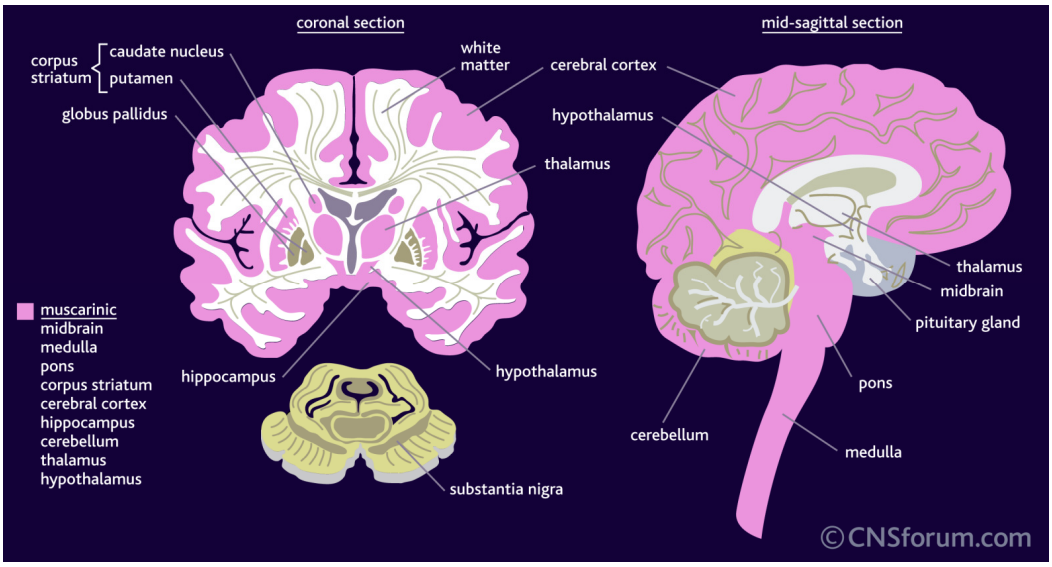

Figure 1. General distribution of muscarinic acetylcholine receptors (mAChRs) in the human brain.

GPCRS are G-protein coupled receptors that bind to a G-protein upon activation by an agonist. Once bound to G-protein, the G_α subunit on the G-protein is activated to release GDP and bind GTP. G_α activation initiates a chain of signal transduction that could stimulate the production of a second messenger or induce interactions with downstream effectors. There are three different classes of GPCRs: A, B, and C or type I, II, or III.[2] These classifications are based on the location of their orthosteric binding domain.[2] However, all three classes have one common structural morphology, they all have seven helical domains that span the transmembrane region. Structurally, mAChRs are classified as class A, or type I, rhodopsin-like GPCRs, which has its orthosteric binding site that is embedded in the hydrophobic core of the transmembrane domains (**Figure 2**).[2] Class B has its orthosteric site that flanks the short extracellular N-terminus.[2] Class C typically exists as a dimer with its orthosteric site flanking the long, extracellular, venus flytrap N terminus.[2]

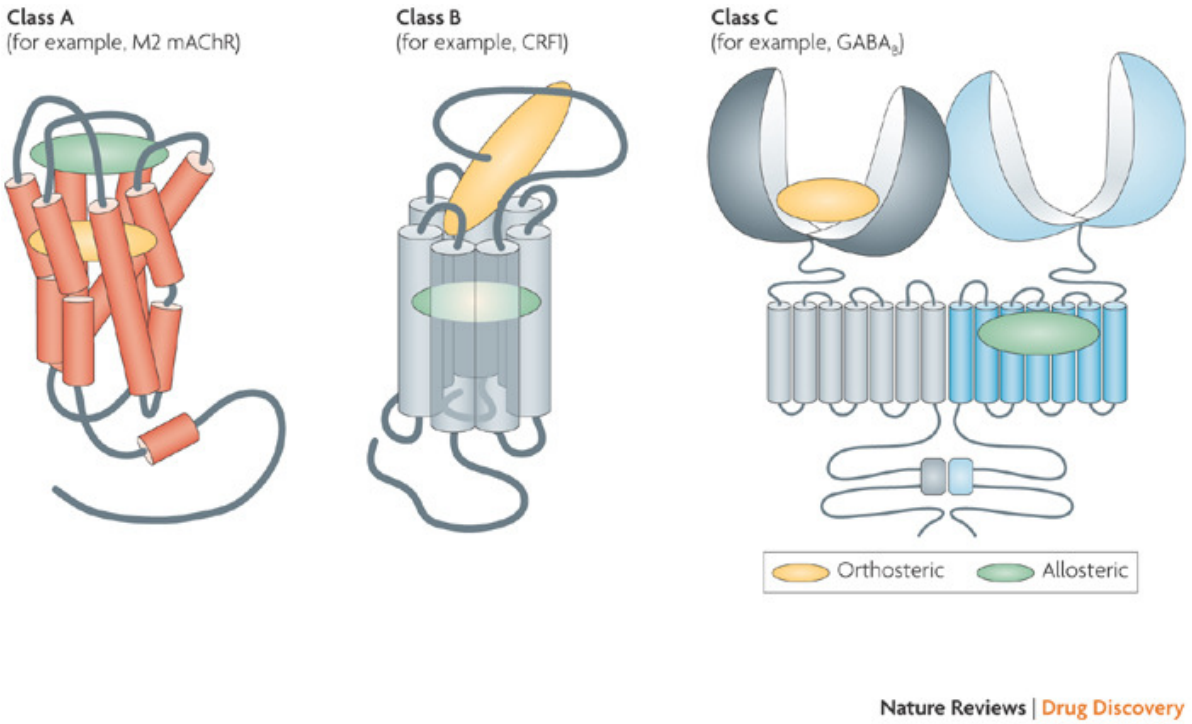

Figure 2. Classes of GPCRs. Class A: orthosteric site is within the transmembrane region. Class B: orthosteric site is located at the periphery on the N-terminus. Class C: orthosteric site is within the large N-terminus.[2]

Allosteric modulation of GPCRs

GPCRs are the largest class of cell-surface receptors and play crucial roles in every organ system. Ligands such as hormones, neurotransmitters, ions, odorants, photons, and various signaling molecules can activate a wide range of GPCRs. They have been implicated in a wide range of disorders. Most modern drugs regulate GPCR activity. Despite past successes of GPCRs as drug targets, there's a limited number of useful ligands that are specific to each type of receptor. There are more than 1000 genes encoded for GPCRs; however, there exist ligands only for a small fraction of these receptors.[4] The search for highly selective tool compounds for this class of receptors is strenuous and often results in failure. Ligands that are not specific could lead

to off-target activities that may have detrimental effects. Therefore, it is important to develop ligands that are highly specific for their targets. Selective ligands are difficult to develop mainly due to high structural homology of the orthosteric site across the members within a single GPCR subfamily making it difficult to achieve selectivity for each subtype. To combat this problem, selective modulators that target an allosteric site, a site other than the orthosteric site, are explored. This has shown to be successful for ligand-gated ion channels[4]. These molecules bind and act at a site that is distinct from the orthosteric site. These ligands can either potentiate or inhibit activation of the receptor by its natural ligand. An example of this alternate approach to obtain better selectivity is Benzodiazephines, which are positive allosteric modulators of gama-aminobutyric acid (GABA) A receptors used for the treatment of anxiety and sleep disorders.[4] By targeting the GABA receptors allosterically, the lethal affects of acting at the receptor directly as agonists are circumvented.

Modes of action of allosteric ligands

Allosteric modulators have a wide range of activities such as positive allosteric modulation (PAM), which enhances the response of the receptor to its endogenous agonists, negative allosteric modulation (NAM), which reduces the responsiveness of receptors, and neutral ligands, which binds to the allosteric site but have no effects on the response of the orthosteric ligand[4]. In recent years, progress has been made in the development PAMs, NAMs, and neutral ligands for each of the three major classes of GPCRs: A, B, and C.[4] These allosteric modulators provide new modes of action compared to the orthosteric ligands.

Allosteric modulators bind to GPCRs at sites that are topographically distinct from the orthosteric site thereby inducing novel receptor conformational changes.[4, 5, 6, 7] As a result the

action of the orthosteric ligands on the receptor and any downstream signaling can be altered. This mechanism of action can alter receptor activity positively, or negatively. Allosteric modulators can exhibit some of the following pharmacological properties: affinity modulation- the orthosteric binding pocket can be impacted such that the association, dissociation rate, or both rates of the orthosteric ligand is modified; efficacy modulation- intracellular responses can be altered leading to a change in the intrinsic efficacy of the orthosteric ligand; agonism/inverse agonism- the allosteric modulator can modulate the receptor activation positively or negatively irrespective of the presence of the orthosteric ligand.[4, 5, 6, 7] Allosteric mechanisms are governed by the affinity of the modulator and the cooperativity factors.[4, 5] The potency of an allosteric ligand is dictated by its affinity for the receptor and its cooperativity with the orthosteric ligand[4].

Allosteric modulators pose many advantages over orthosteric ligands. Those that do not on their own act as agonists do not display activity in the absence of endogenous orthosteric action.[4, 7] They can only exert their effects in the presence of endogenous orthosteric ligands; the degree of their effect is limited to the concentration of endogenous ligand, hence, there is less target-mediated toxicity due to high dosage because its efficacy.[4, 7] Higher selectivity across receptor subtypes can be achieved easier with allosteric modulators due to the potential for higher sequence divergence between allosteric binding sites compared to the conserved orthosteric sites.[4, 5, 6, 7] This higher selectivity could also be due to higher cooperativity between the allosteric site and orthosteric site in one subtype but lower cooperativity in another subtype.[4, 5, 7] Selectivity can also be produced by creating a 'bitopic' ligand that possesses both orthosteric and allosteric pharmacophores.[4] These modulators are able to modify specific signaling pathways associated with a given GPCR to varying degrees giving different output of efficacies. For example, the same ligand may have different efficacies mobilizing calcium and phosphorylating

an effector, though these two pathways are linked to one receptor.[4] This allows for further fine-tuning of intracellular signaling with allosteric modulators.

Several examples of this new mode of pharmacology exist in the drug market: Cinacalcet, a positive allosteric modulator (PAM) of calcium sensing receptor (CaSR) helps increase sensitivity to circulating calcium.[4] CaSR is involved in regulating calcium homeostasis and renal calcium resorption, as well as in the maintenance of inositol triphosphate levels; Maraviroc, a NAM of the chemokine receptor CCR5, is used in the treatment of HIV.[4] These discoveries provide strong proof of concept for the utility of allosteric modulators.[4]

Muscarinic acetylcholine receptors

There are five mAChR subtypes, M_1-M_5, distributed throughout the CNS and the periphery (**Figure 3**).[9, 10] In the periphery, M_1-M_4 expression dominates; they are expressed in the heart, lungs, GI, salivary glands, muscle cells, and the autonomic nerves.[9, 10] In the central nervous system, M_1-M_5 are localized in the cerebral cortex, hippocampus, striatum, thalamus, brain stem, cerebellum, substantia nigra, and the ventral tegmental area.[9, 10] Regulation of these receptors has been implicated in many neurodegenerative diseases.

These subtypes share structure homology with high conservation of the acetylcholine orthosteric binding site. Among these subtypes, they are further classified into two subgroups: M_1, M_3, & M_5 in one group and M_2 & M_4 in another.[9, 10] This classification is derived from similarities in their structural homology and signal transduction pathways. M_1, M_3, and M_5 share the highest structural homology with each other, while M_2 and M_4 have the highest homology with one another. Functionally, M_1, M_3, and M_5 are considered stimulatory receptors in that they exhibit the most similar signaling pathways of stimulating phospholipase C (PLC) and inositol

triphosphate (IP_3) as a result increasing intracellular Ca^{2+} concentration via coupling with G-protein G_q.[9, 10] M_2 and M_4 are most similar to each other both structurally and functionally. They inhibit the production of cyclic adenosine monophosphate (cAMP) by attenuating adenylyl cyclase (AC) via G_i coupling (**Figure 4**).[9, 10]

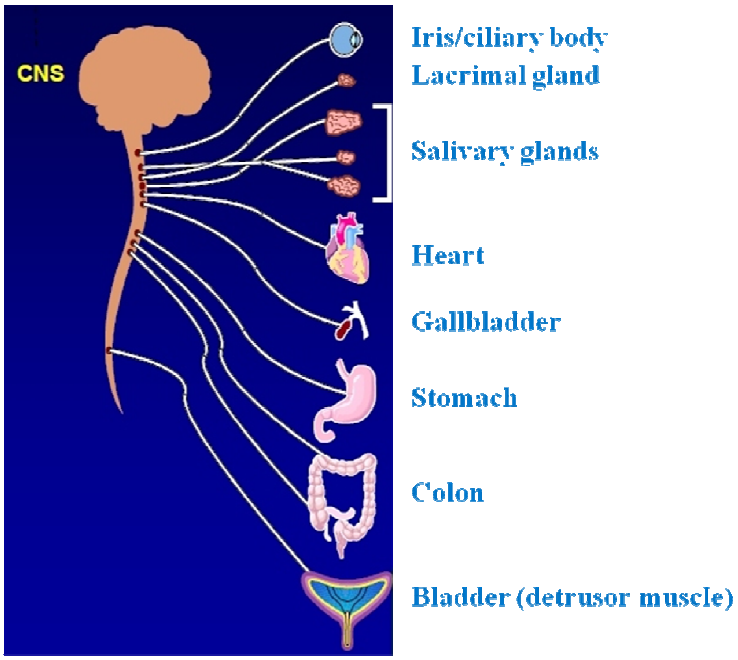

Figure 3. General location of mAChR subtypes in the body. Karl-Erik, Anderson. *Discovery Medicine* 8 (42), 118-124

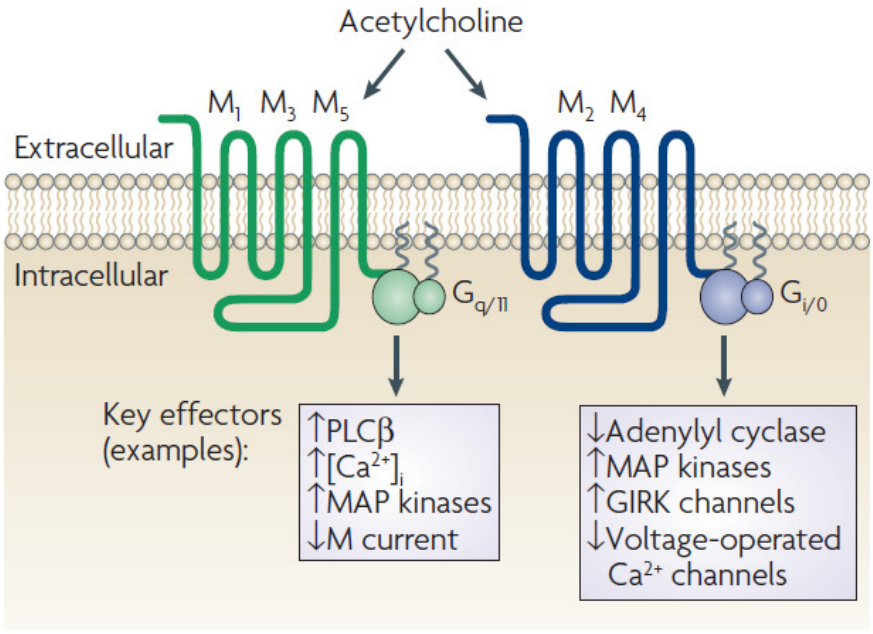

Figure 4. General function of muscarinic acetylcholine subtypes M_1- M_5.[9]

Muscarinic acetylcholine receptors (mAChRs) are involved in a wide variety of biological processes and diseases such as pain, Alzheimer's, schizophrenia, diabetes, and obesity[11]. Numerous non selective mAChR agonists have advanced into clinical development and show efficacy in improving cognition and alleviating psychotic symptoms in patients with Alzheimer's disease or schizophrenia. Symptoms of schizophrenia are thought to be alleviated by activation of the M_1 or M_4 receptor subtypes.[20]

Therapeutic relevance: schizophrenia

M_4 has been found to be linked to a schizophrenic pathway.[11] Throughout the 20th century, schizophrenia was believed to be a unitary illness with one cause, which is dopamine (DA) hyperactivity, and one treatment.[11] Therefore, first and second generation antipsychotics were all antagonists of the D_2 receptors, and they mostly address only the positive symptoms but

not the negative or cognitive symptoms. Due to this and large variability of the symptoms manifested by patients, this unitary pathology is no longer a valid paradigm.[11] The current belief is that this illness is made up of distinct independent but overlapping symptoms that can be distinguished pharmacologically, and that there are multiple molecular pathways involved (**Figure 5A**).[11] Excessive response of the pyramidal neuron induces psychosis.[11, 12] The current theory is that dopamine, serotonin, glutamate, and acetylcholine signaling facilitates the neuronal circuits involved in inducing psychosis (**Figure 5B**).[12]

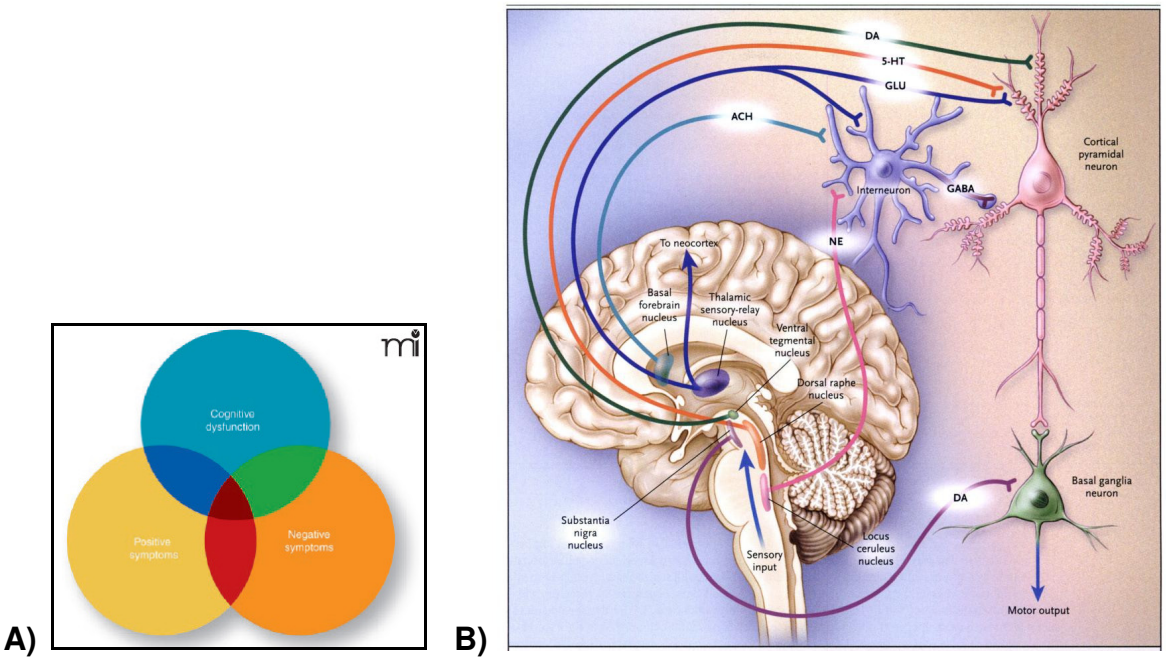

Figure 5. A) Overlapping symptoms. [11] B) Molecular pathway involved.[12]

The rationale for treatments via modification of dopamine signaling came from the idea that many physiological processes having a cognitive, reward, motivational, emotional or motor component are regulated in some way by dopaminergic pathways located in the central nervous system.[13, 14] It has been hypothesized that schizophrenia involves a biphasic dysregulation of dopamine signaling in which the subcortical mesolimbic dopamine pathways are overactive and

the mesocortical DA pathways are underactive.[13, 14] This combination leads to a decrease in the prefrontal DA signaling. Frontal cortical regions functions involve working memory and executive functions.[11, 12, 13, 14] Schizophrenic patients demonstrate abnormal prefrontal activation associated with impaired performance of cognitive tasks. Using DA antagonists to suppress over-activity is beneficial in alleviating positive symptoms but it could further exacerbate negative and cognitive symptoms by further decreasing DA signaling in the frontal cortex.[11, 14] DA agonists alleviate negative and cognitive impairments but exacerbates psychosis.[11, 14] Studies have shown that in addition to regulating the dopamine receptor, regulation of the NMDA receptor directly or indirectly through glutamate receptors, glyT1, or muscarinic acetylcholine receptors can be therapeutic.[11,13]

NMDA (N-methyl-D-aspartate) receptor is a type of ionotropic glutamate receptor. Its antagonists PCP, ketamine, or their analogs have been known to induce positive, negative, and cognitive symptoms of schizophrenia in healthy patients.[11, 15] Clinical observations show that administering NMDA co-agonist, glycine, modestly improves these symptoms.[15] These observations lead to the NMDA receptor hypothesis of schizophrenia. Agents that activate NMDA receptor directly or indirectly by modulating other receptors that activate NMDA could potentially improve symptoms of schizophrenia.[15] Glycine is an agonist of the NR1 subunit of the NMDA receptor.[15] It's been shown that glycine improves the symptoms of schizophrenia. The Javitt lab demonstrated that glycine treatment leads to a significant decline of negative symptoms, a decline in positive symptoms and cognitive symptoms.[15] Therefore, a potential approach to treatment is to increase extracellular glycine levels to increase NMDA activation by preventing its uptake. Synaptic level of glycine is regulated by glycine transporter 1 and 2.[15] GlyT1 inhibitors such as sarcosine have shown to improve positive, negative, and cognitive

symptoms of schizophrenia.[15] The localization of GlyT1 mirrors the localization of NMDA receptors suggesting that they are optimally localized to modulate glycine level at NMDA-receptor expressing synapses.[15]

Metapotropic glutamate receptors (mGluRs) modulate glutamate signaling by pre and post-synaptic and glia mechanisms.[16] Due to its modulatory role and distribution in the forebrain, they are implicated as potential targets for lowering brain excitability seen in various psychiatric disorders.[16] Schizophrenia is associated with excessive glutamate release.[16] Activation of mGluR2/3 decreases the release of glutamate.[16, 17] PCP or phencyclidine and ketamine are agents that antagonize the NMDA receptor (a type of ionotropic glutamate receptor) and increases cortical excitability which results in the induction of psychosis.[16] mGluR2/3 receptor agonists have been shown to block the activity of PCP and related drugs, in other words, they block NMDA antagonist activity.[17] The Schoepp lab demonstrated that PCP increases locomotion in both wildtype and mice that lack mGluR2/3.[17] mGluR2/3 agonists are able to block PCP-induced hyperlocomotion, which is a behavioral model of many neurological disorders including schizophrenia, in wildtype mice but not mice lacking mGluR2/3 receptors suggesting that these receptors are involved in PCP-induced locomotion.[17]

To address negative and cognitive symptoms, muscarinic acetylcholine receptors are also compelling targets.[11, 18, 19] Many studies support the idea of targeting muscarinic acetylcholine receptors for the treatment of schizophrenia. Felder and Wess used M_1- M_5 muscarinic receptor knockout mice to delineate the role of the muscarinic cholinergic subtypes.[20] They demonstrated that hyperlocomotion increases in M_1 and M_4 knockout mice (**Figure 6**).[20] This implicates the role of M_1 and M_4 subtypes in psychiatric disorders.

Table I. Physiological Role of Muscarinic Receptor Subtypes: Effect of Deletion of Muscarinic Receptors

	Muscarinic receptor subtype				
Measurement	M_1	M_2	M_3	M_4	M_5
Parasympathetic effects					
Agonist-induced					
Hypothermia	N	↓↓	↓	N	N
Tremor	N	Absent	N	N	N
Salivation	↓	N	↓↓	↓	N
Bradycardia	N	Absent	N	N	N
Smooth muscle contractility	N	↓	↓↓	N	N
Pupillary dilation	N	N	↑↑	N	N
Central Nervous system effects					
PI hydrolysis in hippocampus	Absent	N	N	N	N
MAPK stimulation	Absent	—	—	—	—
Blockade of dopamine release	—	↓	—	↓	—
Autoreceptor function	—	↓↓	—	↓	—
Cerebral vasculature tone	—	—	—	—	↓↓
Hyperlocomotion	↑	N	N	↑↑	N
Blockade of dopamine-agonist induced hyperactivity	—	N	—	↑	—
Learning and memory	+	—	—	—	—
Weight	N	N	↓	N	N
Agonist-induced seizures	Absent	N	N	N	N
Analgesia	—	↓↓	—	↓	—

Note: N, normal function or no effect; ↓ indicates reduced activity; ↑ indicates increased activity; absent indicates loss of function; number of arrows indicates magnitude of effect, – equals not tested.

Figure 6. Effect of knockout mice on indicated properties.[20]

M_4 is localized in dopamine rich regions of the brain (mesolimbic and nigrostriatal dopaminergic pathways).[21, 22, 23] Knockout studies in mice suggest that M_4 regulates dopaminergic neurons that are involved in motor functions, cognition, and psychosis in these regions.[21, 22, 23] M_4 receptors are localized in brain regions thought to be involved in schizophrenia such as the cerebral cortex and limbic areas.[21, 22, 23] To prove this, Felder et al. measured the effects of prepulse inhibition (PPI) of the acoustic startle response and locomotor activity, which are animal models of schizophrenia, in M_4-knockout mice.[24] The NMDA

antagonist, PCP, acts by stimulating locomotor activity and disrupting PPI (conditioned startle response- second startle response is lower than that of the first).[24] In M_4 knockout mice, it was discovered that locomotor activity increases and prepulse inhibition decreases, meaning that the startling response occurs unabeted even after the conditioned pulse.[24] This result indicates that M_4 activity is necessary in decreasing locomotor activity and increasing PPI (**Figure 7**).[24]

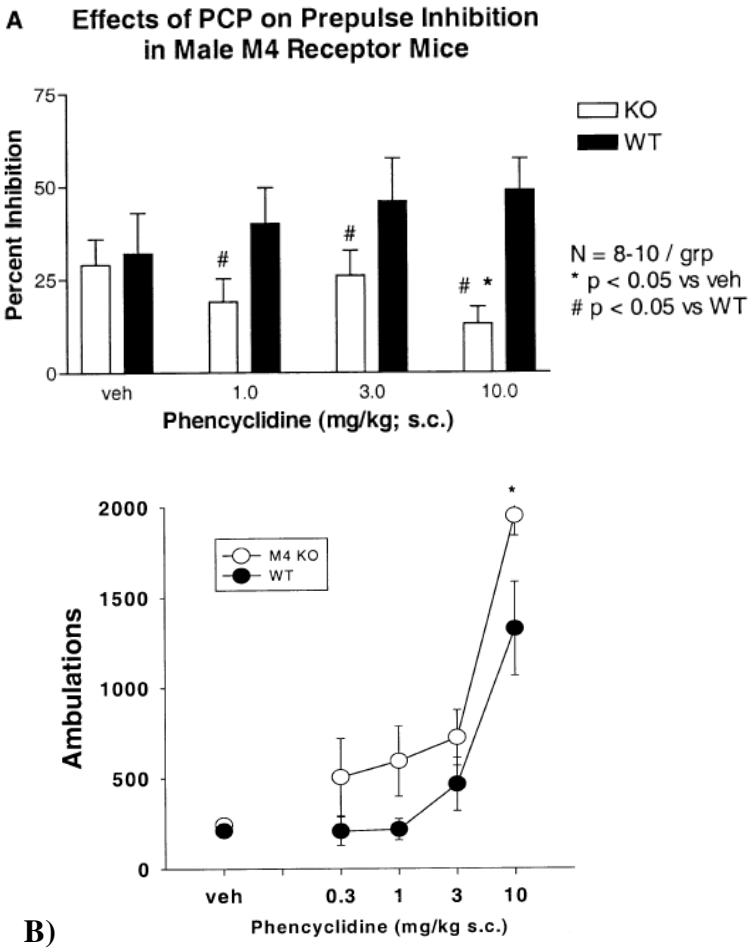

Figure 7. A) Effect of PCP on PPI in M_4 knockout mice. B) Effect of PCP on hyperlocomotion in M_4 knockout mice.[24]

To further establish the involvement of mAChRs in schizophrenia, Dean and Crook performed post mortem studies of the CNS in healthy individuals and unmedicated schizophrenic patients.[25] Their findings suggest that the mRNA density of the M_1 and M_4 receptors is significantly lower in patients with schizophrenia compared to healthy patients.[25] To further support the theory that muscarinic receptors play a role in schizophrenia, Raedler et al. observed muscarinic receptor occupancy *in vivo* in patients with schizophrenia.[27] The following are SPECT brain images of healthy patients and schizophrenic patients (**Figure 8**).[27] Muscarinic receptor occupancy is significantly less in patients with schizophrenia compared to normal subjects.[27]

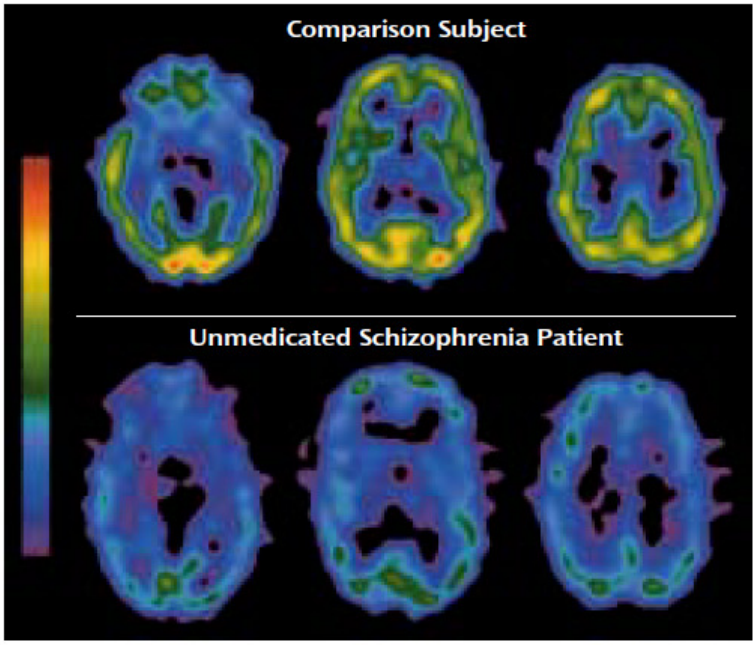

Figure 8. Muscarinic receptor occupancy in healthy patients and schizophrenic patients. Red = high receptor occupancy; blue = low receptor occupancy[27].

To support this muscarinic hypothesis even more, studies show that an M_1/M_4 preferring agonist, xanomeline, has antipsychotic efficacy. In large clinical trial studies of patients with

Alzheimer's disease, xanomeline shows robust therapeutic effects in reducing psychosis and behavioral disturbances that are similar to those found in people with schizophrenia.[27] In a study performed by Neil Bodick et al., an increasing concentration of xanomeline in patients improves symptoms such as delusions, wandering, vocal outburst, and hallucinations.[28] Additional studies of xanomeline establish that it is efficacious in improving cognitive symptoms of schizophrenia. At high concentration of xanomeline, cognition and simple reaction time response improve.[29] In a cognitive test battery, patients treated with xanomeline show the most robust improvement in measures of verbal learning, short-term memory function, list learning, story recall, delayed memory, and digit span tests (**Figure 9**).[29] Xanomeline is unable to progress further in the clinical development process due to its lack of specificity. It is both M_1 and M_4 preferring, and it also has some affinity and efficacy at M_2, M_3, and M_5; therefore, clinically it displays adverse peripheral effects expected from non-selective muscarinic agonists.[28, 29, 30]

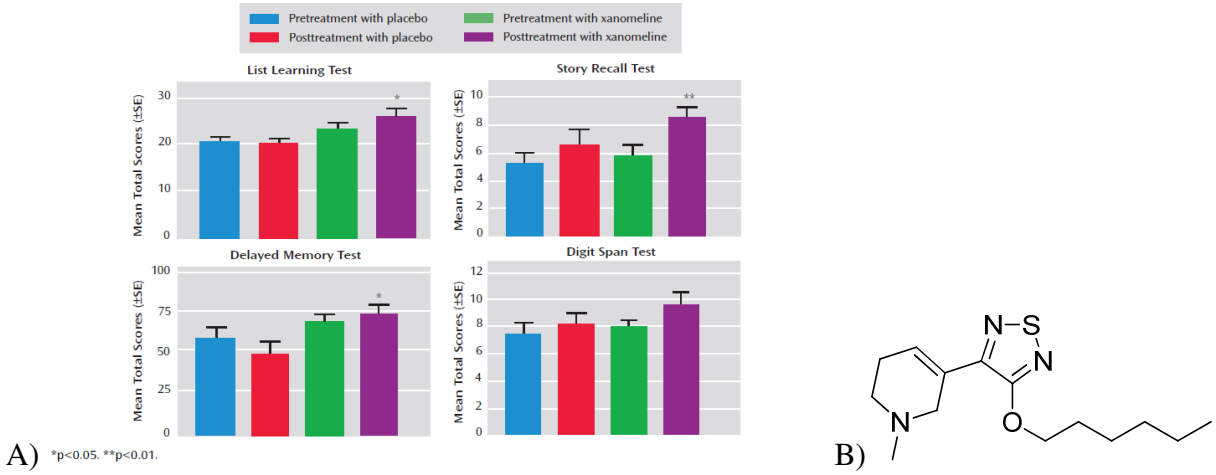

Figure 9. A) Effect of xanomeline in a cognitive test battery.[29] B) Structure of xanomeline.

Following the clinical data obtained from xanomeline, significant efforts have been put forth in developing both M_1 and M_4 modifying agents. Due to the high structural homology of the muscarinic receptor subtypes, historical agonists such as oxotremorine and carbachol, and antagonists, such as atropine and scopolamine, are promiscuous towards these receptor subtypes. Hence, these non-selective ligands are not ideal as tool compounds (**Figure 10**)[32].

Agonists

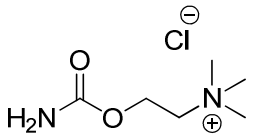

Carbachol

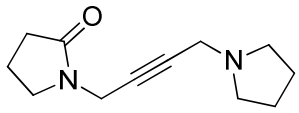

Oxotremorine

Antagonists

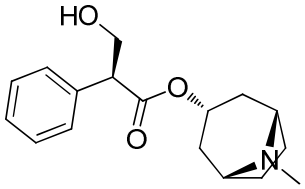

Atropine

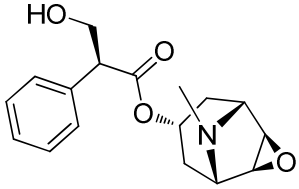

Scopolamine

Figure 10. Structures of historical agonists and antagonists.

Recently, Chan and coworkers report a highly potent (EC_{50} < 100 nM) PAM called LY2033098 which has high selectivity for the human M_4 mAChR.[35] This compound also shows efficacy in paradigms predictive of antipsychotic drug efficacy such as reducing condition avoidance response and reversal of apomorphine-induced disruption of prepulse inhibition.[35] Due to its lower efficacy in the rat model, in *in vivo* studies, LY2033298 has to be co-dosed with oxotremorine in order for it to potentiate receptor function rendering it a less than ideal tool

compound.[35] Major progress has been made in the discovery of selective allosteric modulators of M_4. In addition to LY2033298, VU10010, VU0152099, and VU0152100 are reported as highly selective M_4 PAMs (**Figure 11**).[35, 36, 37]

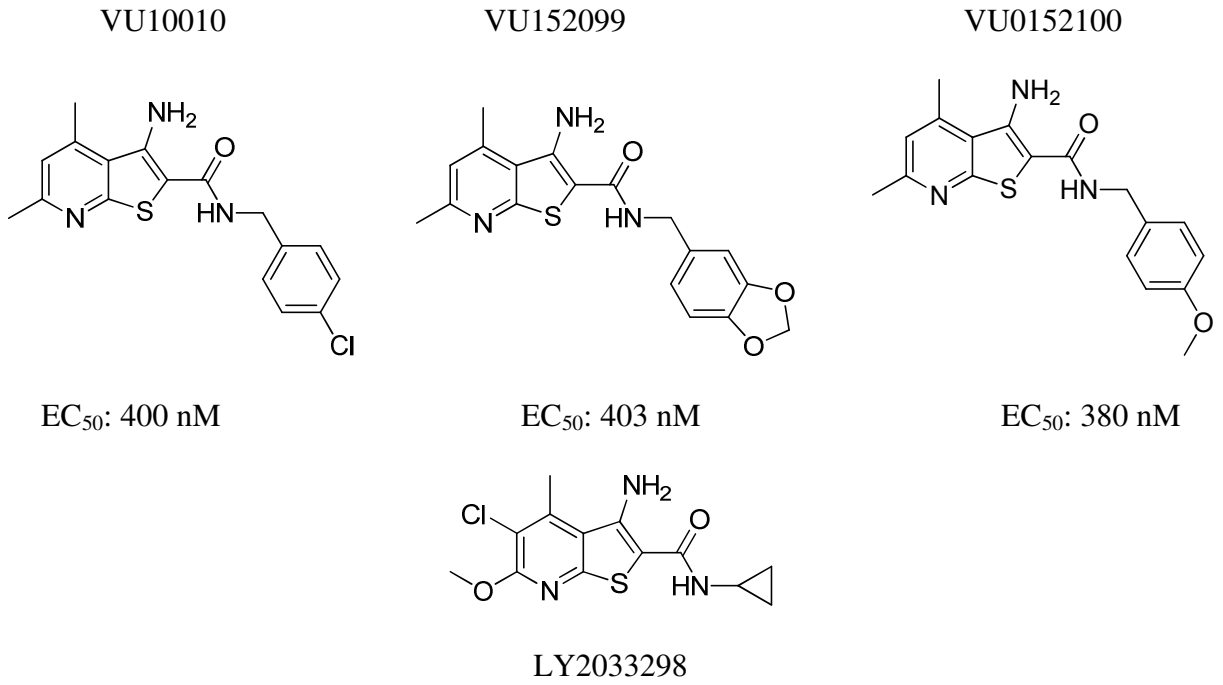

Figure 11. Reported M_4 PAMs.

They all bind an M_4 allosteric site and induce leftwards shifts in the ACh concentration response curve by increasing both the affinity and efficacy of ACh for the M_4 receptor.[35, 36, 37] VU10010 displays no agonist activity in the absence of ACh; which differs than LY2033298 in that LY2033298 displays variable agonist activity on its own.[35, 36] The development of analogs of VU10010 leads to the discovery of VU0152099 and VU0152100. Both are shown to have great efficacies and significantly reverse amphetamine-induced hyperlocomotion in rats.[37] The discoveries of these modulators spur further research into the field of allosteric modulation of M_4 PAM in search for more selective and efficacious ligands that could be useful as tool compounds to further prove the involvement of M_4 in schizophrenia.

Chapter II

OPTIMIZATION AND CHARACTERIZATION OF M_4 POSITIVE ALLOSTERIC MODULATORS

Discovery of M_4 PAM VU010010, VU0152099, and VU0152100

Nomenclature of basic structure

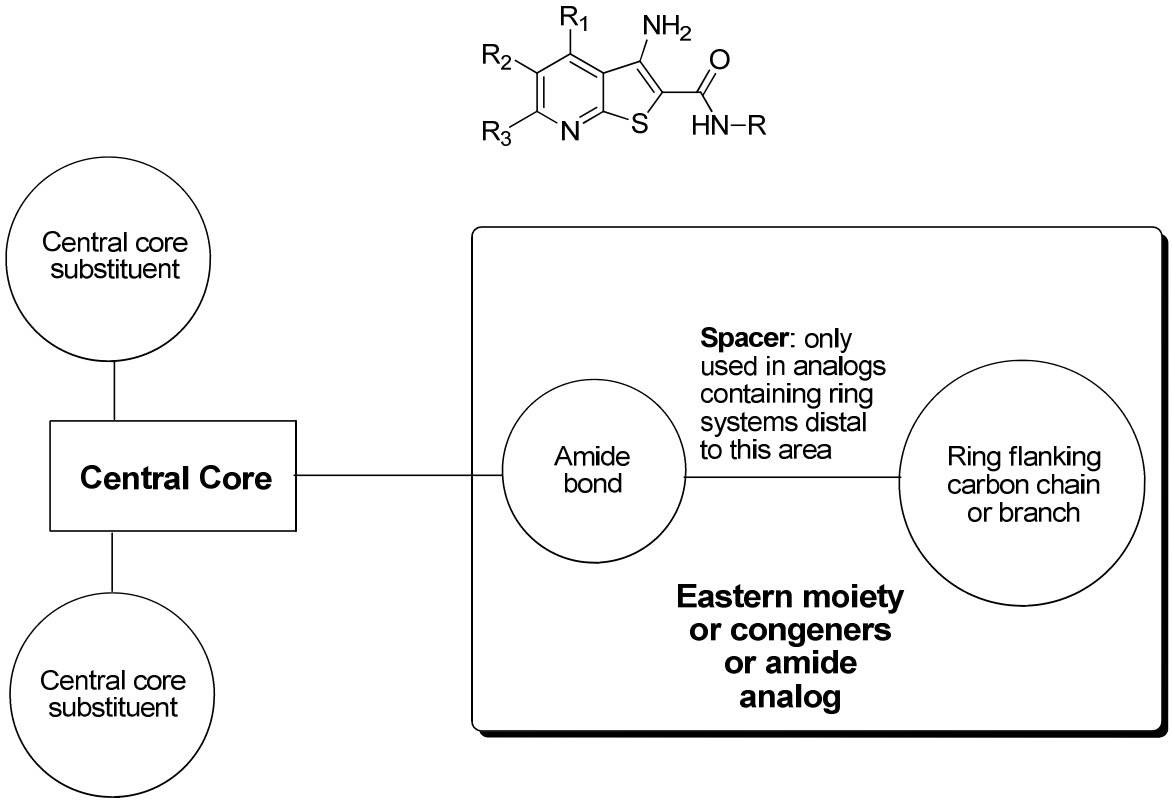

Figure 12. Nomenclature of basic structure.

Discovery of VU10010[36]

The discovery of LY2033298 spurs extensive research in this field. We are able to identify a series of compounds with robust allosteric potentiation and high selectivity for the rat M_4

receptor utilizing chemi-informatics and structure activity (SAR) methods. At the start of the M_4 project, we perform data mining of the ChemBridge database for compounds with similar core structures to LY2033298. 232 compounds are identified and tested for allosteric potentiator activity on M_4 receptors in Chinese hamster ovary (CHO) cells stably expressing rM_4 and the chimeric G protein G_{qi5}.[36] This chimera allows for the immobilization of calcium, since M_4 is not natively coupled to calcium. G_q activation initiates calcium mobilization, which is the readout that is typically used to monitor the direct effect of compounds on muscarinic acetylcholine receptors. The M_4 receptor does not typically bind to G_q, therefore, it is necessary to generate a mutant receptor that allows for the binding of this G-proteins to induce an appropriate readout. The potentiation ability of the compound on an effective concentration of acetylcholine that induces 20% maximal response is determined by a functional fluorescence-based calcium assay. Out of the 232 compounds tested, several hits are identified. (**Figure 13**).[36] On their own, these hits did not induce agonist response at M_4. In the presence of acetylcholine, they enhance the response of the submaximal concentration of acetylcholine, indicating they are PAMs.

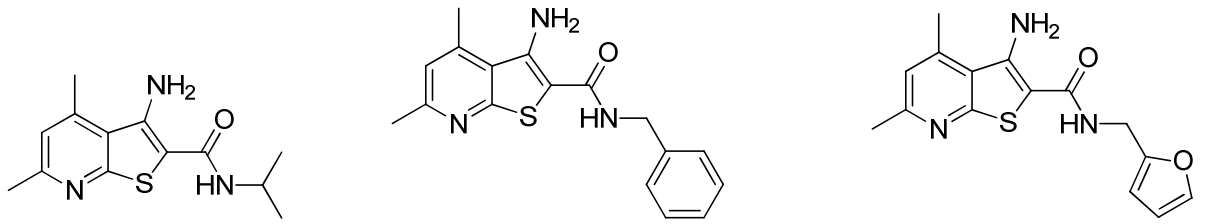

7904200; EC_{50} = 6 μM 7911703; EC_{50} = 1.3 μM 7912361; EC_{50} = 395 nM

Figure 13. Hits identified in screening of ChemBridge compounds purchased commercially.[36]

To determine the potency of each compound, cells are incubated with an increasing concentration of the test compound. Then an EC_{20} concentration of ACh is added to generate a

concentration response curve. It is noted that these compounds did not generate a clear efficacy plateau. The insolubility of these compounds prevented further testing at high concentration.

Next, the effect of a maximal concentration of these compounds on ACh CRC is determined. Cells are incubated with a fix concentration of the test compound that would generate a maximal response. Then increasing concentration of ACh is added. All of the above compounds (7904200, 7911703, 7912361) are tested, and they all cause a leftward shift of the ACh CRC, which is indicative of robust potentiation of the agonistic effect of ACh on the M_4 receptor.[36] It indicates that a lower concentration of ACh is need for the induction of a specific level of response; for examples, hypothetically, to induce 50% receptor response 30 μM of ACh is required. However, in the presence of the positive allosteric modulator, to induce 50% receptor response, only 30 nM of ACh is required (shifting the ACh concentration response curve leftward- EC_{50} is shifted leftward). Therefore, the effect of a leftward shift of the ACh CRC is indicative of potentiation of the acetylcholine agonist activity. This further supportss that these compounds act allosterically, and that they exert their effects from a binding site that is different than that of the acetylcholine binding site.

To test for functional selectivity for the M_4 mAChR receptor, cells expressing other subtypes (M_1, M_2, M_3, and M_5) are incubated with the test compound, then an increasing concentration of ACh is added. Across all other subtypes, these M_4 potentiators fail to initiate potentiation effects on the ACh CRC.

Structurally, the most active compounds all contain a dimethyl thienopyridine core. It is discovered that substitution of these methyl groups with larger groups demolish all functional activity.[36] Substitution of the primary amine also results in reduction of efficacy. Therefore, further chemical derivation occurs at the amide site generating the "VU10000" series. Further *in*

vitro SAR studies of this series utilizing the mentioned assays result in compounds with good potentiation of tan EC_{20} of acetylcholine. Compounds VU10005, VU10008, VU10010 have the highest efficacy and potency (**Figure 14**). VU10010 is the most robust allosteric potentiator; it was able to shift the ACh CRC 47-fold to the left and has an rM4 EC_{50} of 400 nM.[36] To confirm the selectivity of VU10010 for M_4, a selectivity functional assay is performed as mentioned earlier using all five mAChR subtypes. It is found to be inactive across all muscarinic receptor subtypes, except for M_4.

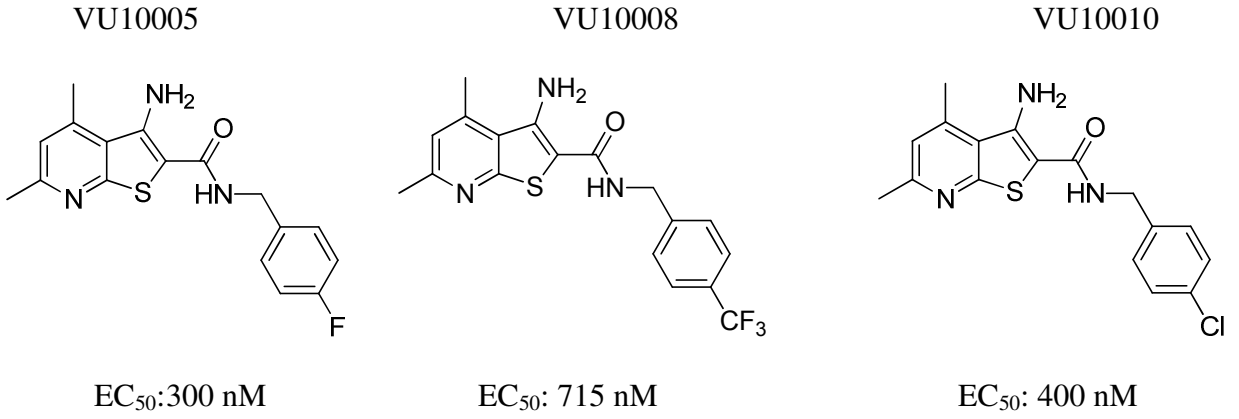

Figure 14. Compounds from optimization effort.

Optimization of VU10010[37]

VU10010 suffered from poor physiochemical properties, such as low solubility (log P of 4.5), and poor pharmacokinetic properties, such as low brain penetration, preventing it from being further characterized.[37] Low brain penetration could be due to the activity of P-glycoprotein (P-gp) efflux. P-gp is an efflux transporter on the luminal membrane of epithelial cells in the blood-brain barrier.[37] It has specificity for a wide range of substrates in order to protect the brain from substances that are toxic. This efflux is known to impair the brain

penetrability of many drugs. The aminoamide motif (**Figure 15**) could potentially be a P-gp liability.

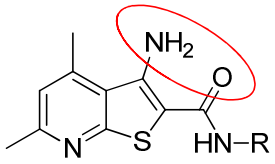

Figure 15. Aminoamide motif: possible P-gp liability.

This susceptibility to P-gp can be reduced by cyclizing the amide and the amine onto the central core or introducing a distal fluorine to attenuate the basicity of the amine moiety. To improve this pharmacokinetic property, VU10010 has to be chemically optimized. Modifications of the central thienopyridine core range from the addition of a CF_3 moiety to the core, removal of the flanking primary amine, replacing the amine with a methyl group, to completely truncating the core by removing all substitutents.[37] The SARs are "flat". In attempts to improve the physiochemical properties and solubility of VU10010, alternative amides are explored while keeping the central core the same. This derivatization generates a few analogs with interesting activity. Within this set of analogs, all aliphatic and non-benzyl amides are inactive at M_4. Only benzyl, functionalized benzyl, and heteroaryl analogs retained some M_4 activity. From this library, two compounds (VU0152099 and VU0152100) are discovered to retain M_4 activity comparable to VU10010 (**Figure 16**).

VU152099

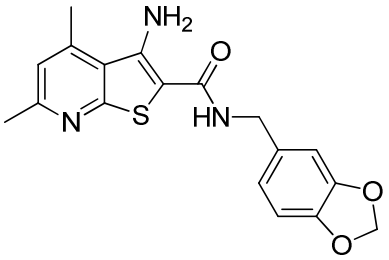

rM4 EC_{50}: 403 nM

VU0152100

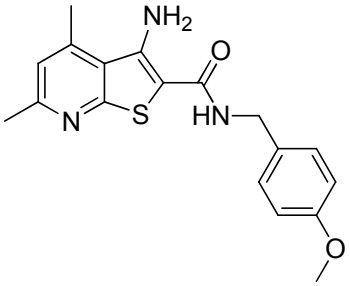

rM4 EC_{50}: 380 nM

Figure 16. VU0152099 and VU0152100

Both VU0152099 and VU0152100 are confirmed to selectively bind M_4 and potentiate ACh response from an allosteric site. These compounds are further characterized to show that their physiochemical and pharmacokinetic properties are better than those of VU10010. Compared to VU10010 with log a P of 4.5, both VU0152099 and VU0152100 have improved log P values of 3.65 and 3.6, respectively. They are almost an order of magnitude less lipophilic than VU10010. Lower lipophilicity could contribute to their higher solubility property. Because they are more soluble, they allow more homogenous dosing for *in vivo* studies. In vivo brain and plasma exposure studies are performed in rats at 56.6 mg/kg administered intraperitoneally. Both compounds exhibit high absorption and brain penetration. Therefore, P-gp susceptibility is not a major concern for this scaffold. Because both analogs have high brain exposure, they were evaluated in a model that is predictive of antipsychotic effect, amphetamine-induced hyperlocomotion. Rodent hyperlocomotion is induced with amphetamine, which is a drug that mimics hyperlocomotion of the schizophrenic state. VU0152099 and VU0152100 appear to reverse the hyperlocomotion activity of amphetamine. Activation or potentiation of the agonist response of acetylcholine on M_4 muscarinic acetylcholine receptor by these compounds activates

NMDA receptors, which increases dopamine turnover, which thereby, reverses amphetamine-induced hyperlocomotion (**Figure 17**).[37]

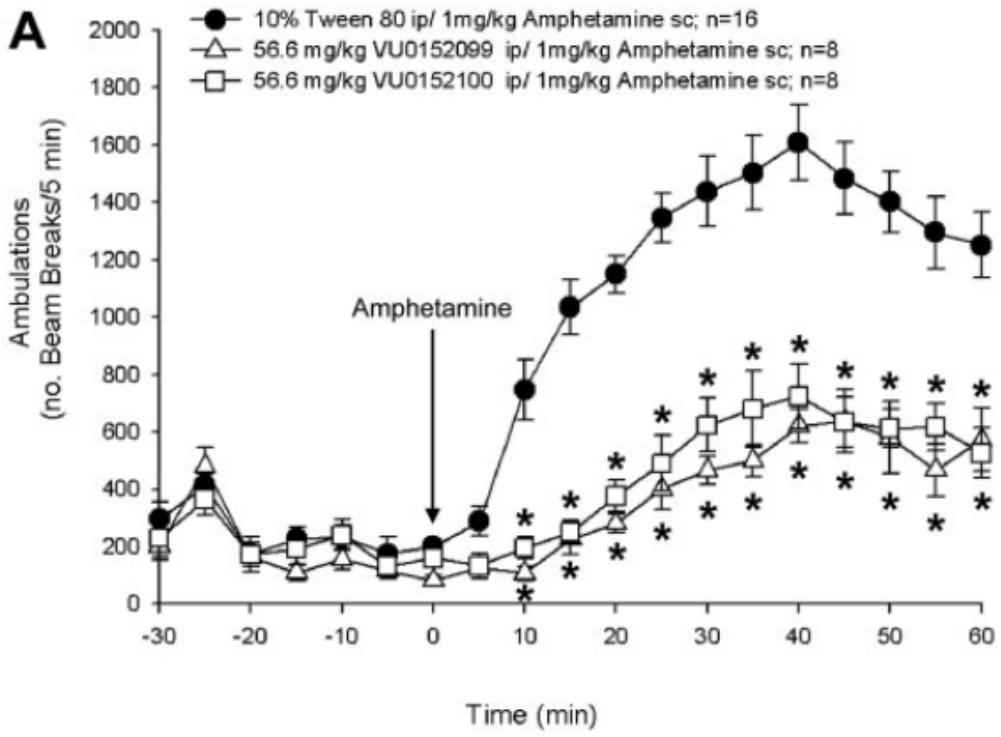

Figure 17. Amphetamine-induced hyperlocomotion is reversed in rats by VU0152099 and VU0152100.[37]

Initial optimization of VU0152099 and VU0152100[38]

VU0152099 and VU0152100 are efficacious, potent, and selective compounds that enhance acetylcholine response via allosteric modulation at the M_4 muscarinic receptor with no inherent agonistic activity on their own. Their metabolic PK profile is still not ideal for *in vivo* studies. Both analogs have poor metabolic stability leaving only less than 10% of the parent compound remaining in human and rat liver microsomes.[38] In attempts to search for tool

compounds that have improved physiochemical and pharmacokinetic properties, further derivitization of VU0152099 and VU0152100 is necessary. Modifications of VU0152100 include replacing the methyl substituent on the thienopyridine core with various aliphatic, aromatics, and functionalized ethers and amines.[32] Most modifications result in "flat" SAR with no potentiation of the acetylcholine response. The groups that are tolerated generating low micromolar potency are analogs containing methylpyridine ethers. Further derivatizations involve keeping the Western moiety (ether linkage) constant and varying the amides flanking the central core. Out of these analogs, the compound with the best combination of potency and fold shift carries a 4-pyridyl ether moiety on the left and a 2,3-difluorobenzyl amide moiety on the right with a potency of 2.44 μM and an acetylcholine fold shift of 44 (**Figure 18**).[38] Other analogs within this set of compounds also have micromolar potency and fold shifts ranging from 7 to 67.

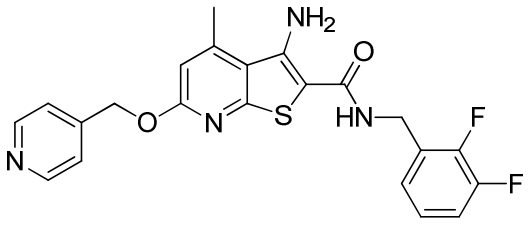

Figure 18. Most potent compound from the initial optimization of VU0152100.

Further Optimization M_4 PAMs

Out of the initial screen of 232 compounds purchased from ChemBridge, along with hits that lead to the generation of VU10010, there was also another hit with micromolar potency. Here we utilize diversity-oriented synthesis to explore the structure activity relationship of hit **1**

(**Figure 19**) from the ChemBridge screen in addition to continuing the optimization of VU0152100.

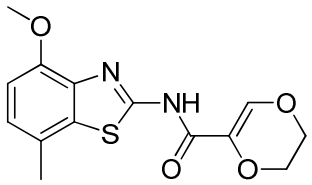

1

Figure 19. Another hit from the initial screen of 232 compounds purchased from ChemBridge.

Compound **1** has a potency (EC_{50}) of 4.5 μM in the rat M_4/G_{qi5} cell line and a potency of 1.7 μM in the human M_4/G_{qi5} cell line. Though these values are within the micromolar range, it can still be improved. However, they are a good starting point for SAR studies. We further explore this hit by derivatizing both the central core and the amide portion.

We previously showed that VU0152099 and VU0152100 posses high potency, efficacy, and selectivity. However, their *in vitro* metabolism PK profile indicates that they are heavily metabolized after 90 minutes of incubation in rat liver microsomes leaving less than 10% of the active parent compound remaining. As a continuing effort to generate compounds that are more metabolically stable and posses better pharmacological profile, we further optimize VU0152100 and its analogs. Two key regions of VU0152100 were derivatized. The new analogs differ from those of VU0152100 in the central core and the amide regions.

General chemistry procedure

Using iterative parallel library synthesis, several sets of compounds are generated from the following general amide coupling procedure: amines are coupled to various carboxylic acids

using *O*-(7-Azabenzotriazol-1-yl)-*N,N,N′,N′*-tetramethyluronium hexafluorophosphate (HATU), N,N-diisopropylethyl amine (DIEA), and either dichloromethane (DCM) or N,N-dimethylforamide (DMF). Reactions are stirred at room temperature until complete. For those carboxylic acids that are not reactive under this amide coupling procedure, they are converted to acid chlorides using $POCl_3$ in pyridine at -15 °C. Then they are coupled to their corresponding amines (**Scheme 1**). All compounds are purified to >95% purity using Gilson HPLC or ISCO Combiflash Rf systems. Purities are determined with the Agilent liquid chromatography/ mass spectroscopy (LCMS) system. Selected compounds were verified using 400MHz Bruker proton nuclear magnetic resonance (NMR).

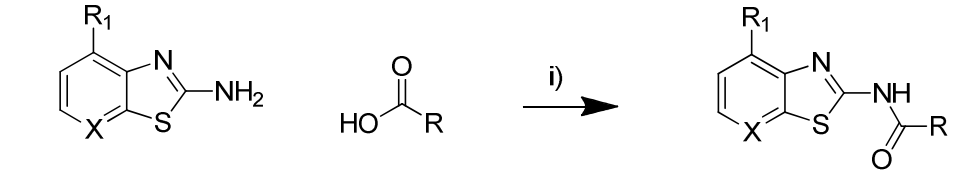

R_1: H, Cl, Br
R_2: H, CH_3
X: N, CR_2

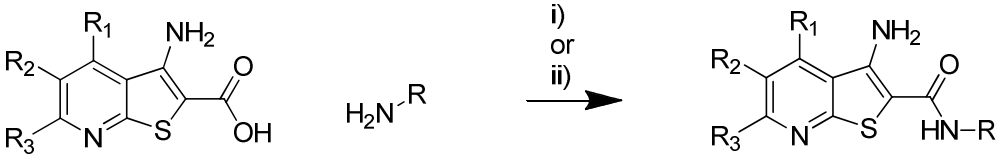

R_1: H, CH_3
R_2: Cl, Br, OH
R_3: CH_3, cyclopropane

Scheme 1. Amide coupling general schemes. i) HATU, DIEA, DMF, RT overnight, ii) $POCl_3$ pyridine, -15°C until completion, then add amine

Characterization of allosteric modulators of GPCRsin calcium mobilization assays

Various assays are used to characterize allosteric modulators. Most functional cell-based assays utilize cells that stably express the receptor in question and readouts that are quantifiable such a fluorescence of calcium mobilization. The assays used typically are in a 'double-add' or 'triple-add' format[8]. Under a 'triple add' format, 10 μM of the test compound is first incubated in human M_4/G_{qi5} cells in the absence of the endogenous ligand (Ach). This incubation establishes a baseline to determine whether the compound itself has intrinsic agonist activity.[8] If the test compound is in fact an agonist, it will potentiate the baseline (**Figure 20A**).[8] Then a submaximal concentration of the acetylcholine (EC_{20}) is added. This second add should reveal the ability of the compound to amplify agonist activity by the orthosteric ligand. If there is a potentiation of activity on top of the submaximal response of the orthosteric ligand, then the compound is considered a positive allostertic modulator (PAM) (**Figure 20B**).[8] All potention response is compared to the positive control, VU0152100. Next, the third add requires the addition of a concentration of the orthosteric ligand that induces a maximal response. If the maximal response is not reached, one possibility of this result is an inhibition of agonist activity (**Figure 20C**).[8] This result is also indicative of no receptor reserve or the receptor is undergoing recovery from an earlier agonist or PAM add, therefore, no additional activation can be induced (**Figure 20A and 20B**).[8] When the compound is antagonizing the activity of the orthosteric ligand, it is either an orthosteric antagonist or a negative allosteric modulator (NAM).[8] To determine whether the test compound is an orthosteric antagonist or NAM, further characterization is required. Competition binding assay can be used to elucidate whether the compound binds orthosterically or allosterically.

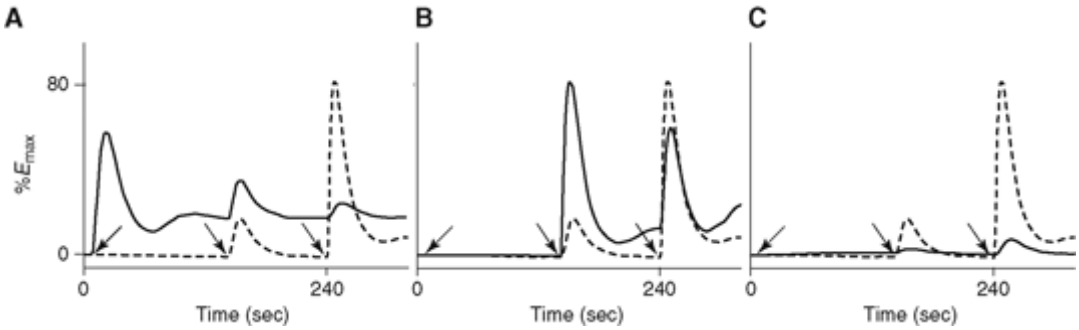

Figure 20. Dotted line displays the action of the endogenous ligand such as acetylcholine for the mAChRs. A) when the compound tested acts as an agonist, it displays agonistic activity even before the endogenous ligand is added B) when the compound is a potentiator, it is not efficacious on its own, but upon the addition of a submaximal concentration of the endogenous agonist, it is able to potentiate activity beyond the efficacy of the agonist C) orthosteric antagonist or NAM inhibits response even with the addition of near maximal concentration of agonist.[8]

Those that show good efficacy from this single point experiment are submitted for further *in vitro* characterization such as its ability to generate a concentration response curve (CRC). The concentration response curve of each compound is generated by incubating increasing concentration of the test compound in cells then adding a submaximal concentration of acetylcholine. The CRC curve determines the effective concentration of the compound required to generate 50% response (EC_{50}) (**Figure 21**).

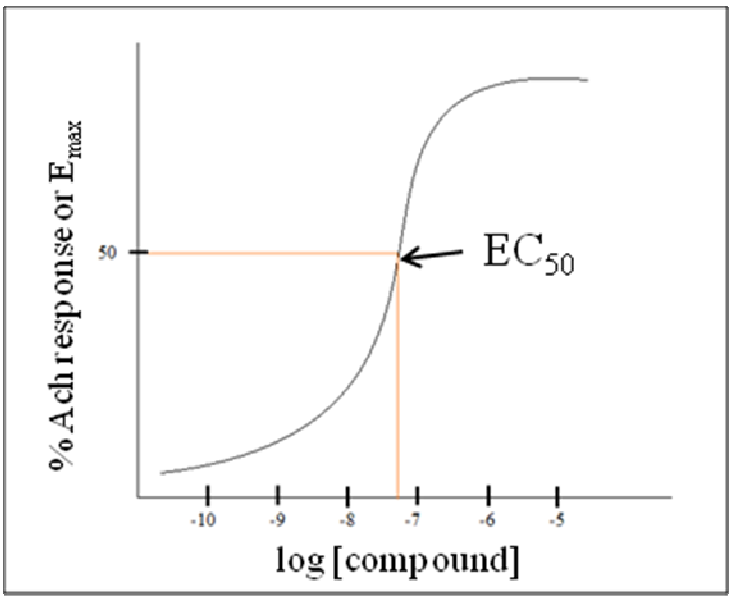

Figure 21. Concentration response curve (CRC).

The allosteric potentiation ability of the test compound is further tested in ACh CRC fold-shift assay (**Figure 22**). Cells are incubated with a fix concentration of the test compound that would generate a maximal response. Then an increasing concentration of ACh is added. A leftward shift of the ACh CRC is indicative of robust potentiation of the agonistic effect of ACh on the M_4 receptor.[36]

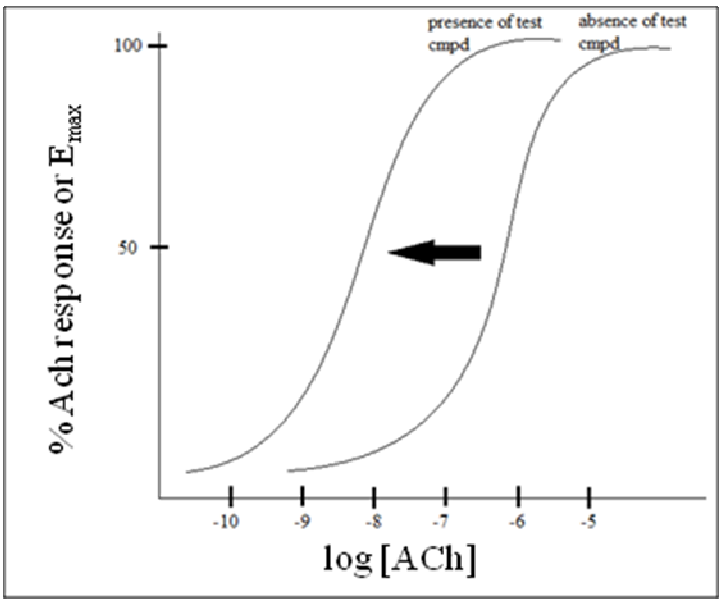

Figure 21. Fold shift of ACh CRC by test compound.

To test for selectivity for the M_4 muscarinic acetylcholine subtype, the same single point $Ca2^+$ mobilization assay is run using other mAChR subtypes. Then this selectivity is confirmed by generating a concentration response curve of the test compound using the corresponding subtypes. Compounds that are selective for the M_4 receptor should not have activity across the other subtypes.

Compounds that have high efficacy, potency, and selectivity against other muscarinic subtypes are further characterized for their pharmacokinetic (PK) properties. For those selected compounds that display good PK profiles, they are further tested in animal models of antipsychotic behavior.

Optimization of HTS hit 1

Using diversity-oriented synthesis, we generate a set of compounds with a wide range of amides in an attempt to probe for functional groups that yield better efficacy and potency compared to the hit compound **1**. This library is synthesized using the amide coupling procedure described above. The carboxylic acids used ranges from aliphatic groups to aromatics and heterocyclic groups. The results from this set of compounds ranges from no potentiation to robust potentiation at the human M_4 receptor. Compounds that potentiate the activity of the submaximal concentration of acetylcholine (EC20) have response higher than the response generated by the EC_{20} (**Figure 22**).

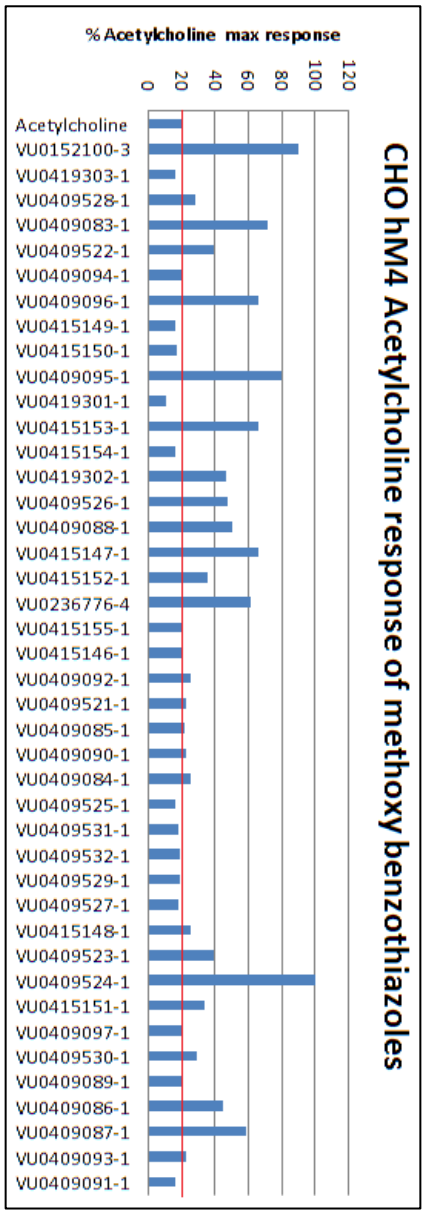

Figure 22. Single point data of methoxy benzothiazole analogs at the human M_4 receptor.

We resynthesize the original hit to reconfirm its activity. The resynthesized hit compound **1** (VU0236776) has an EC_{max} of 61.23 and potency of 1.86 μM, which reconfirms the original data. Results show that a few compounds do in fact potentiate the EC_{20} of acetylcholine. To further investigate the effect of the dihydrodioxine amide from **1** on potency, we investigate

similar ring systems such as tetrahydropyran, methylated dihydrodioxine, and benzodihydrodioxine (**Figure 23**). Compared to the lead compound, 2-amide tetrahydropyran (VU0415147-1) and 3-amide tetrahydropyran (VU0415152-1) congeners are less efficacious and less potent. They have EC_{max} of 66.24, 35.40 and potencies of 3.6 μM and 9.5 μM, respectively. When dihydrodioxine is methylate (VU0415155-1), activity is completely abolished.

Structure	**VU Number**	**EC_{max}**	**EC_{50} (nM)**
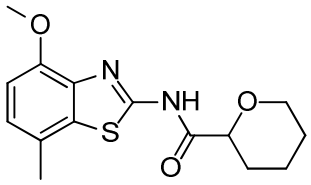	VU0415147-1	66.24	3640
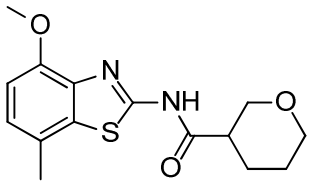	VU0415152-1	35.40	9530
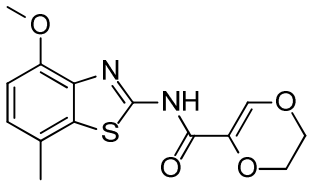	VU0236776-4	61.23	1890
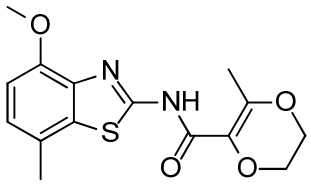	VU0415155-1	20.04	inactive
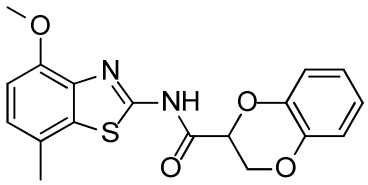	VU0415146-1	20.62	inactive

Figure 23. Analogs of **1** with similar ring systems.

Among the aliphatic groups used, it is observed that as the chain size increases, efficacy and potency increase (**Figure 24**). Foramide (VU0419303-1) is inactive compared to acetamide (VU0409528-1), which has a potency of >10 μM, and butyramide (VU0409083-1), which has an EC_{50} of 6.1 μM. As these chains become branched, activity is abolished as seen in the t-butyl analog (VU0409094-1). With the addition of an oxygen onto the butyramide chain (VU0409096-1), potency remains around 6.5 μM.

Structure	**VU Number**	**EC_{max}**	**EC_{50} (nM)**
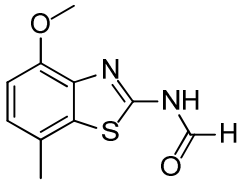	VU0419303-1	16.87	inactive
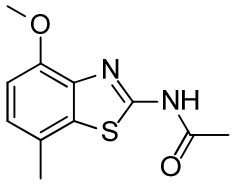	VU0409528-1	28.44	>10000
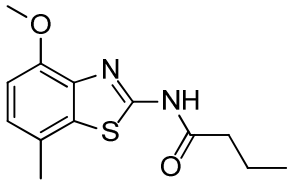	VU0409083-1	71.84	6050
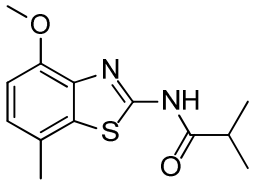	VU0409522-1	39.58	>10000

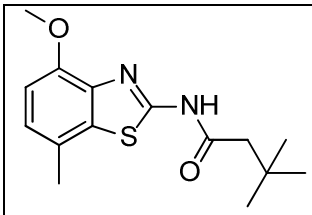	VU0409094-1	21.48	inactive
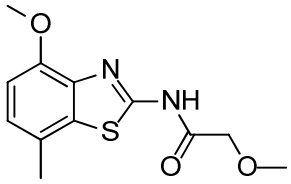	VU0409096-1	65.79	6540
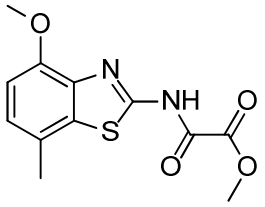	VU0415149-1	16.70	inactive
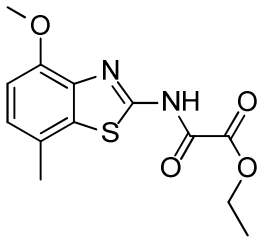	VU0415150-1	17.79	inactive

Figure 24. Aliphatic analogs of **1**.

As for the cyclized aliphatic groups, there is no clear trend with increasing ring size (**Figure 25**). Cyclopropane (VU0409095-1) and cyclobutane (VU0419302-1) have potencies that are comparable to each other (EC_{50} of 4.6 μM and 3.4 μM). Both cyclopentane (VU0409526-1) and cyclohexane (VU0409088-1) have potencies greater than 10 μM. Among the cyclopropane analogs, potency is completely abolished when a methyl spacer (VU0419301-1) is introduced between the cyclopropane ring and the amide. With the addition of a methyl group to the

cyclopropane ring (VU0415153-1), potency decreases to an EC_{50} of 5.3 μM, and no activity is detected when a longer chain is tethered to cyclopropane (VU0415154-1).

Structure	VU Number	EC_{max}	EC_{50} (nM)
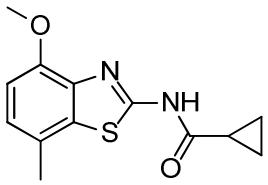	VU0409095-1	79.55	4600
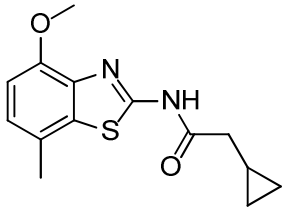	VU0419301-1	11.05	inactive
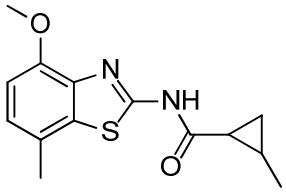	VU0415153-1	65.85	5280
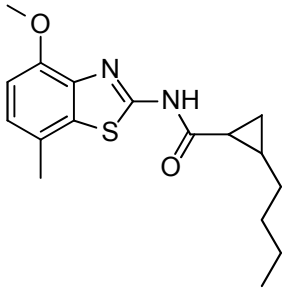	VU0415154-1	16.70	inactive
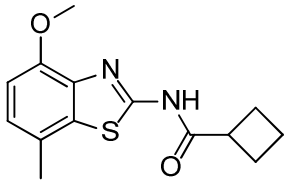	VU0419302-1	47.17	3410

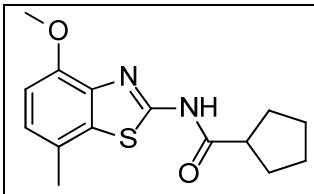	VU0409526-1	47.53	>10000
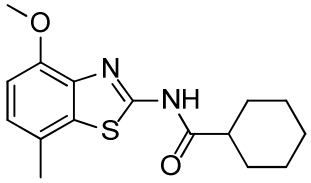	VU0409088-1	50.73	>10000

Figure 25. Cyclized aliphatic analogs of **1**.

It appears that the most efficacious compound among this series with the highest EC_{max} (100.27) contains a 4-pyridyl amide (VU0409524-1). Its counterparts are less potent in comparison; 2-pyridyl amide (VU0415148-1) has an EC_{max} of 25.22, and 3-pyridyl amide (VU0409524-1) has an EC_{max} of 39.62 (**Figure 26**). The 4-position seems to yield the highest efficacy. Their potencies do not clearly distinguish a major difference between the 3 and 4 position of the substitution, but a 10-fold difference can be seen in comparison to the 2-position. The 4-pyridyl substituted analog has an EC_{50} of 1.1 μM while the 3-pyridyl analog has an EC_{50} of 2.5 μM, and the 2-pyridyl analog has potency greater than 10 μM. In comparison to the 3-pyridyl moiety, the addition of a nitrogen onto the 3-pyridyl ring (VU041515-1) decreases acetylcholine max response. However, this pyrazine analog appears to be the most potent compound of this set with an EC_{50} of 744 nM. Though this pyrazine analog has nanomolar potency, its low efficacy prevents it from being a useful compound.

Structure	VU Number	EC_{max}	EC_{50} (nM)
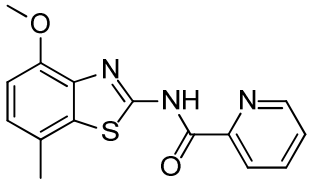	VU0415148-1	25.22	>10000
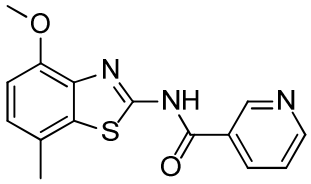	VU0409523-1	39.62	2480
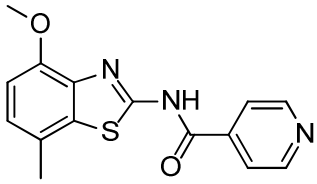	VU0409524-1	100.27	1120
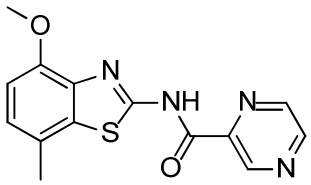	VU0415151-1	33.90	744

Figure 26. Pyridine analogs of **1**.

All other analogs of this series are inactive, with the exception of 4-fluorobenzamide (VU0409084-1), which has a potency of 3.5 μM, and furan (VU0409087-1), which has a potency of 1.6 μM (**Figure 27**). In terms of efficacy, the furan analog is the most efficacious among the remaining analogs with an EC_{max} of 58.85. The subtle trend of increasing efficacy as the substitution position changes can be seen in both fluoro-substituted and cyano-substituted rings. However, because potentiation by these analogs is so low, they are deemed inactive.

Structure	VU Number	EC_{max}	EC_{50} (nM)
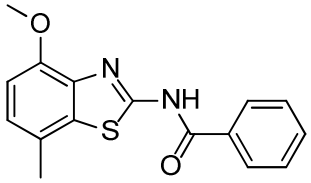	VU0409092-1	26.10	inactive
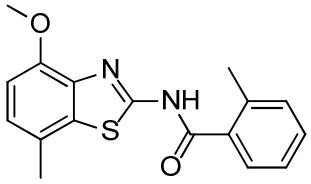	VU0409521-1	22.46	inactive
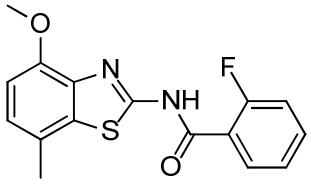	VU0409085-1	21.56	inactive
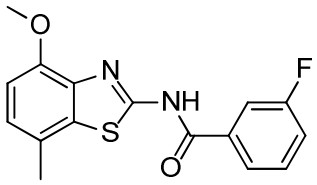	VU0409090-1	22.58	inactive
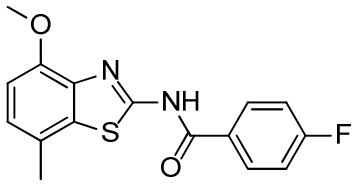	VU0409084-1	25.44	3540
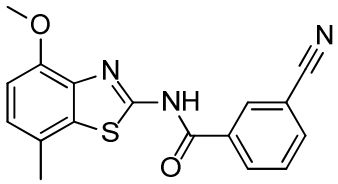	VU0409525-1	16.45	inactive

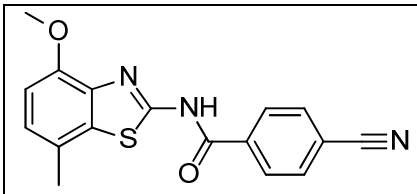	VU0409531-1	18.25	inactive
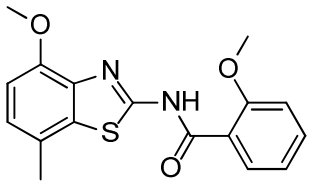	VU0409532-1	19.62	inactive
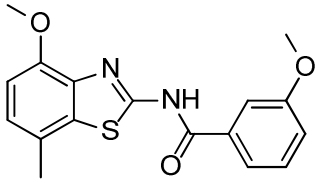	VU0409529-1	18.90	inactive
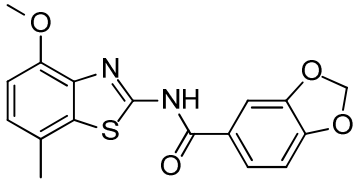	VU0409527-1	18.40	inactive
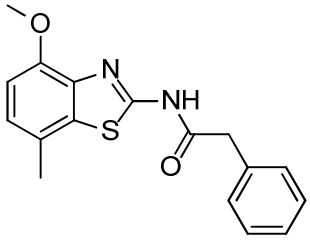	VU0409097-1	20.96	inactive
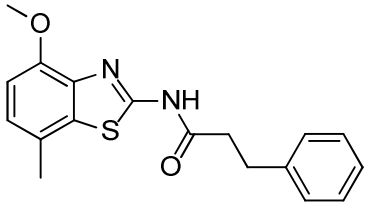	VU0409530-1	29.43	inactive
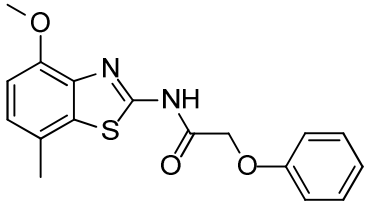	VU0409089-1	20.35	inactive

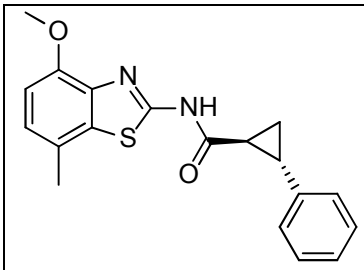	VU0409086-1	44.50	inactive
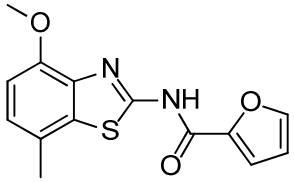	VU0409087-1	58.85	1620
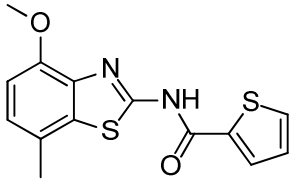	VU0409093-1	22.81	inactive
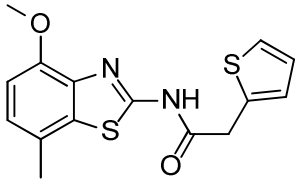	VU0409091-1	16.07	inactive

Figure 27. Additional analogs of **1**.

Compounds among this methoxy methyl benzothiazole series do not appear to have significantly better potency in comparison to **1**. It is observed that pyridines are better tolerated. Structure activity relationship between aliphatics, aromatic, and functionalized aromatic analogs within this subset of compounds indicate a possible discrimination against ring size and position of functionalization.

To further derivatize **1**, the methoxy methyl benzothiazole core is replaced with benzothiazole (**Figure 28**). This truncation of the central core is an experiment to test whether

efficacy and potency are driven from substitution of the central core. The same amide coupling protocol described earlier is used to generate this set of compounds. No active compounds are observed. Some of the same side chains that display efficacy and potency from the previous set of analogs do not produce similar profile with this core substitution. From the previous set of analogs, it is observed that the 4-pyridyl substituent (VU0409524-1) has good efficacy and low micromolar potency. When the methoxy and methyl substituents are removed from the central core, activity is abolished. No potentiation is seen among analogs that were active in the previous series. This benzothiazole core produces no active PAMs.

Structure	**VU Number**	**EC_{max}**	**EC_{50} (nM)**
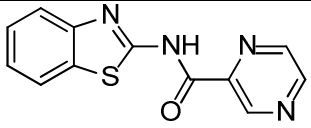	VU0166610-4	20.31	inactive
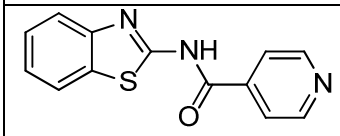	VU0419287-1	20.20	inactive
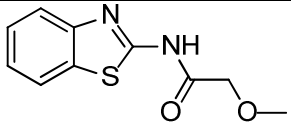	VU0155360-3	16.75	inactive
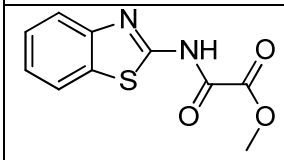	VU0419283-1	16.44	inactive
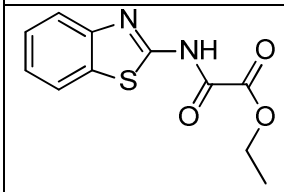	VU0419284-1	15.70	inactive

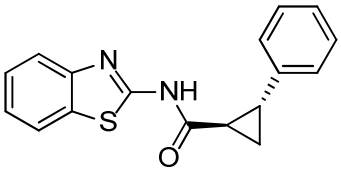	VU0419285-1	15.19	inactive
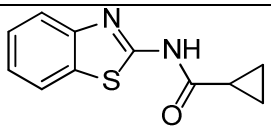	VU0419286-1	18.30	inactive
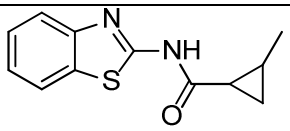	VU0419288-1	18.43	inactive
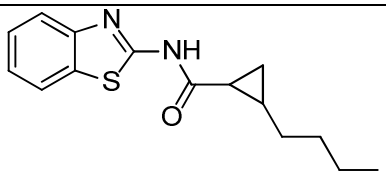	VU0419291-1	16.01	inactive
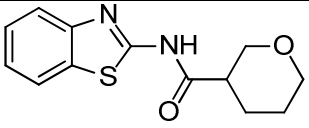	VU0419290-1	16.18	inactive
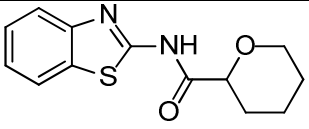	VU0419282-1	19.81	inactive
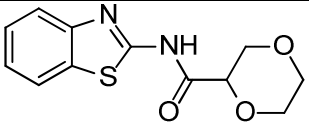	VU0419289-1	17.71	inactive
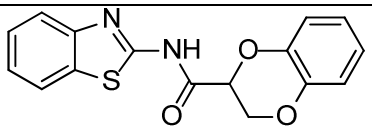	VU0195412-5	12.73	inactive
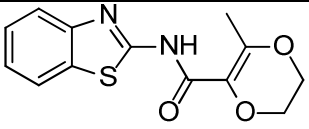	VU0419292-1	15.23	inactive

Figure 28. Analogs of truncated central core (benzothiazole).

To examine whether the introduction of a heteroatom within the central core has any affect on efficacy and potency, we replace the truncated benzothiazole core with thiazolopyridine (**Figure 29**). Using some of the same congeners that previously showed activity in the methoxy methyl benzothiazole series, we generate a library using thiazolopyridine. Similarly to benzothiazole, this thiazolopyridine core produces only inactive compounds.

Structure	VU Number	EC_{max}	EC_{50} (nM)
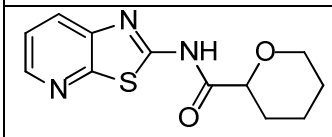	VU0419293-1	13.80	inactive
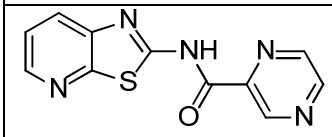	VU0419294-1	18.98	inactive
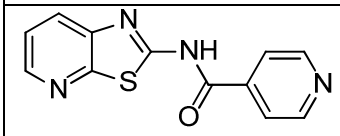	VU0419297-1	15.77	inactive
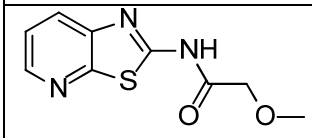	VU0419296-1	16.18	inactive
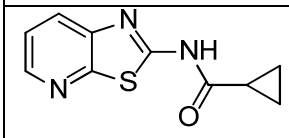	VU0419295-1	16.11	inactive
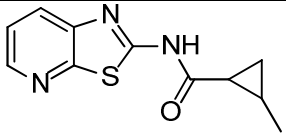	VU0419298-1	16.35	inactive

Figure 29. Replacing the methoxy methyl benzothiazole core. Analogs of thiazolopyridine core.

To further examine the effect of altering the central core on efficacy and potency, we replace the methoxy methyl benzothiazole core with hydroxymethyl benzothiazole (**Figure 30**). The congener of choice for this set is cyclopropane, which has good efficacy of 79.55 and a potency of 4.6 μM. As seen here, replacing the methoxy substituent of the central core with hydroxy does not have dramatic effects on the efficacy and potency of these analogs.

		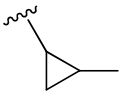
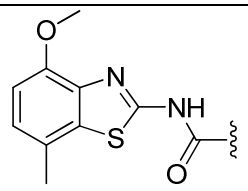	VU0409095-1 EC_{max}: 79.55 EC_{50}: 6.00 μM	VU0415153-1 EC_{max}: 65.85 EC_{50}: 5.28 μM
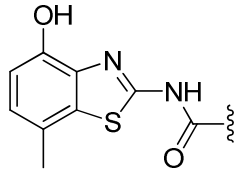	VU0419299-1 EC_{max}: 43.80 EC_{50}: 5.16 μM	VU0419300-1 EC_{max}: 44.74 EC_{50}: 4.97 μM

Figure 30. Result of replacing the methoxy substituent on the central core with hydroxy in comparison to the analogs carrying the original central core.

Among the analogs generated, those with high potency and efficacy are selected for further characterization. The effect of a maximal concentration of these compounds on the ACh CRC is determined (ACh fold-shift assay). VU0409524-2, VU0409095-1, and VU0409523-1 are selected for further analysis (**Figure 31**). The methoxy methyl benzothiazole analog that carries the 4-pyridine eastern moiety (VU0409524-2) has the highest fold shift of 15. Out of the three

compounds tested, it is observed that VU0409524-1 has the highest potentiation amd it shifts the ACh CRC leftward the farthest. The analog carrying the cyclopropyl moiety (VU0409095-1) is able to shift the ACh CRC leftward by 4.9 fold, and the 3-pyridyl moiety (VU0409523) is able to shift the ACh CRC leftward by 2.7 fold.

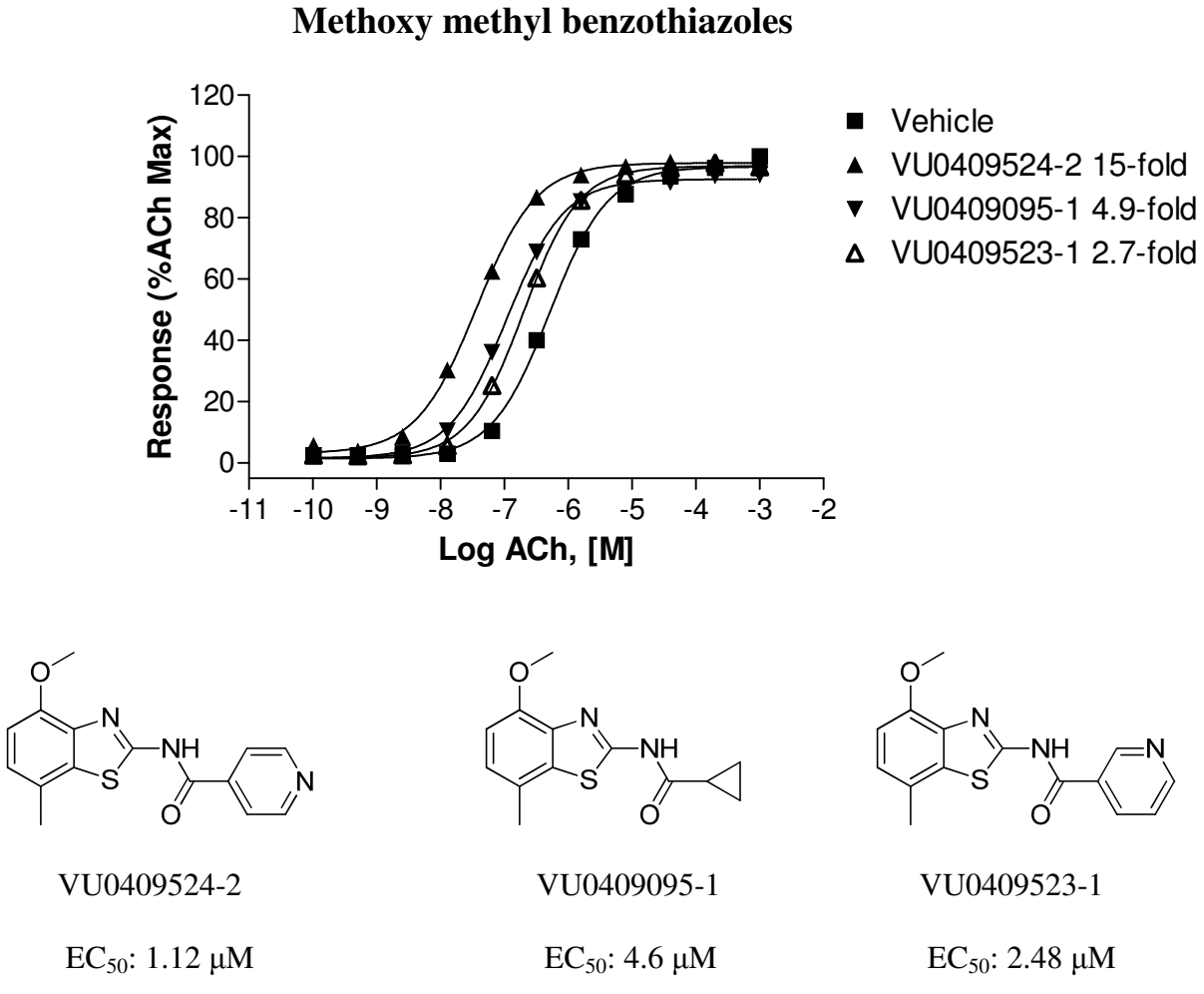

Figure 31. Fold shift result of most efficacious and potent analogs of **1**.

In conclusion, attempts to improve efficacy and potency of **1** result in analogs with potencies within the low micromolar range that are comparable to **1**. It is observed that the

methoxy methyl substituents on the central core are important for activity. Truncating the central core, by removing these substituents, results in analogs with no activity. A subtle trend among the pyridine congeners is detected. The position of the nitrogen affects activity. The 4-pyridyl analog is most potent in comparison to the 2- and 3-pyridyl analogs.

Optimization of VU0152100

As mentioned earlier, even though VU0152099 and VU0152100 have good efficacy, potency, and selectivity, their metabolic PK profile is still not ideal. They are metabolized in human and rat liver microsomes leaving less than 10% of the parent compound remaining. Paralleling the optimization effort of VU0152100 mentioned earlier, in an attempt to optimize VU0152100, the central core and the amide linker are modified. For comparison, some of the same amines previously used to generate VU0152100 and their analogs are utilized. Kennedy P., et al. shows that some of the amides that are tolerated in the analogs that they generated range from aliphatic groups such as t-butyl to di-fluorinated aromatic groups.[38]

We first observe the effect of modifying the central core. A set of analogs are generated using bromocyclopropyl thienopyridine (**Figure 32**). It is seen that among all the congeners synthesized, the most efficacious analog contains a cyclopropane ring (VU0448244-1). It has an EC_{max} of 59 and a potency of 1.6 μM. This set of analogs produce "flat" SAR; all other analogs are inactive.

Structure	VU Number	EC_{max}	EC_{50} (nM)
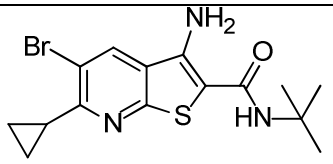	VU0448215-1	17	inactive
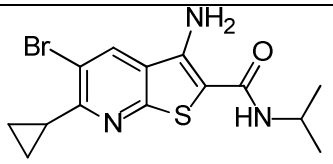	VU0448181-1	29	inactive
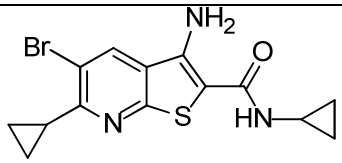	VU0448244-1	59	1630
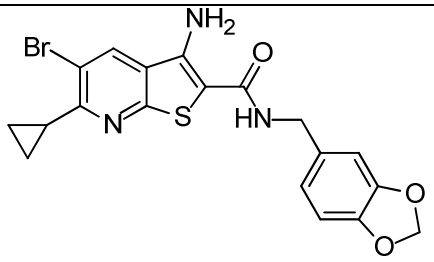	VU0448120-1	24	inactive
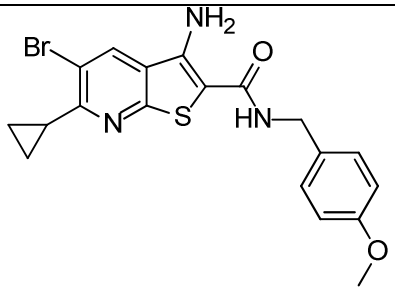	VU0448145-1	25	inactive
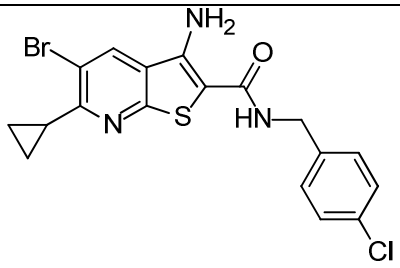	VU0448146-1	27	inactive

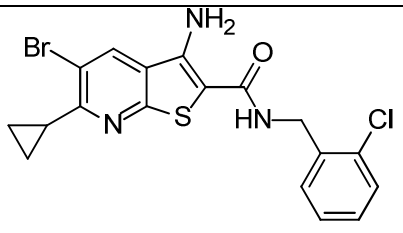	VU0448162-1	31	inactive
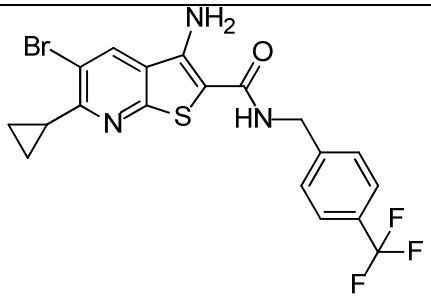	VU0448177-1	28	inactive
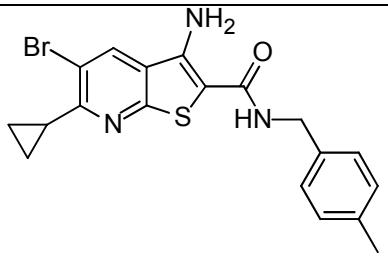	VU0448188-1	26	inactive
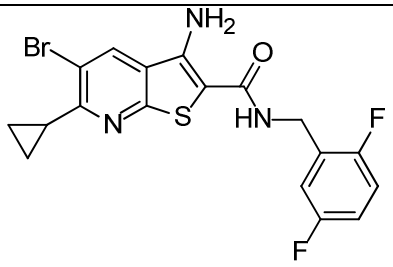	VU0448247-1	24	inactive
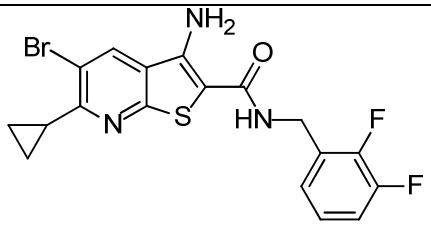	VU0448230-1	27	inactive

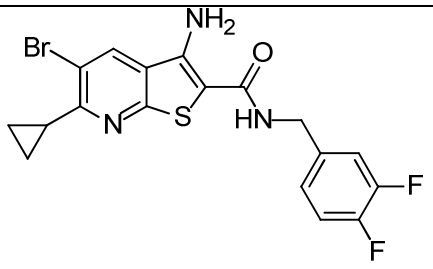	VU0448196-1	23	inactive

Figure 32. Results of replacing the central core of VU0152100. All analogs are inactive, except for the analog carrying cyclopropylamide.

To further modify the central core of VU0152100, we substitute the dimethyl thienopyridine core with chlorodimethyl thienopyridine. Then we proceed with amide coupling with various amines ranging from aliphatics to aromatics and functionalized aromatics.

Synthesis of 3-amino-5-chloro-4,6-dimethylthieno[2,3-b]pyridine-2-carboxylic acid

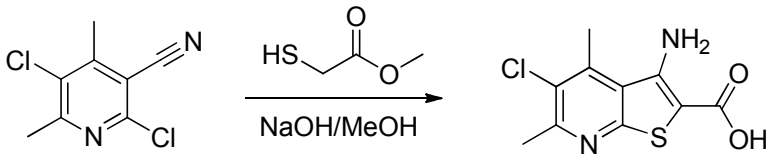

To a 20 mL microwave vial fitted with a magnetic stir bar, 2,5-dichloro-4,6-dimethylnicotinonitrile (1 g, 5.0 mmol) and MeOH (10 mL) are added. Methyl thioglycolate (490 µL, 5.5 mmol) is added followed by the addition of a 1 M solution of NaOH (aq, 10 mL, 25 mmol). The microwave vial is sealed and the solution is heated to 125 °C for 30 min. The reaction is cooled to room temperature and a solution of HCl is added until the solution reaches the pH of 1. The precipitate that formed is filtered and dried in a vacuum oven at 50 °C for 24 h.

The solids are of sufficient purity to use without further purification. ^{1}H NMR (400 MHz, d_6-DMSO, δ (ppm)): 6.833 (s; 2H), 2.84 (s; 3H), 2.63 (s; 3H).

Synthesis of 3-amino-N-(benzo[d][1,3]dioxol-5-ylmethyl)-5-chloro-4,6-dimethylthieno[2,3-b]pyridine-2-carboxamide

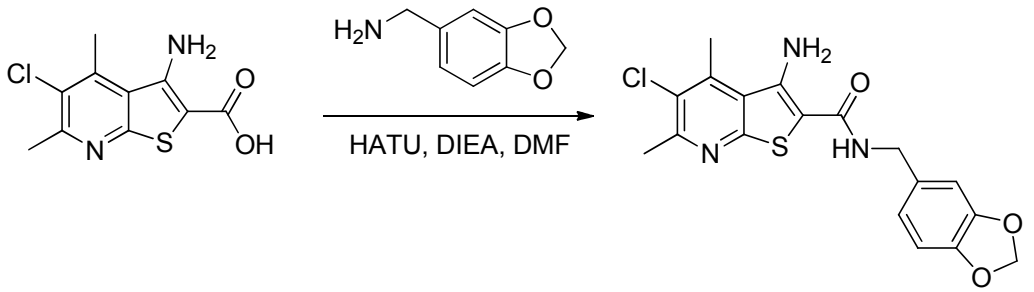

To a 20 mL vial fitted with a stir bar and a setum cap, 3-amino-5-chloro-4,6-dimethylthieno[2,3-b]pyridine-2-carboxylic acid (125 mg, 0.50 mmol) and and DMF (3 mL) are added. Then piperonylamine (90.9 μL, 0.75 mmol) is added followed by diisopropylethylamine (499 μL, 1.0 mmol) and 2-(1H-7-Azabenzotriazol-1-yl)-1,1,3,3-tetramethyl uronium hexafluorophosphate methanaminium (HATU, 190 mg, 0.50 mmol). The solution is stirred at ambient temperature overnight. Then it was concentrated and purified via Gilson HPLC purification system. ^{1}H NMR (400 MHz, d_6-DMSO, δ (ppm)): 8.3 (t; J = 6.0 Hz; 1H), 6.9 (broad s; 2H), 6.8 (d; J = 8.0 Hz; 1H), 6.75 (dd, J = 8.0 Hz; 1H), 5.9 (s; 2H), 6.9 (bs; 2H), 4.3 (d; J = 6.0 Hz; 2H), 2.8 (s; 3H), 2.6 (s; 3H).

Synthesis of all other analogs follows this procedure.

The SAR of these analogs produces a number of compounds with robust potentiation. The potencies of these compounds range from greater than 10 μM down to 10 nM. Of the aliphatic amides used, there is no clear trend between chain/branched versus cyclized analogs.

The potencies of some analogs from this series are better in comparison to the potencies of VU0152099 (EC_{50} 403 nM) and VU0152100 (EC_{50} 380 nM) such as potencies of the following aliphatic compounds (**Figure 33**). The most notable compound is VU0449033-1 carrying cyclopropyl amide, which has a high potency of 19.4 nM. In comparison, potency decreases 10-fold (188 nM) as the ring size increases to cyclohexyl amide (VU0452029); potency decreases even further by 100-fold (1.1 μM) when a methyl spacer is added between the amide and the cyclohexyl ring (VU0452142). In general, these analogs generate submicro molar potencies that are better than VU0152099 and VU015210.

Structure	**VU Number**	**EC_{max}**	**EC_{50} (nM)**
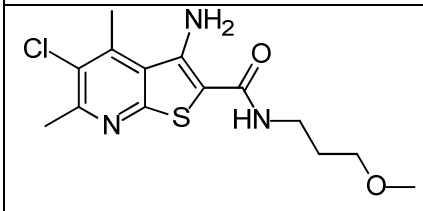	VU0448053-1	89	337
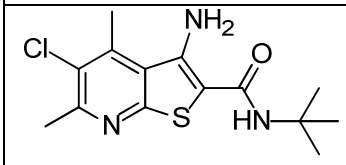	VU0448042-1	90	293
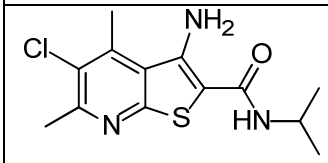	VU0449064-1	----	183
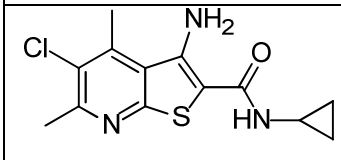	VU0449033-1	----	19.4
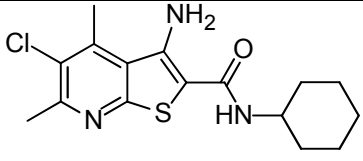	VU0452029-1	----	188

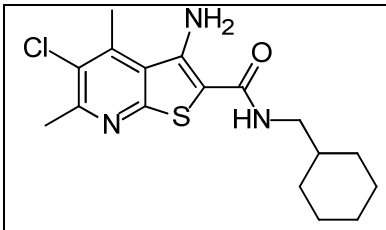	VU0452142-1	----	1090

Figure 33. Aliphatic analog results of replacing the central core of VU0152100.

In comparison to the cyclohexyl amide analog, the introduction of an oxygen into the cyclohexyl ring (tetrahydropyran analog VU0452127-1) does not dramatically change the potency. Its EC_{50} of 220 nM remains near that of the cyclohexane moiety. In comparison to the tetrahydropyran analog, oxetane (VU0459382-1) has a lower potency of 906 nM. With an EC_{50} of 28.7 nM, tetrahydrofuran (VU0459381-1) is the most potent analog of these oxygen containing aliphatic rings. It is 10-fold more potent than the tetrahydropyran analog and is 30 fold more potent compared to oxetane. No clear trend is detected among these analogs, however tetrahydrofuran has a notable potency (**Figure 34**).

Structure	**VU Number**	**EC_{max}**	**EC_{50} (nM)**
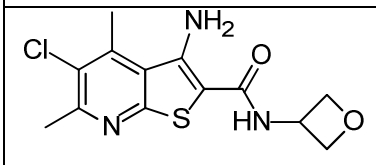	VU0459382-1	----	906
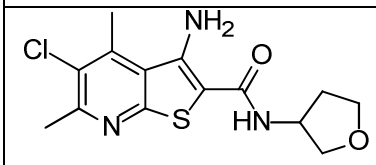	VU0459381-1	----	28.7

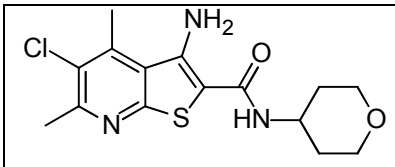	VU0452127-1	----	220

Figure 34. results of oxygen containing cyclized aliphatic analogs.

In comparison to VU0152099 and VU0152100, analogs of this series are more potent (**Figure 35**). Replacing the central core of VU0152099 increases potency 7-fold from 403 nM to 56.9 nM. Potency of VU0152100 increases about 3-fold from 380 nM to 117 nM.

	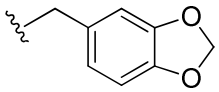	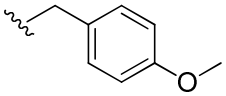
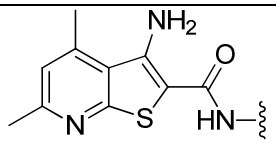	VU0152099 EC_{50}: 403 nM	VU0152100 EC_{50}: 380 nM
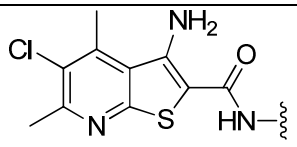	VU0448057-1 EC_{50}: 56.9	VU0448098-1 EC_{50}: 117

Figure 35. Comparing VU0152099 and VU0152100 to their analogs in the chlorodimethyl thienopyridine series.

Similarly to the pyridyl analogs of **1** mentioned above, pyridine analogs within this series also display similar trend of nitrogen position-dependent activity. Potency is affected by the

position of the nitrogen on the pyridine ring (**Figure 36**). 2-pyridine (VU0452032-1) has a potency of 293 nM, while 3-pyridine (VU0452129-1) is more potent with an EC_{50} of 94.9 nM, and 4-pyridine (VU0448088-1) is the most potent with EC_{50} of 40.0 nM. As a result of this robust potentiation among the pyridyl analogs, additional pyridyl analogs are generated. Similarly to the pyridyl analogs, this trend of nitrogen position-dependent potency is also observed among analogs containing a methylated methyl spacer. When the nitrogen is in the 2-position (VU045367-18) the EC_{50} is 1.41 μM; when the nitrogen is in the 3-position (VU0453649-1), potency increases an additional 10-fold to an EC_{50} of 601 nM; when the nitrogen is moved to the 4-position (VU0453628-1), the potency remains near that of the 3-position displaying an EC_{50} of 600 nM. Potency decreases when the methyl spacer is homologated. Compared to the 2-methylpyridine analog (VU0452032-1), which has a potency of 293 nM, the 2-ethylpyridine analog (VU0459327-1) is slightly less potent producing an EC_{50} of 686 nM. The 3-ethylpyridine moiety (VU0459383-1) is unable to potentiate acetylcholine agonist activity, while the 3-methylpyridine (VU0452129-1) moiety has a potency of 94.9 nM. When the nitrogen is moved to the 4-position (4-ethypyridine VU0456952-1), activity is regained producing an EC_{50} of 121 nM, which is 10-fold less than that of 4-methylpyridine (VU0448088-1). In general, among these pyridine analogs, the 4-position is more preferable. The length of the spacer is important to potency. It is observed that the shorter spacer generates better potency.

Structure	VU Number	EC_{max}	EC_{50} (nM)
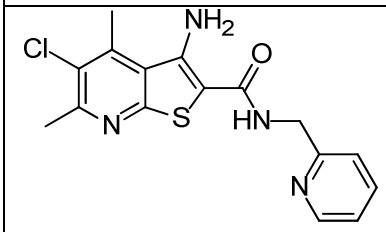	VU0452032-1	----	293
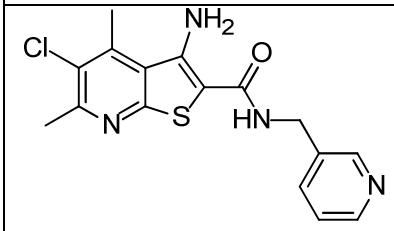	VU0452129-1	----	94.9
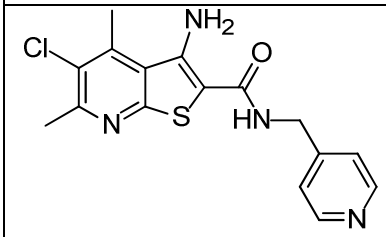	VU0448088-1	93	40.0
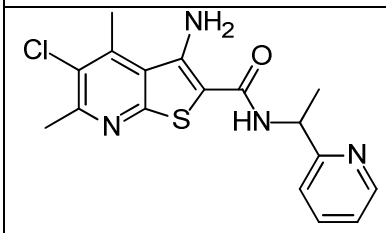	VU0453678-1	----	1410
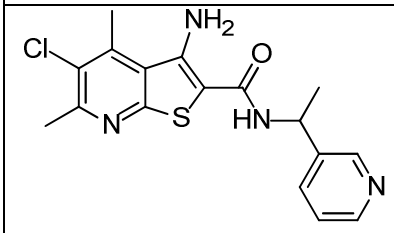	VU0453649-1	----	601
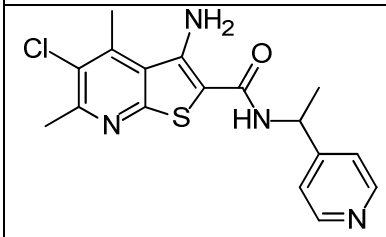	VU0453628-1	----	600

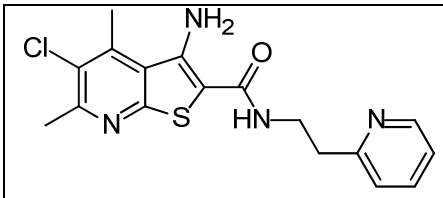	VU0459327-1	----	686
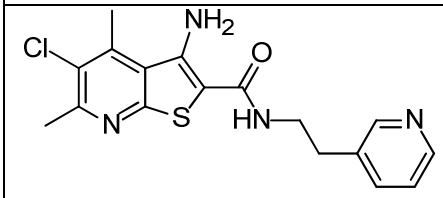	VU0459383-1	----	inactive
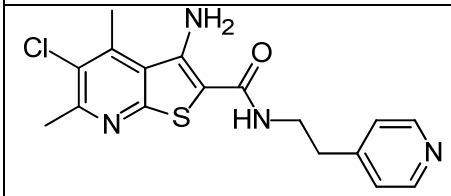	VU0456952-1	----	121

Figure 36. Results of pyridine analogs.

Next, we observe the effect of adding an additional nitrogen to the pyridine ring (**Figure 37**). Data from the pyridine analogs above establish that potency increases as nitrogen is moved from 2- to 3- to 4-position. Of the di-nitrogen containing rings, this trend can subtly be seen. The potency displays by each nitrogen in these analogs is additive; the final potency of each analog is the summation of the potency of each nitrogen on the ring. For example from the above data, 2-pyridine displays the lowest potency (293 nM). Hence, when when the nitrogens are in the 2- and 6-position (VU0456925-1), potency is even lower (EC50 1.07 μM). Having a nitrogen in the 6-position is similar to having a nitrogen in the 2-position if atom count starts on the side containing the 6-nitrogen (like having nitrogen in two 2-positions). When the 2-position nitrogen is held constant and the other nitrogen is walked around the ring, potencies are still lower than those of pyridines above (additive effect). However, it can still be observed that walking the

second nitrogen from 2- to 3- to 4-postion increases potency within this series. VU0459384-1 has nitrogens at the 3- and 4-position, which are the more potent positions; therefore, its potency of 222 nM is better than the other analogs in the same series.

Structure	VU Number	EC_{max}	EC_{50} (nM)
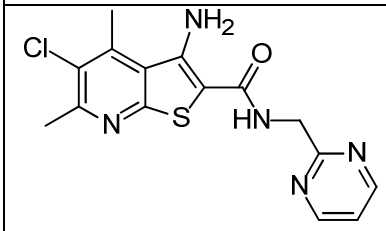	VU0456925-1	----	1070
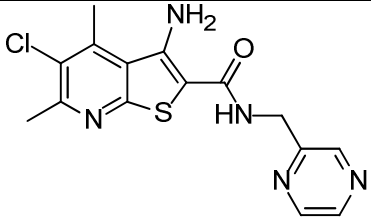	VU0452102-1	----	262
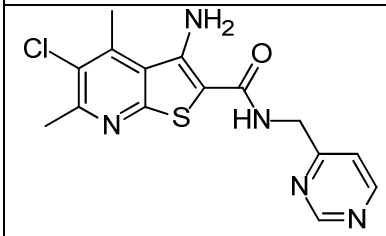	VU0456953-1	----	243
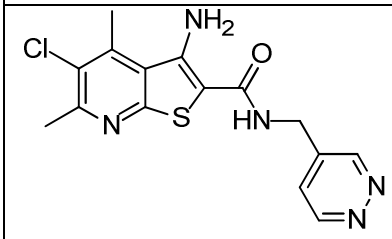	VU0459384-1	----	222

Figure 37. Results of dinitrogen-containing analogs.

Next, the chlorodimethyl thienopyridine core is replaced with hydroxydimethyl thienopyridine (**Figure 38**). It is observed that replacement of the chlorine with hydroxyl abolishes activity shown with VY0458326. Potency of the benzyl analog decreases from 90.8 nM to greater than10 μM.

	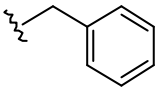
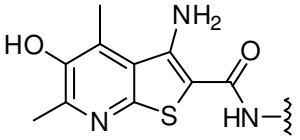	VU0458326 EC_{50} > 10 μM
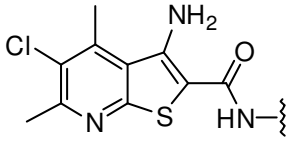	VU0448087 EC_{50} = 90.8 nM

Figure 38. Replacing the chlorodimethyl thienopyridine with hydroxydimethyl thienopyridine.

To conclude, there is a strong correlation between the position of the nitrogens on the benzene ring and potency. As nitrogen is moved from 2- to 3- to 4-position, potency increases. It is observed that the 4-postion is better tolerated. Also, it is observed that some analogs of the chlorodimethyl thienopyridine core are more potent than VU0152100. This chlorodimethyl thienopyridine core is essential for activity. Replacing it with bromocyclopropyl thienopyridine or hydroxydimethyl thienopyridine yields inactive compounds or compounds with low potencies.

Fold shift

We further characterize a selected set of compounds that have good efficacy and potency to establish their ability to shift the acetylcholine concentration response curve. There is also a

subtle trend accompanying the fold shift data (**Figure 39**). As we have observed before, potencies of analogs containing the pyridyl moiety is dependent on the position of the nitrogen. This can also be seen in the ACh CRC fold-shift ability. In the absence of nitrogen in the phenyl ring (VU0448087-1), the fold shift is 38. In the presence of a nitrogen (pyridyl moieties), fold shift increases dependent on the position of the nitrogen. The 4-methylpyridine analog (VU0448088-1) has a fold shift of 139, while its counterpart, 3-methylpyridine (VU0452129-1), has a much lower fold shift of 55. Fold shift increases dramatically as the nitrogen migrates from the 3- to 4-position.

As mentioned earlier, it is observed that potency of those analogs carrying pyridine congeners decreases with increasing spacer length. This decrease in potency also translates to fold shift. In comparison to VU0448088-4 (fold shift 139), which has a spacer that is one carbon long, the 4-ethylpyridine moiety (VU0456952-1), containing a homologated spacer, has a much smaller fold shift of 91. The potency additive theory mentioned earlier involving the addition of a second nitrogen to the 2-pyridine ring is observed with VU0456953-1 and VU0448088-4. VU0456953-1, which contains nitrogens in the 2- and 4-position, has a fold shift that is lower than VU0448088 (139 versus 62), which contains a nitrogen in the 4-position, because it also contains a nitrogen in the less potent position. Another important analog with a significant fold shift carries a cyclopropane ring (VU0449033-1). It has the largest ACh CRC fold shift of 380. Some analogs if this series appears to have better fold shifts in comparison to VU0152100 (fold shift 27). See Appendix for ACh CRC fold shift curves.

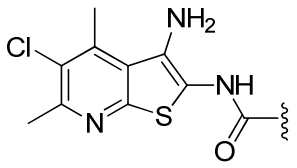	
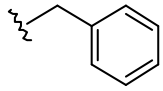	VU0448087-1 EC_{50} = 90.8 nM Fold shift = 38
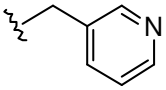	VU0452129-1 EC_{50} = 94.9 nM Fold shift = 55
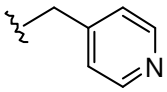	VU0448088-4 EC_{50} = 40 nM Fold shift = 139
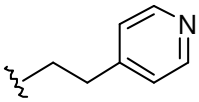	VU0456952-1 EC_{50} = 121 nM Fold shift = 62
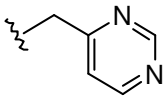	VU0456953-1 EC_{50} = 243 nM Fold shift = 62
	VU0449033-1 EC_{50} = 19.4 nM Fold shift = 380

Figure 39. Some subtle fold shift trends.

Selectivity

To further characterize compounds with good potency and fold shift, selectivity of these analogs for the M_4 muscarinic acetylcholine receptor is evaluated. This selectivity screen is performed in both human M_4/G_{qi5} and rat M_4/G_{qi5} cells. As mentioned earlier, to test for selectivity for the M_4 mAChR receptor, single point Ca^{2+} mobilization functional assay and concentration response curve of the test compound has to be generated in cells expressing the other subtypes (M_1, M_2, M_3, and M_5). These M_4 potentiators ideally fail to potentiate acetylcholine response across all other subtypes, except for M_4.[36] Here, only a few example data sets are shown. Data for the remaining compounds can be viewed in the Appendix. VU0449033 has the largest fold shift of 380 and an EC_{50} of 19.4 nM. In human cells, it is active at hM_4, hM_1, and hM_2 muscarinic receptors (**Figure 40**). It has efficacy and potency in all three receptors, but the highest effect is in M_4. Its potency in M_4 is 35.5 nM, while in M_1 and M_2 are 969 nM and 548 nM, respectively. VU0449033 is not completely selective for the human M_4 mAChR. Similarly in rat, it shows potentiation in rM_4, rM_1, and rM_2 (**Figure 41**).

Another analog submitted to selectivity screening is VU0448088, which is shown to be selective for both human and rat M_4/G_{qi5} (**Figure 42 and 43**). Its potency (EC_{50}) of 83.3 nM is reconfirmed in the human cell line. In rM_4, it is slightly less potent generating an EC_{50} of 173.3 nM. There's a 10-fold difference in potency between the human and rat cell line. All other analogs from the fold shift experiment above (VU0452129, VU0448099, VU0452055, VU0452127, VU0456952, VU0456953) are selective for the M_4 subtype (see Appendix).

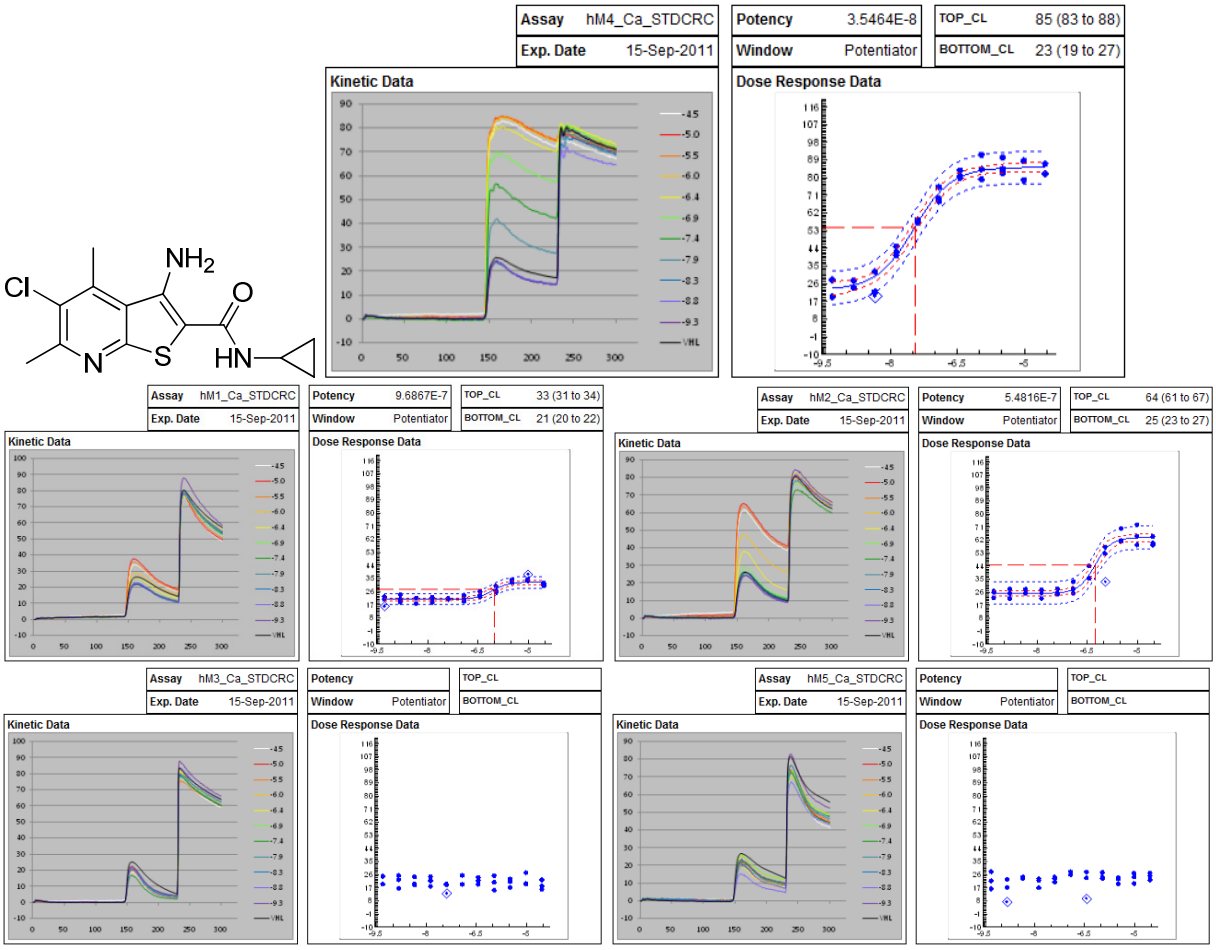

Figure 40. Human cell line selectivity data across all subtypes.

VU0449033

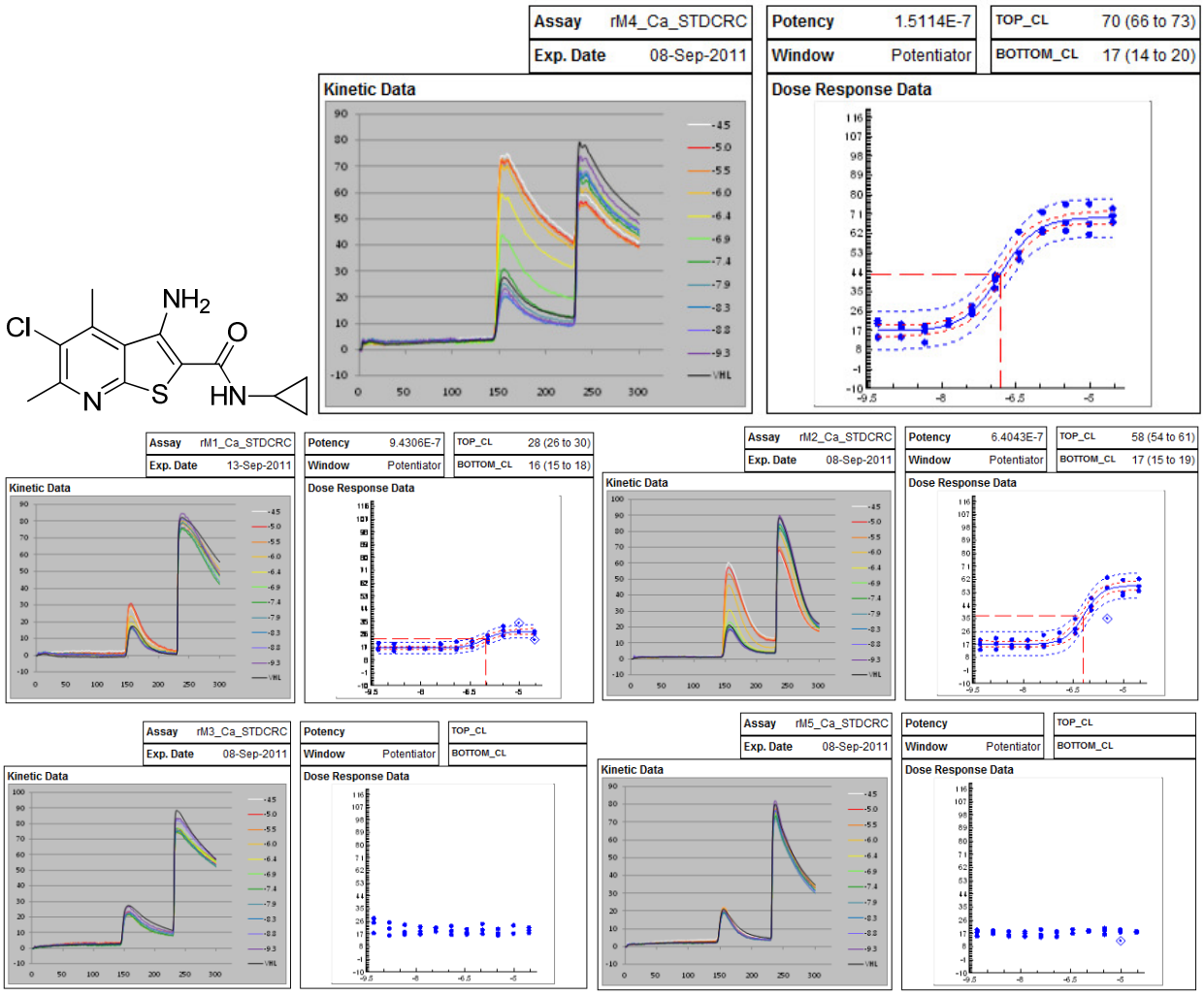

Figure 41. Rat cell line selectivity data across all subtypes.

VU0448088

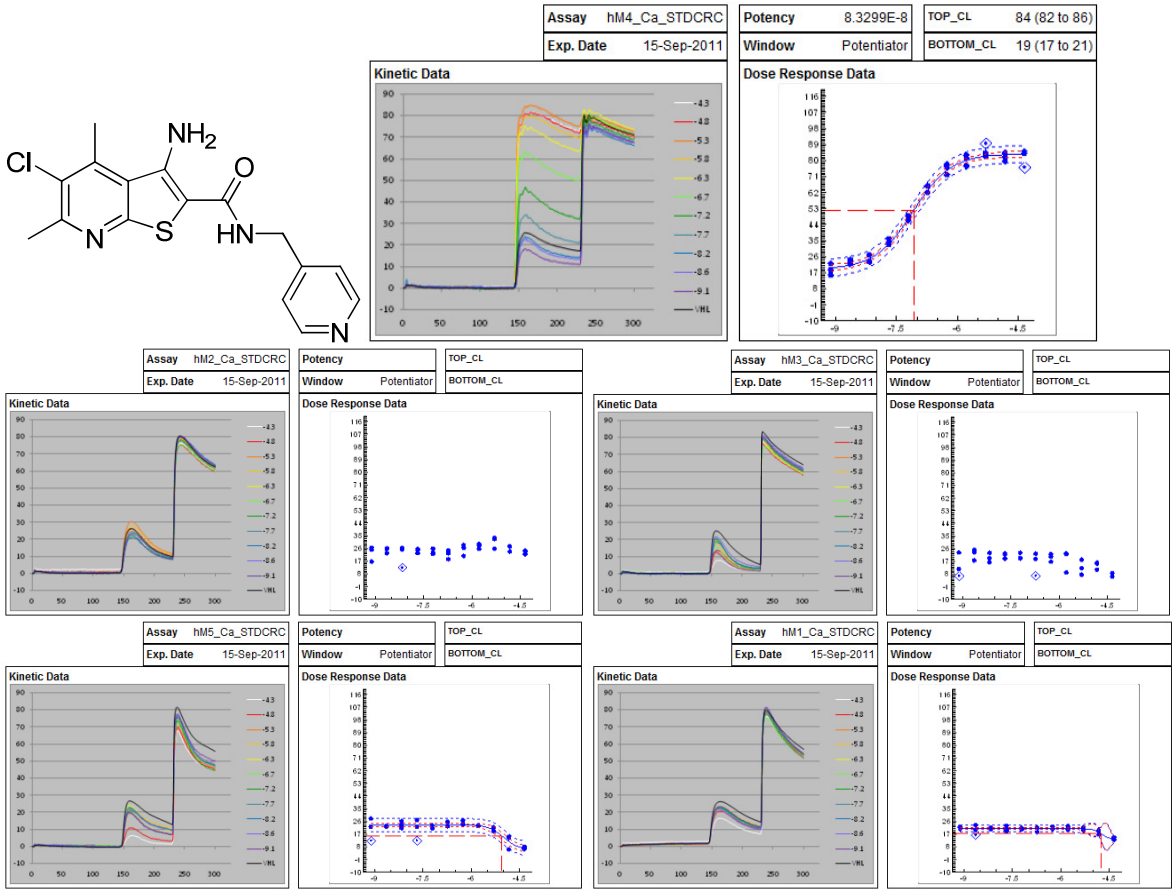

Figure 42. Human cell line selectivity data across all subtypes.

VU0448088

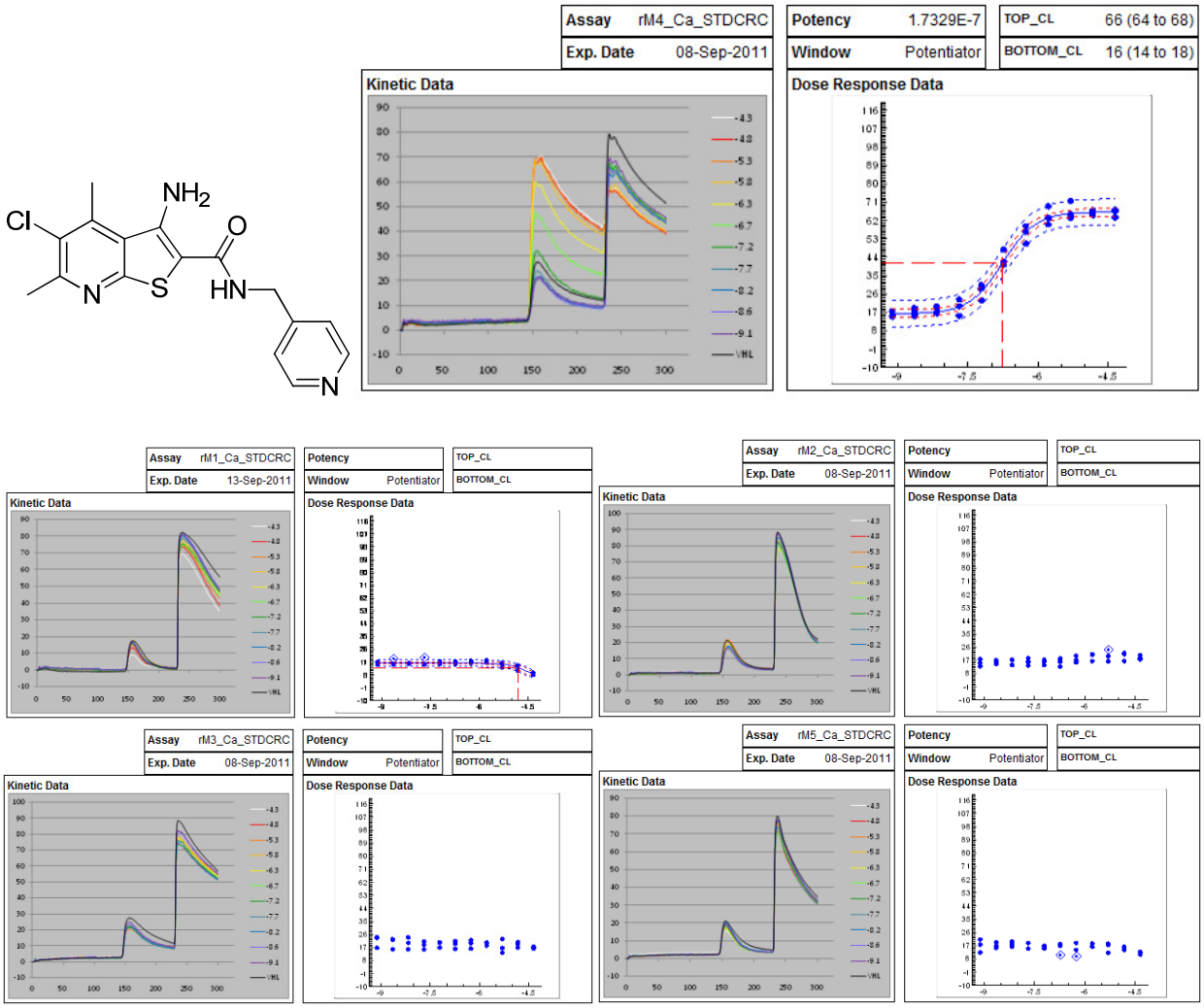

Figure 43. Rat cell line selectivity data across all subtypes.

*Pharmacokinetic (**Figure 44**)*

A few selected analogs are chosen for further pharmacokinetic evaluation. Some of the important properties to consider are solubility, clearance, fraction of free drug available for action, and metabolism. The ability of a compound to be absorbed is partially dependent on its ability to be solubilized for dosing, which is partially determined by its lipophillicity. High lipophillicity, or high cLogP, could is predictive of low solubility. Low solubility interferes with absorption into cells. cLogP values of greater than 5 is typically associated with low absorption[39]. We previously showed that VU10010 has low solubility, has a cLogP of 4.5, and has low brain penetration. VU0152099 and VU0152100 both have cLogP values lower than VU10010 (3.65 and 3.6, respectively).[37] They both are more soluble, and they both display better brain penetration. Some analogs of this chlorodimethyl thienopyridine series have better cLogP values. Since lower cLogP values could potentially contribute to better solubility, more homogenous dosing would be possible.

Another parameter to consider is clearance. Intrinsic clearance is the ability of the liver to remove or metabolize drugs. It measures the activity of drug metabolizing enzymes in the liver. High clearance indicates that the drug is being highly metabolized or cleared. The data below shows that VU0449033 carrying the cyclopropyl congener and VU0456925 have the lowest clearance[40, 41].

Next, we examine the protein plasma binding of these compounds. The extent to which a drug is bound to plasma protein is expressed as fraction unbound (fu). Fraction unbound is dependent on the binding affinity of the drug and the protein, the concentration of drug available, and the concentration of protein available[40]. The higher the fraction of drug is unbound to plasma

protein, the higher the concentration of drug is likely available for action. Both VU0449033 and VU0448088 display the highest fraction of unbound drug.

Cytochrome P450 is a family of enzymes responsible for most drug metabolism due to their ability to bind many substrates. Metabolism can range from the catabolism of the compound to deactivation of the compound therefore attenuating its biological activity and accelerating its clearance[42]. Compounds that have no activity at these enzymes have a better chance of getting to the target site. It appears that all the analogs tested display low micromolar inhibition of CYP450 1A2. VU0449033, and VU0456925 are inactive at all the other CYP45 subtypes with potency greater than 10 μM.

Figure 44. Pharmacokinetics data. Data table is adopted from Corey Hopkin

	VU0448088	VU0452129	VU0449033	VU0448057	VU0448087	VU0456925
	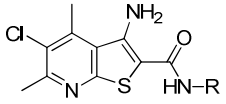	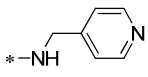	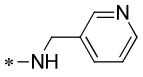	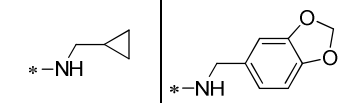	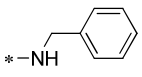	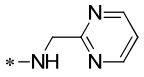
M4 EC_{50} (nM)	**34**	**95**	**31**	**48**	**73**	**1070**
MW	**346.83**	**346.83**	**295.79**	**389.86**	**345.85**	**347.82**
cLogP / **TPSA**	**2.19** / **80.9**	**2.19** / **80.9**	**2.25** / **68.0**	**3.20** / **86.5**	**3.44** / **68.0**	**1.23** / **93.8**
In Vitro Clearance (mL/min/kg)						
hCL_{INT}	**183.4**	**261**	**41.1**	**577**	**452**	**32.7**
rCL_{INT}	**261.0**	**275**	**188**	**397**	**626**	**Stable***
PPB (% fu)						
rPPB (% fu)	**1.7**	**3.4**	**6.4**	**0.1**	**0.2**	**4.4**
hPPB (% fu)	**2.6**	**0.9**	**1.1**	**0.1**	**0.2**	**2.5**
CYP450 (mM)						
1A2	**0.12**	**0.18**	**<0.1**	**1.30**	**0.17**	**1.2**
2C9	**<0.1**	**4.32**	**>10**	**6.42**	**2.08**	**>30**
2D6	**0.70**	**>30**	**>30**	**24.71**	**8.66**	**>30**
3A4	**2.75**	**3.46**	**>30**	**6.87**	**>30**	**>30**

Behavioral characterization

VU0448088 is selected for further characterization in an animal behavioral paradigm that is indicative of antipsychotic effects. Its ability to inhibit amphetamine induced hyperlocomotion is observed with dosing of the compound from 3mg/kg up to 100mg/kg. Amphetamine is a drug that mimics hyperlocomotion of the schizophrenic state. Compounds that have antipsychotic-like effects will be able to reverse amphetamine induced hyperlocomotion. At higher concentration, VU0448088 appears to exhibit some reversal of hyperlocomotion effects immediately after administration (**Figure 45**). It slightly inhibits the action of amphetamine on locomotion (decrease in mean breaks). However, the effect is short acting. After exerting some modest reversal in hyperlocomotion activity for 40 seconds, hyperlocomotion is reverted back to the same level as amphetamine. This short acting effect is seen at low concentrations of VU0448088 (3mg/kg, 10mg/kg, and 30mg/kg). At 100mg/kg, the reversal effect seems to last about 60 seconds. VU0448088 does not completely reverse amphetamine induced hyperlocomotion; its efficacy is slight and short acting.

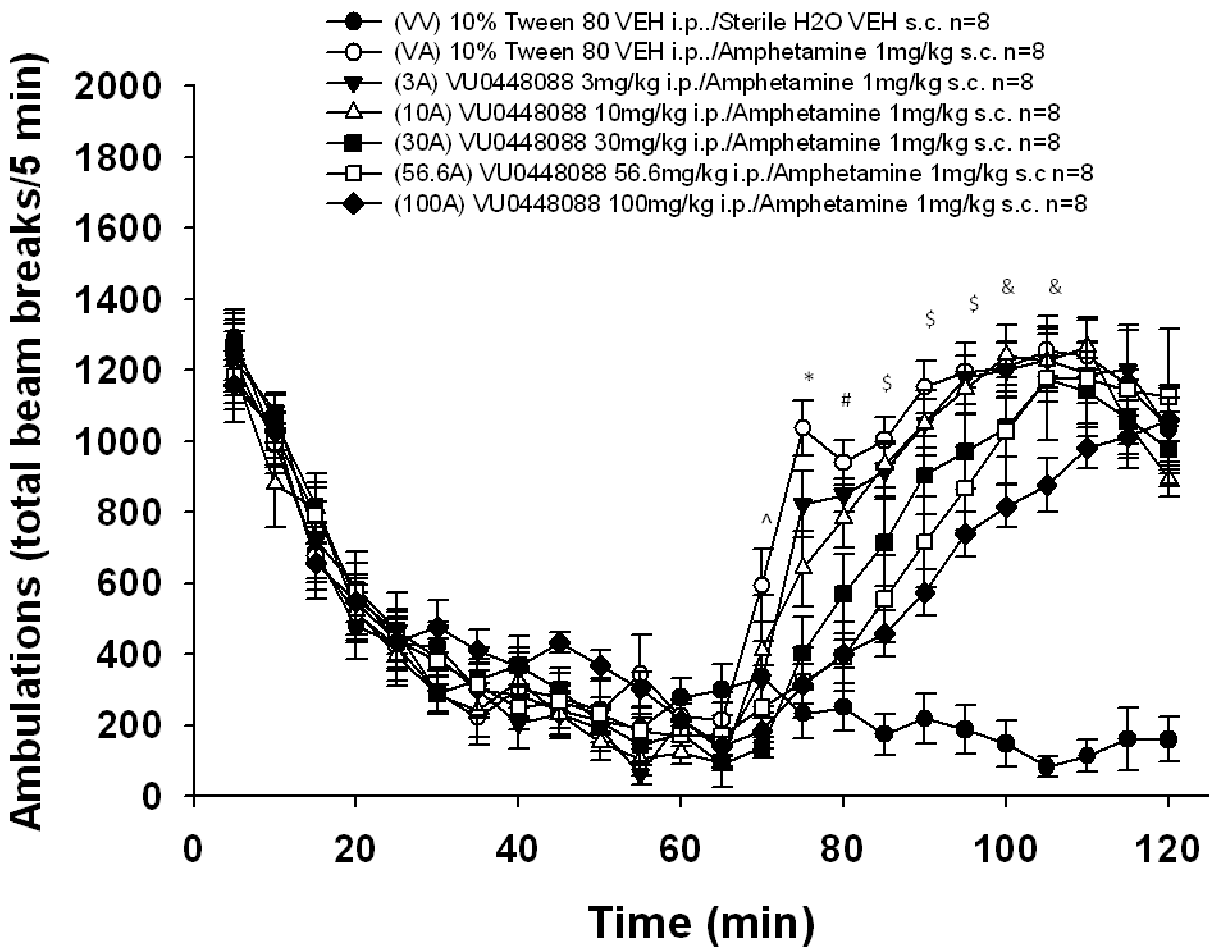

* - VV, 10A, 30A, 56.6A, 100A significant p <0.05 from VAMP, Dunnett's test
\# - VV, 30A, 56.6A, 100A significant p <0.05 from VAMP, Dunnett's test
^ - VV, 30A, 100A significant p <0.05 from VAMP, Dunnett's test
$ - VV, 56.6A,100A significant p <0.05 from VAMP, Dunnett's test
& - VV, 100A significant p <0.05 from VAMP, Dunnett's test

08/7/11 – 08/08/11
Lawson, N= 8

Vehicle: 10% Tween 80
30 minute pretreatment
amphetamine dosed at 60 minute interval
3mg/kg & 10mg/kg: clear, solution
30mg/kg, 56.6 mg/kg, 100mg/kg: white microsuspension

No overt behavioral disturbances observed

Figure 45. Amphetamine-induced hyperlocomotion data ov VU0448088.

Chapter III

SUMMARY

Schizophrenia is a complex neurological disorder that is represented by a large spectrum of symptoms. These symptoms can fall into 3 categories: positive, negative, and cognitive. Positive symptoms include hallucinations, delusions, disorganized thinking, and hearing of voices. Negative symptoms include social withdrawal, and cognitive symptoms include memory loss, lack of attention, and being unable to process information. Current antipsychotics provide symptomatic relief for psychoses; however, their effectiveness is variable and side effects are occassionally greater than their benefits.

The current atypical antipsychotics are successful at treating positive symptoms; however, they have little efficacy on negative and cognitive symptoms. Most atypical antipsychotics are GPCR antagonists which inhibit dopamine and serotonin receptors. However, due to their lack of selectivity numerous undesirable side effects are associated with these treatments. Therefore, this leads to the search for a new mode of pharmacology in an attempt to reduce side effects and better control symptoms.

Studies using muscarinic receptor knockout mice implicate M_1 and M_4 in the pathophysiology of schizophrenia. Muscarinic receptors are mechanistically linked to schizophrenia and cognitive deficits. Pharmacologically, non-selective muscarinic antagonists exacerbate, whereas agonists ameliorate, cognitive deficits and psychotic behaviors in animal models and patients suffering from Alzheimer's disease and schizophrenia.

Xanomeline, an M_1/ M_4 preferring partial agonist is efficacious in animal models predictive of antipsychotic behaviors. In clinical trials, it reduces psychotic behaviors and improves cognitive deficit in Alzheimer's patients. In a small schizophrenia trial, it improves positive, negative, and cognitive symptoms. Due to lack of subtype selectivity, xanomeline exhibits intolerable side effects rendering it an unsuccessful clinical candidate.

The current thought of the etiology of schizophrenia is one of an imbalanced dopaminergic system. M_4 muscarinic acetylcholine receptors are highly expressed in dopamine rich regions of the brain. In knockout mice studies, M_4 is implicated in the regulation dopaminergic neurons involved in movement and cognition. Therefore, M_4 mAChR emerges as the key regulator of dopaminergic hyperactivity. Selective M_4 activator may be a useful antipsychotic agent. However, no selective small molecule tools exist to provide pharmacological validation of the M_4 subtype being involved in pathways relating to schizophrenia. Attempts to develop selective M_4 compounds have been unsuccessful at the orthosteric binding site, site which the endogenous agonist, acetylcholine, binds. This is due to the high structural homology across the five muscarinic subtypes. Muscarinic receptors also display allosteric binding sites that have greater sequence divergence across the five subtypes and, hence, provide an alternative means of attaining selectivity.

The recent discovery of LY2033298 by Chan and coworkers spur further research into the field (**Figure 46**). LY2033298 is a positive allosteric modulator discovered to have high potency and selectivity at the M_4 muscarinic acetylcholine receptor. However, it is not an ideal tool compound because it has to be co-dosed with oxotremorine *in vivo* (5). Because oxotremorine is a non-selective agonist, data obtained from this co-dosing will be the results of the action of both

LY2033298 and oxotremorine. Therefore, no definitive conclusion can be made about the action of LY2033298 alone.

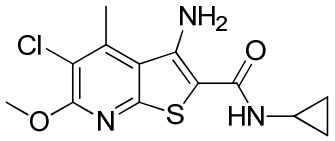

LY2033298

Figure 46. Structure of LY2033298.

Over the years our lab, in collaborations with Dr. Jeff Conn's lab, has developed several M_4 PAMs (VU10010, VU0152099, VU0152100) (**Figure 47**) that display good pharmacological properties such as efficacy, potency, and selectivity. VU10010 was discovered through optimizations of several hit compounds from a screen of compounds purchased from ChemBridge. Though VU10010 exhibits good efficacy, potency, and selectivity, it has solubility issues and low brain penetration. Its optimization leads to VU0152099 and VU0152100, which also display good efficacy, potency, and selectivity. In addition to those properties, they also exhibit higher brain penetration. However, because they are rapidly metabolized leaving only less than 10% of the parent compound remaining in rat and human liver microsomes, they became less attractive tool compounds. Therefore, optimization of VU0152100 is necessary to improve its pharmacological and pharmacokinetic properties. Among the initial hits, **1** was also found to have micromolar potency as an M_4 PAM (**Figure 48**). We further explored this hit in conjunction with optimization of VU0152100.

VU10010 VU152099 VU0152100

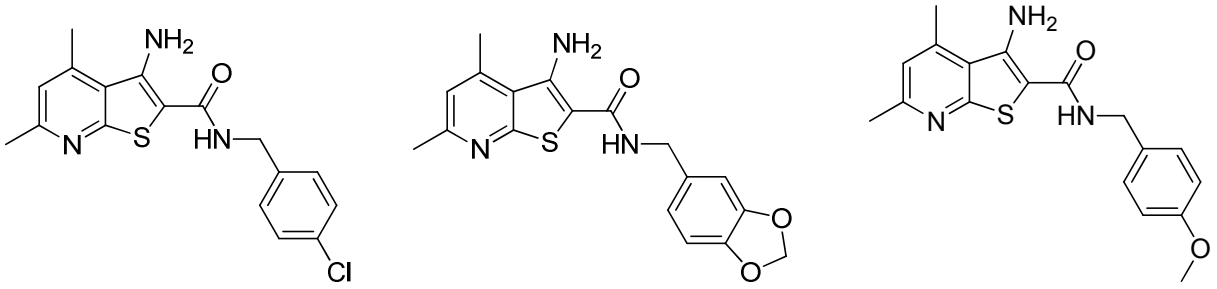

EC_{50}: 400 nM EC_{50}: 403 nM EC_{50}: 380 nM

Figure 47. M_4 PAMs developed at Vanderbilt.

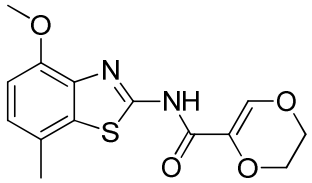

1

Figure 48. Hit from initial PAM screen.

Optimization of **1** occurs with derivation of the amide portion and the central core. Diversity-oriented synthesis is utilized to generate a library of compounds carrying the same central core as **1** and diversified amides. Of the analogs tested, short aliphatic chains are more tolerable than long chains and branched chains. Small cyclized aliphatic groups have better potencies compared to larger ones, especially cyclopropane (VU0409095). Nitrogen containing rings are very well tolerated (VU0409523 and VU0409524). Their potencies are comparable to that of **1** (EC_{50} 1.7 μM). Substitution of other aromatic amides results in no activity. Replacement of the methoxymethyl benzothiazole central core with a truncated core (benzothiazole) and thiazolopyridine core generates analogs with no activity. When

methoxymethyl benzothiazole is replaced with hydroxymethyl benzothiazole, micromolar potency is retained in a few analogs.

Of those analogs generated for the optimization of **1**, a few displayed comparable potencies (**Figure 49**).

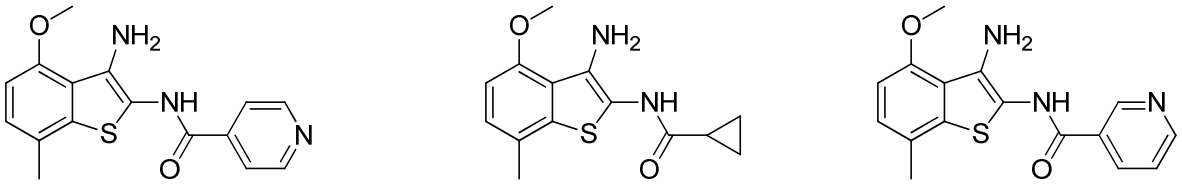

VU0409524-2 EC_{50}: 1.12 μM

VU0409095-1 EC_{50}: 4.6 μM

VU0409523-1 EC_{50}: 2.48 μM

Figure 49. Some of the best analogs of 1 with comparable potencies.

The VU0152100 optimization effort includes replacement of the central core with bromocyclopropyl thienopyridine and chlorodimethyl thienopyridine. All analogs carrying the bromocyclopropyl thienopyridine core are inactive, with the exception of cyclopropyl amide. As for analogs generated using chlorodimethyl thienopyridine, most display micromolar to nanomolar potency. Notable ones are listed below. In comparison to VU0152099 and VU0152100, some chlorodimethyl thienopyridine analogs display better potencies (**Figure 50**). One clear trend exhibits among the functionalized nitrogen rings. As nitrogen is moved from 2- to 3- to 4-position on pyridines, potency increases.

	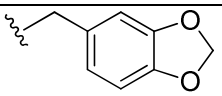	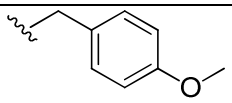
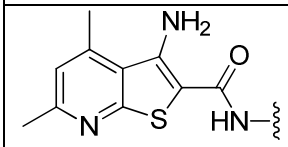	VU0152099 EC_{50}: 403 Fold shift: 26	VU0152100 EC_{50}: 380
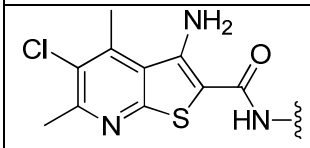	VU0448057 EC_{50}: 56.9 Fold shift: 7.6	VU0448098 EC_{50}: 117

Figure 50. Analogs of VU0152099 and VU0152100.

Other notable compounds are listed below with their potency, fold shift and selectivity.

Structure	**VU Number**	**EC_{max}**	**EC_{50} (nM)**	**Fold shift**	**Selective for M_4**
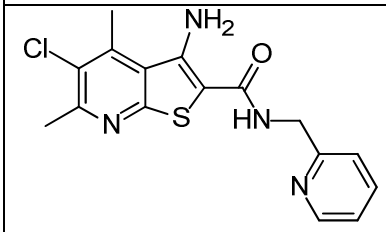	VU0452032-1	----	293	----	----
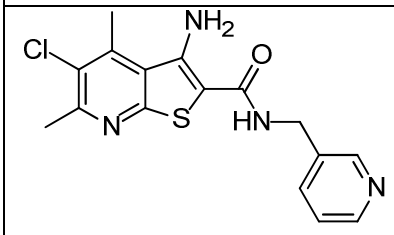	VU0452129-1	----	94.9	55	Yes

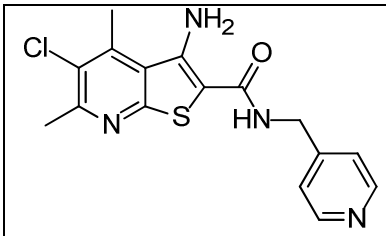	VU0448088-1	93	40.0	139	Yes
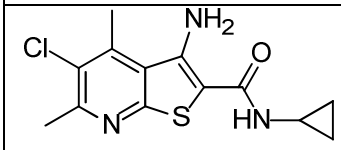	VU0449033-1	----	19.4	380	M_4, M_1, M_2

Figure 51. Other notable compounds with better potencies compared to VU0152100.

In comparison to VU0152099 and VU0152100, the analogs generated using the chlorodimethyl thienopyridine core are more potent and have better fold shifts. A couple of examples are VU0449033 and VU0448088, which have potencies that are more than 10 fold better than VU0152100 (**Figure 51**). They are both able to shift the ACh concentration response curve leftward more than 10 fold compared to VU0152100. Their lipophilicity values (clogP) are less than those of VU0152099 and VU0152100, which could contribute to their greater solubility. Further structure activity relationship studies are needed to fully characterize these analogs to confirm that they have better pharmacological and pharmacokinetic profiles.

Additional chemical modifications can be made to fully flush out the SAR to help better understand the functional groups tolerated and their binding modes. Modifications can range from reversing the amide linker to derivatizing the substituents of the central core to increase its functionality, alkylating the primary amine flanking the core, and tying the amine to the core forming three fused heterocyclic rings. These modifications are not only necessary for probing the binding pocket, but it is also necessary for optimizing pharmacological properties. Other

characterizations such as competitive radioligand binding and G-protein binding affinity have to be assessed to further prove the allosteric properties of these analogs. Good M_4 tool compounds with ideal pharmacological and pharmacokinetic profile are needed to further elicit the role of M4 in schizophrenia.

Chapter IV

MATERIALS and METHODS

Medicinal Chemistry

M_4 PAM Synthesis

Amide coupling general procedure. To a solution of carboxylic acid and amine in solvent, base and catalysts were added. The solution was stirred at room temperature overnight. Then the reaction was concentrated on a heating block. Each compound was purified via liquid chromatography/mass spectrometry purification system (Gilson) or flash chromatography system (ISCO Combiflash Rf). Purity is verified via liquid chromatography/mass spectrometry system (LCMS) and nuclear magnetic resonance (NMR).

Synthesis of thieno pyridine carboxylic acid core. To a solution of commercially available 2,5-dichloro-2,6-dimethyl nicotinonitrile in ethanol (1M) in a microwave vial, methyl thioglycolate, and 5M LiOH or NaOH were added. The reaction was heated to 125°C for 20 minutes. The cyclized product was confirmed via LCMS. The lithium salt carboxylate product was protonated with 1M hydrochloric acid (HCL) solution. HCl was added until the pH of the reaction reaches 1.

Pharmacology: *All of the below in vitro procedures are adopted from Alice Rodriguez from Dr. Jeff Conn's lab. The behavioral assay protocol is adopted from Analisa Thompson from Carrie Jones's lab.*

M_4 *in vitro* Functional Assay. The human M_4 cDNA in pcDNA3.1 (+) was purchased from www.cDNA.org. CHO cells purchased from the ATCC (www.atcc.org), were stably transfected with hM_4 cDNA along with the chimeric G protein G_{qi5} (Conklin et al., 1993) in pIREShygro (Invitrogen, Carlsbad, CA). Single hygromycin- and neomycin-resistant clones were isolated and screened for M_4-mediated calcium mobilization. CHO cells expressing human M_4 receptor were plated (Greiner Bio-One, Monroe, North Carolina) at 15,000 cells/20µL well in assay media (20mM HEPES, 10% FBS, Ham's F-12). The plates were incubated overnight at 37°C in 5% CO_2. Media was removed and assay buffer (10mL of 1M HEPES, HBSS, 2.5 mM Probenecid) containing 8uL of Fluo4-AM dye (Invitrogen), and 8uL of pluronic acid was added. Cells were incubated for 45 minutes at 37°C in 5% CO_2 to allow for dye loading. Dye was removed, and 45uL of assay buffer was added to each well. The plate is allowed to incubate in the dark at room temperature for 10-15 minutes. After incubation, the cell plates were loaded into Flexstation II (Molecular Device Corp). Test compound in assay buffer was added at 19 seconds. Then at 109 seconds, a submaximal concentration of acetylcholine was added. Negative control was compound vehicle (0.2% DMSO) plus assay buffer; positive control was ACh CRC and positive control compounds that previously yielded maximal acetylcholine response. Fold shifts were determined using the same functional assay by varying the amount of acetylcholine in the presence of either a concentration of compound (10 µM) or vehicle. A concentration response curve was generated using acetylcholine concentrations ranging from 10pM to 100 µM. Assays were performed in triplicate on different days. Concentration response curves were generated using GraphPad Prism 4.0.

Fold Shift Protocol

Cell line creation and culture of the human M_4/G_{qi5}/CHO line. The human M_4 (hM_4) cDNA in pcDNA3.1 (+) was purchased from www.cDNA.org. CHO cells purchased from the ATCC (www.atcc.org), were stably transfected with hM_4 cDNA along with the chimeric G protein G_{qi5} (Conklin et al., 1993) in pIREShygro (Invitrogen, Carlsbad, CA) and single hygromycin- and neomycin-resistant clones were isolated and screened for M_4-mediated calcium mobilization using the method described below. hM_4/CHO-G_{qi5} cells were cultured in Ham's F-12; 10% FBS, 20mM HEPES, 50µg/mL G418 (Mediatech, Inc., Herndon, VA), 500 µg/ml Hygromycin. All cell culture reagents were purchased from Invitrogen Corp. (Carlsbad, CA) unless otherwise noted.

Fold-Shift Assay. Assays were performed within the Vanderbilt Center for Neuroscience Drug Discovery's Screening Center. Human M_4/G_{qi5}/CHO cells (15,000 cells/20 µL/well) were plated in black-walled, clear-bottomed, TC treated, 384 well plates (Greiner Bio-One, Monroe, North Carolina) in Ham's F-12, 10% FBS, 20 mM HEPES. The cells were grown overnight at 37 °C in the presence of 5% CO_2. The next day, the medium was removed and replaced with 20 µL of 2.3 µM Fluo-4, AM (Invitrogen, Carlsbad, CA) prepared as a 2.3 mM stock in DMSO and mixed in a 1:1 ratio with 10% (w/v) pluronic acid F-127 and diluted in Assay Buffer (Hank's balanced salt solution, 20 mM HEPES and 2.5 mM Probenecid (Sigma-Aldrich, St. Louis, MO)) for 45 minutes at 37 °C. Dye was removed and replaced with 20 µL of Assay Buffer. Test compounds were prepared in Assay Buffer to generate a 2x stock in 0.6% DMSO (0.3% final). Acetylcholine concentration responses were prepared at a 5X stock solution in assay buffer prior to addition to assay plates. Ca^{2+} mobilization was measured at 37 degrees C using a Functional Drug Screening System 6000 (FDSS6000, Hamamatsu, Japan) kinetic plate reader according to the following protocol. Cells were preincubated with test compound (or vehicle) for 144 seconds

prior to the addition of a concentration response of the agonist ACh and the fluorescence was monitored for a total of 5 min. The signal amplitude was first normalized to baseline and then as a percentage of the maximal response to acetylcholine. EC_{50} values for ACh in the presence of vehicle or compound were determined using GraphPad Prism (4.0c), which fits curves using standard non-linear regression (variable slope). Fold-Shift values were calculated by dividing the ACh EC_{50} in the presence of 10 μM compound by the ACh EC_{50} in the presence of vehicle. Compounds showing greater than a 3-fold shift were assigned 'Outcome' = 'Active', 'Fold-Shift' ='Value', and '% ACh max' = Value'.

***In vivo* Pharmacology**

All experiments were conducted in accordance with the National Institutes of
Health regulations of animal care covered in Principles of Laboratory Animal Care

Drugs

d-Amphetamine hemisulfate (AMPH) was obtained from Sigma (Cat#A5880-1G; St. Louis, MO). Salt-correction was used to determine the correct amount of the *d*-amphetamine hemisulfate form in mg to add to sterile water in order to yield a 1 mg/ml solution; injected with a volume equal to the body weight of each animal. VU0448088 was formulated in volumes specific to the number of animals dosed each day. The appropriate amount according to the dosage was mixed into a 10% Tween 80 in sterile water solution. Each mixture was vortexed with for 2-3 min and then sonicated in a 40˚C sonication bath for 45 min until in a solution or a very fine microsuspension. Next, the pH of all solutions was checked using 0-14 EMD pH strips and adjusted to a pH of 6-7 if necessary with 1N NaOH.

Animals

Animals were housed in the animal care facility certified by the American Association for the Accreditation of Laboratory Animal Care (AAALAC) under a 12-hour light/dark cycle (lights on: 7 a.m.; lights off: 7 p.m.) and had free access to food and water. The animals used in this experiment were food-deprived the evening before experimentation for oral administration of test compound. For enrichment purposes, animals were housed 2-3 per cage. The experimental protocols performed during the light cycle were approved by the Institutional Animals Care and Use Committee of Vanderbilt University and conformed to the guidelines established by the National Research Council Guide for the Care and Use of Laboratory Animals.

Amphetamine-induced Hyperlocomotion

Male Harlan Sprague Dawley rats (Harlan Laboratories, Indianapolis, IN) were habituated in the locomotor activity test chambers for 30 min. Animals were next pretreated for an additional 30 min with either vehicle or a dose VU0448088, i.p. followed by a subcutaneous injection of 1 mg/kg amphetamine or vehicle and monitored for an additional 60 min. Changes in locomotor activity were recorded for a total of 120 min. Data were expressed as changes in ambulation defined as the total number of photobeam breaks per 5 min interval.

Behavioral Data Analysis

Behavioral data were analyzed using a one-way ANOVA with main effects of treatment and time. *Post hoc* analyses were performed using a Dunnett's *t*-test with all treatment groups compared to the Vehicle+AMPH group using JMP ® 9.0 (SAS Institute, Cary, NC) statistical

software. Data were graphed using SigmaPlot for Windows Version 11.0 (Saugua, MA). A probability of $p \leq 0.05$ was taken as the level of statistical significance.

APPENDIX

Fold Shift Curves

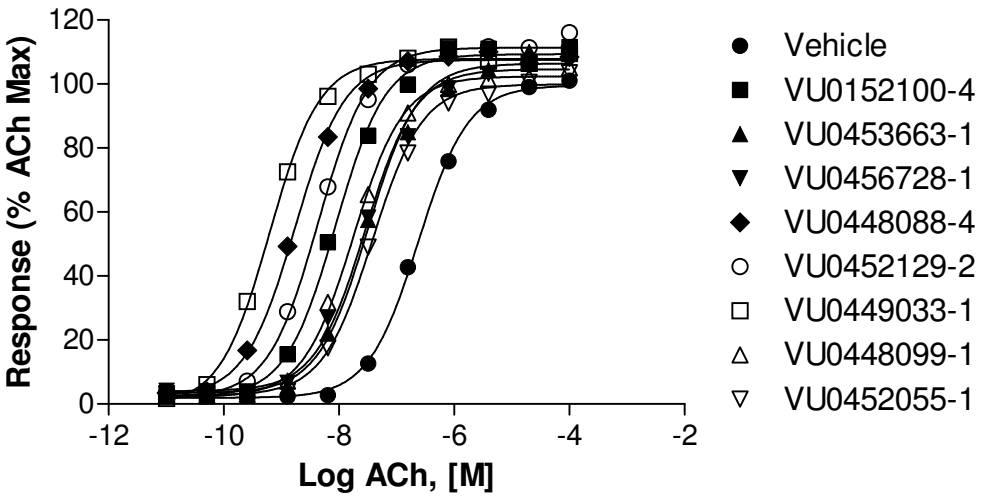

	EC_{50}	
VU Number	**ı**	**Fold shift**
Vehicle	2.39E-07	1
VU0152100-4	8.72E-09	27
VU0453663-1	3.21E-08	7
VU0456728-1	2.86E-08	8
VU0448088-4	1.72E-09	139
VU0452129-2	4.37E-09	55
VU0449033-1	6.3E-10	380
VU0448099-1	1.78E-08	13
VU0452055-1	3.83E-08	6

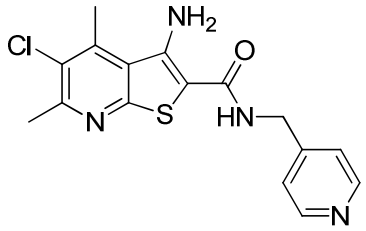

VU0448088

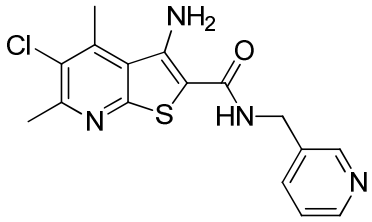

VU0452129

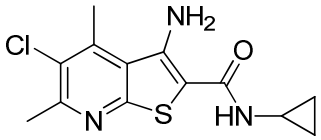

VU0449033

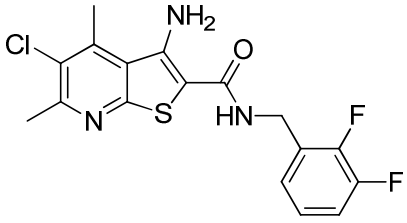

VU0448099

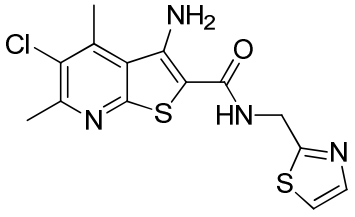

VU0452055

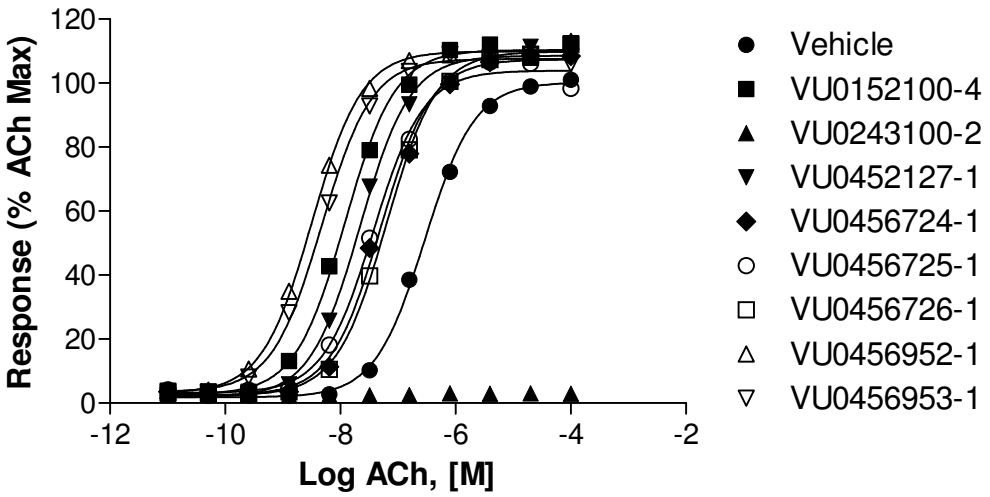

VU Number	EC_{50}	Fold shift
Vehicle	2.92E-07	1
VU0152100-4	1.21E-08	24
VU0243100-2		full block
VU0452127-1	2.19E-08	13
VU0456724-1	5.04E-08	6
VU0456725-1	3.71E-08	8
VU0456726-1	6.36E-08	5
VU0456952-1	3.21E-09	91
VU0456953-1	4.75E-09	62

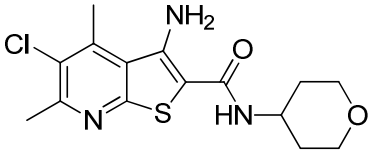

VU0452127

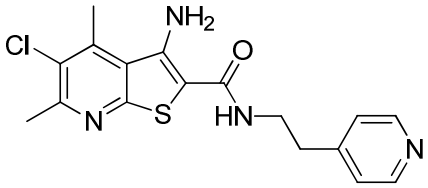

VU0456952

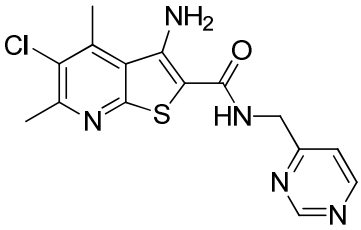

VU0456953

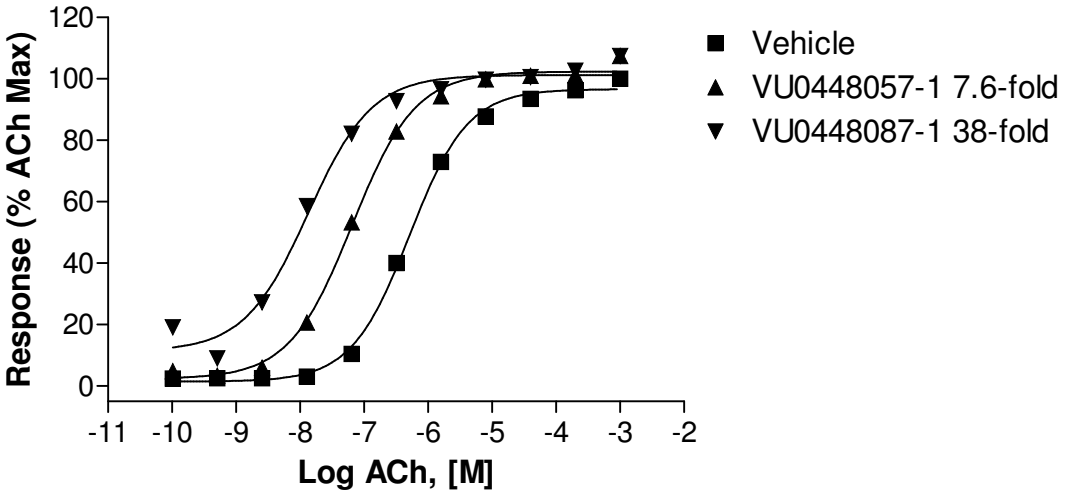

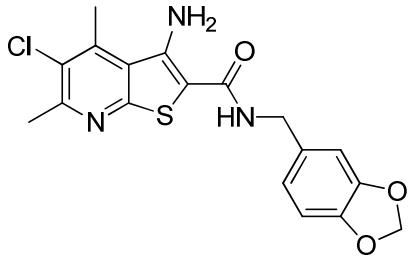

VU0448057

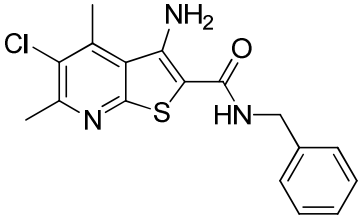

VU0448087

Human Selectivity

VU0448099

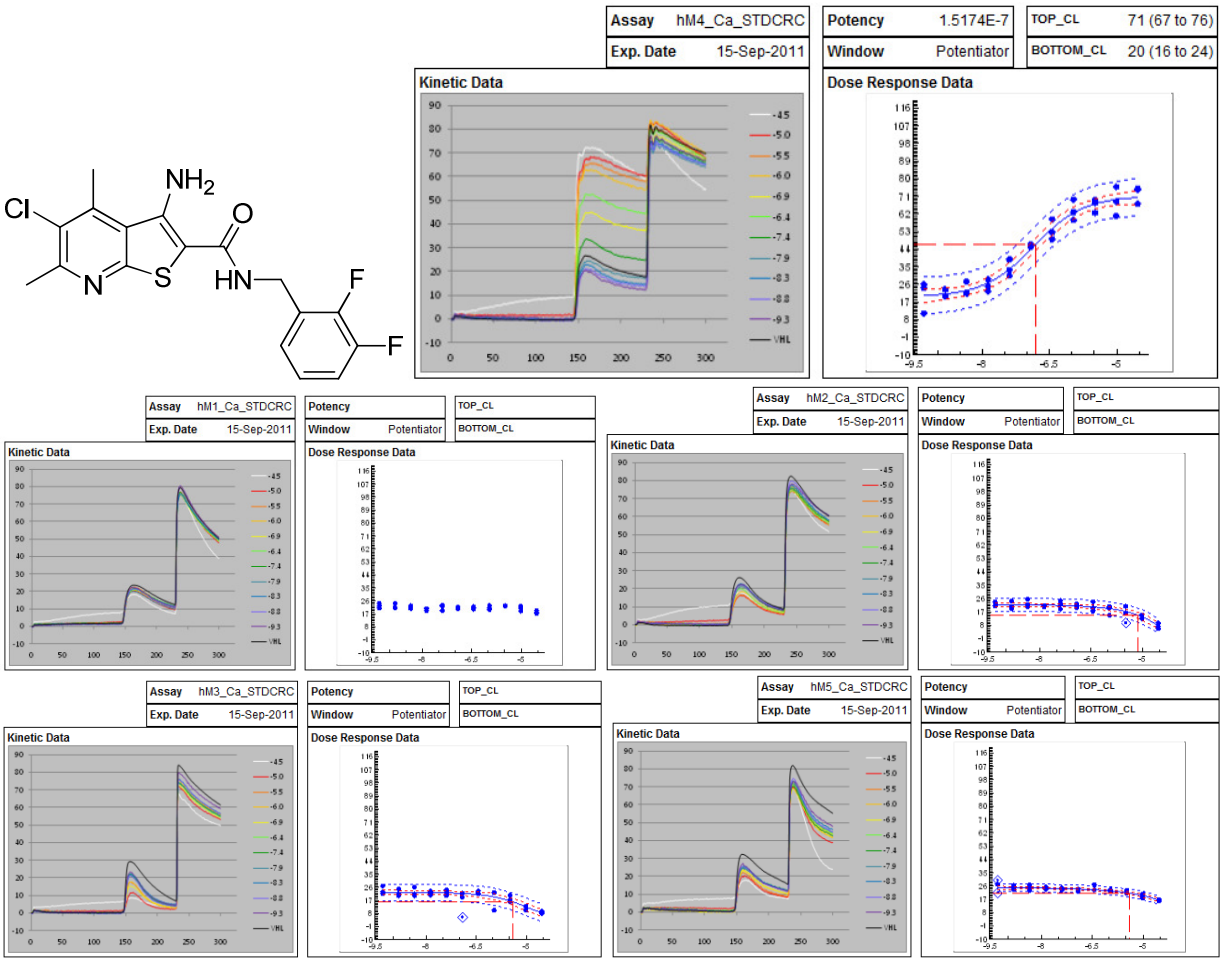

VU0452055

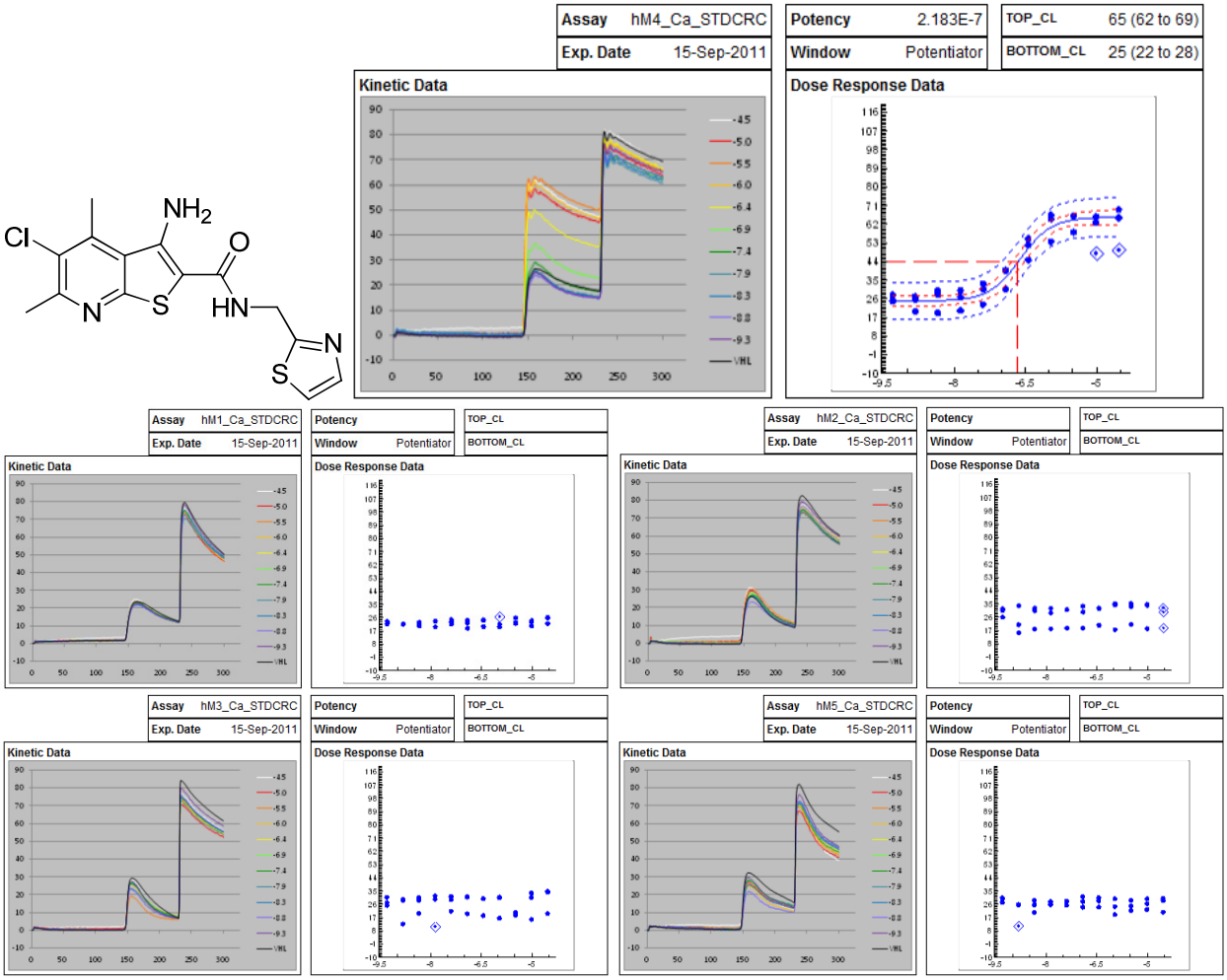
Assay hM4_Ca_STDCRC
Exp. Date 15-Sep-2011
Potency 2.183E-7
Window Potentiator
TOP_CL 65 (62 to 69)
BOTTOM_CL 25 (22 to 28)
Kinetic Data
Dose Response Data
Cl
NH2
O
N
S
HN
N
S
Assay hM1_Ca_STDCRC
Exp. Date 15-Sep-2011
Potency
Window Potentiator
TOP_CL
BOTTOM_CL
Kinetic Data
Dose Response Data
Assay hM2_Ca_STDCRC
Exp. Date 15-Sep-2011
Potency
Window Potentiator
TOP_CL
BOTTOM_CL
Kinetic Data
Dose Response Data
Assay hM3_Ca_STDCRC
Exp. Date 15-Sep-2011
Potency
Window Potentiator
TOP_CL
BOTTOM_CL
Kinetic Data
Dose Response Data
Assay hM5_Ca_STDCRC
Exp. Date 15-Sep-2011
Potency
Window Potentiator
TOP_CL
BOTTOM_CL
Kinetic Data
Dose Response Data

VU0452129

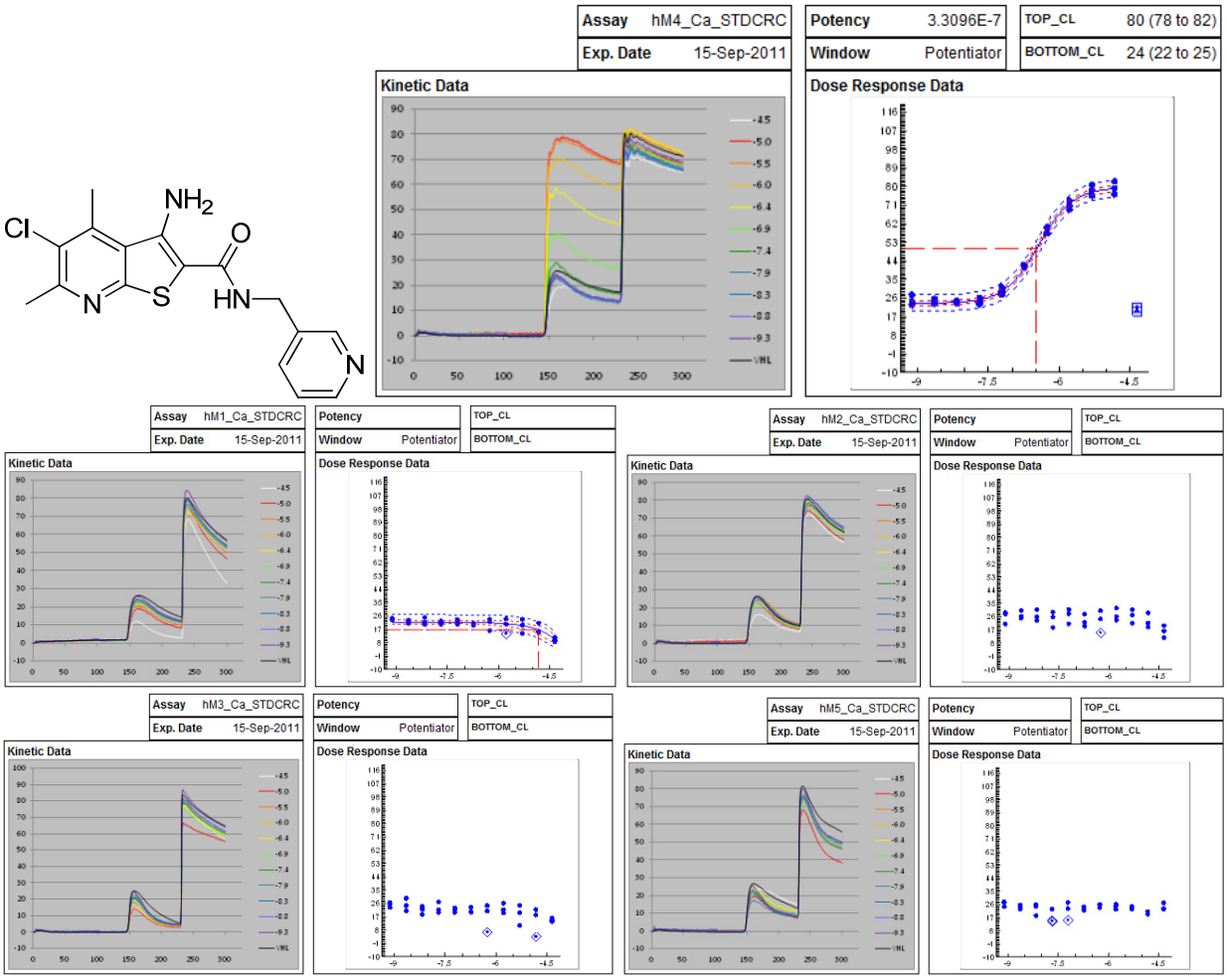
Assay hM4_Ca_STDCRC
Exp. Date 15-Sep-2011
Potency 3.3096E-7
Window Potentiator
TOP_CL 80 (78 to 82)
BOTTOM_CL 24 (22 to 25)
Kinetic Data
Dose Response Data
Cl
NH2
O
HN
N
S
N
Assay hM1_Ca_STDCRC
Exp. Date 15-Sep-2011
Potency
Window Potentiator
TOP_CL
BOTTOM_CL
Kinetic Data
Dose Response Data
Assay hM2_Ca_STDCRC
Exp. Date 15-Sep-2011
Potency
Window Potentiator
TOP_CL
BOTTOM_CL
Kinetic Data
Dose Response Data
Assay hM3_Ca_STDCRC
Exp. Date 15-Sep-2011
Potency
Window Potentiator
TOP_CL
BOTTOM_CL
Kinetic Data
Dose Response Data
Assay hM5_Ca_STDCRC
Exp. Date 15-Sep-2011
Potency
Window Potentiator
TOP_CL
BOTTOM_CL
Kinetic Data
Dose Response Data

VU0456952

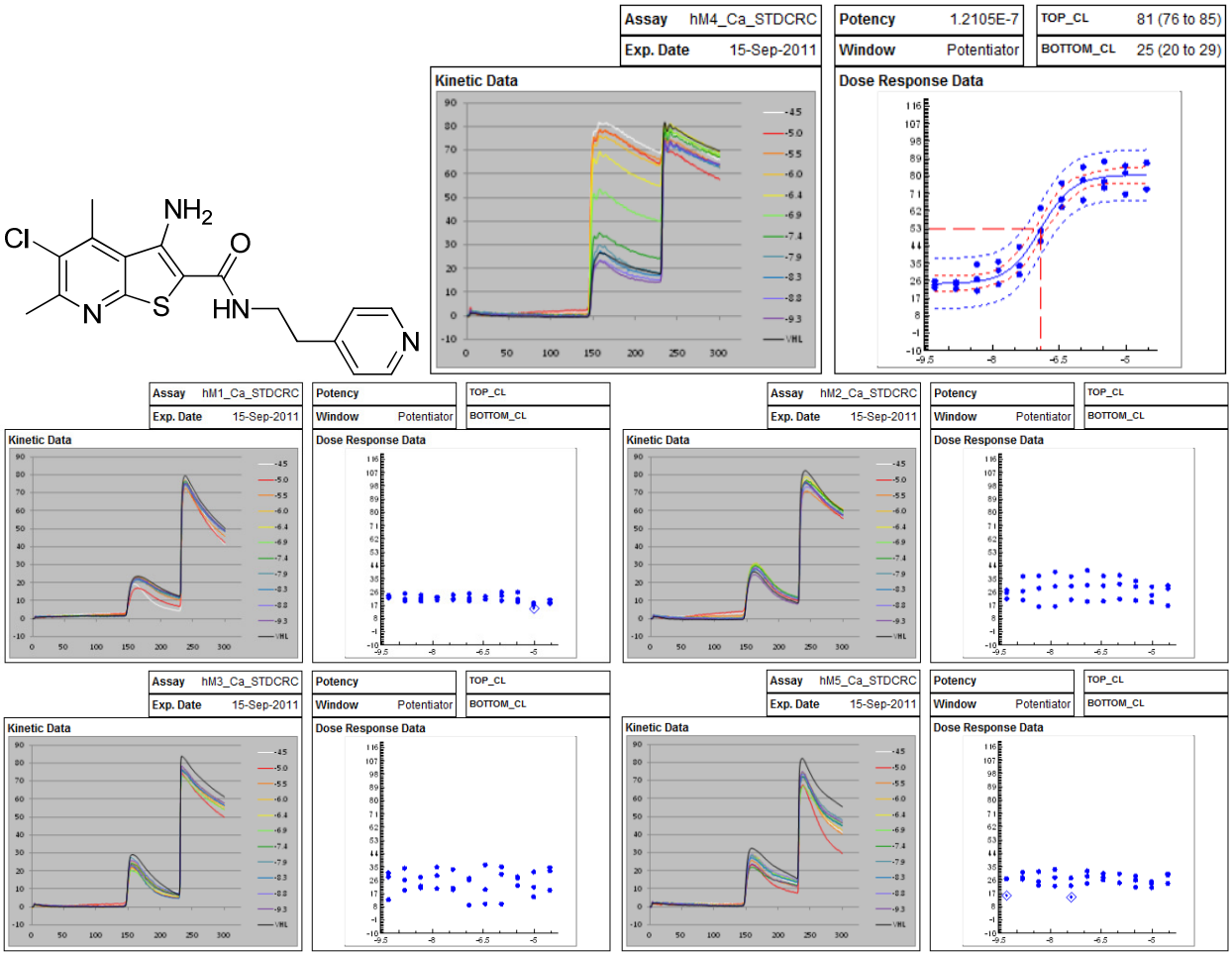
Assay hM4_Ca_STDCRC
Exp. Date 15-Sep-2011
Potency 1.2105E-7
Window Potentiator
TOP_CL 81 (76 to 85)
BOTTOM_CL 25 (20 to 29)
Kinetic Data
Dose Response Data
Cl
NH2
O
N
S
HN
N
Assay hM1_Ca_STDCRC
Exp. Date 15-Sep-2011
Potency
Window Potentiator
TOP_CL
BOTTOM_CL
Kinetic Data
Dose Response Data
Assay hM2_Ca_STDCRC
Exp. Date 15-Sep-2011
Potency
Window Potentiator
TOP_CL
BOTTOM_CL
Kinetic Data
Dose Response Data
Assay hM3_Ca_STDCRC
Exp. Date 15-Sep-2011
Potency
Window Potentiator
TOP_CL
BOTTOM_CL
Kinetic Data
Dose Response Data
Assay hM5_Ca_STDCRC
Exp. Date 15-Sep-2011
Potency
Window Potentiator
TOP_CL
BOTTOM_CL
Kinetic Data
Dose Response Data

VU0456953

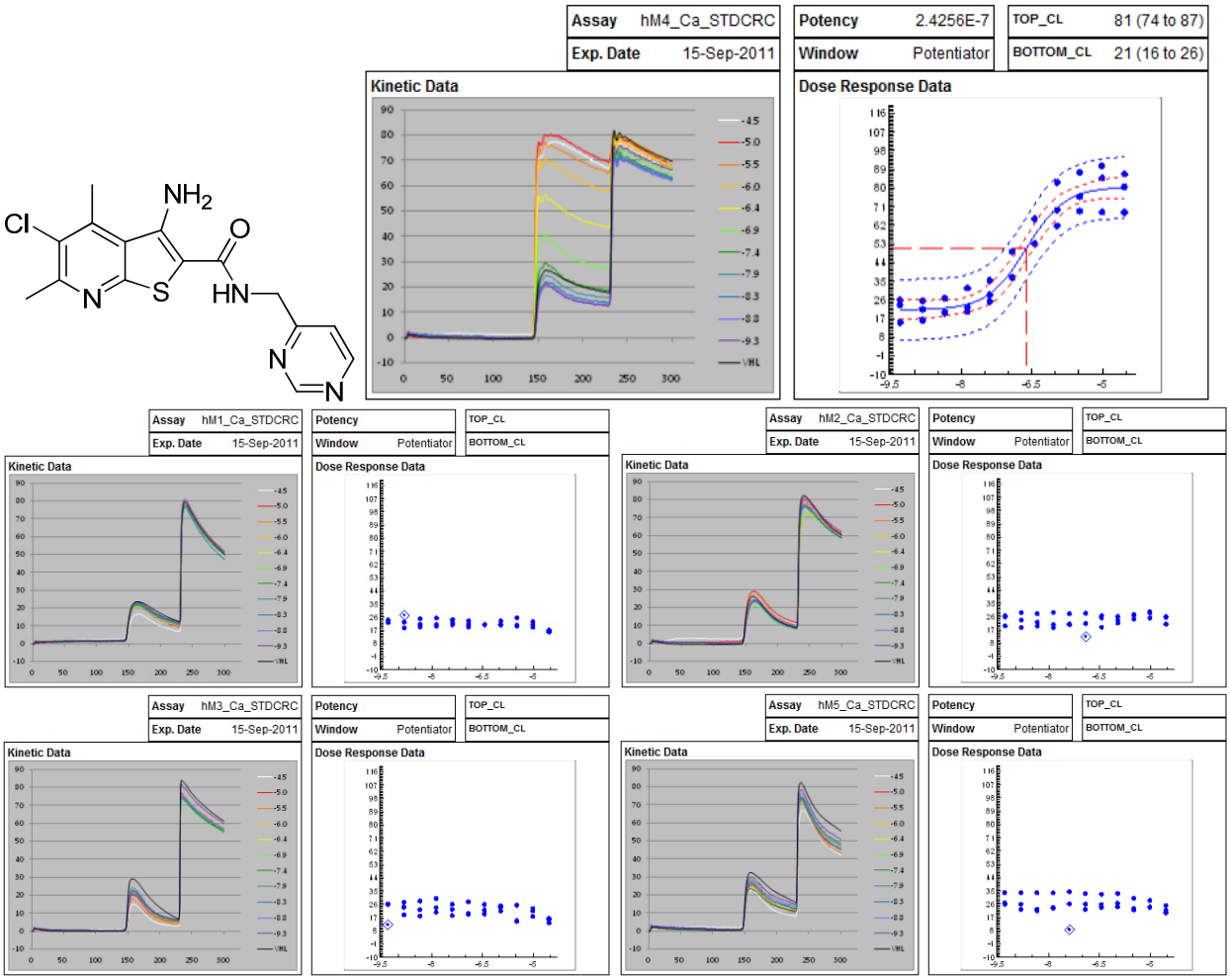
Assay hM4_Ca_STDCRC
Exp. Date 15-Sep-2011
Potency 2.4256E-7
Window Potentiator
TOP_CL 81 (74 to 87)
BOTTOM_CL 21 (16 to 26)
Kinetic Data
Dose Response Data
Assay hM1_Ca_STDCRC
Exp. Date 15-Sep-2011
Potency
Window Potentiator
TOP_CL
BOTTOM_CL
Kinetic Data
Dose Response Data
Assay hM2_Ca_STDCRC
Exp. Date 15-Sep-2011
Potency
Window Potentiator
TOP_CL
BOTTOM_CL
Kinetic Data
Dose Response Data
Assay hM3_Ca_STDCRC
Exp. Date 15-Sep-2011
Potency
Window Potentiator
TOP_CL
BOTTOM_CL
Kinetic Data
Dose Response Data
Assay hM5_Ca_STDCRC
Exp. Date 15-Sep-2011
Potency
Window Potentiator
TOP_CL
BOTTOM_CL
Kinetic Data
Dose Response Data

Rat selectivity

VU0448099

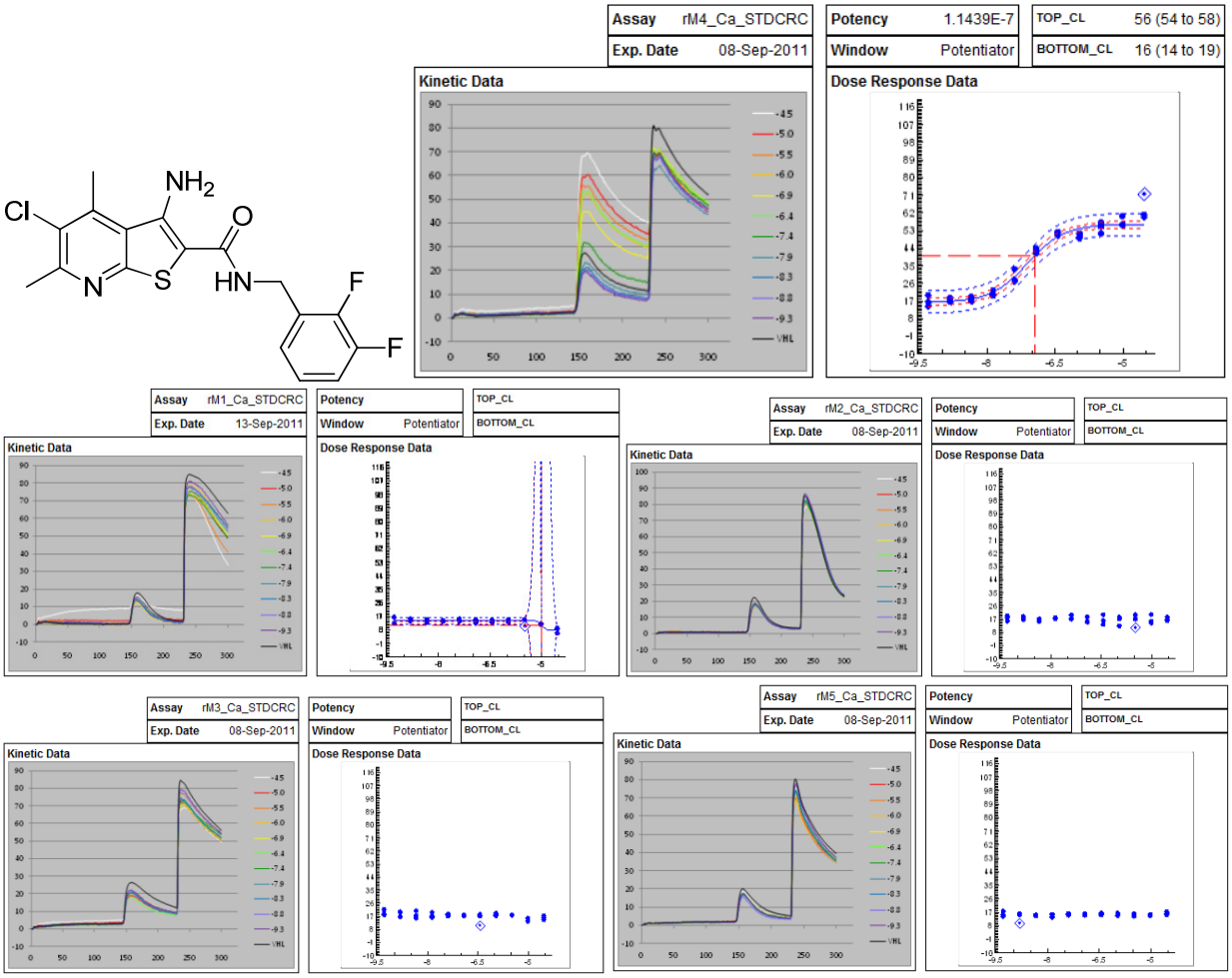

VU0452055

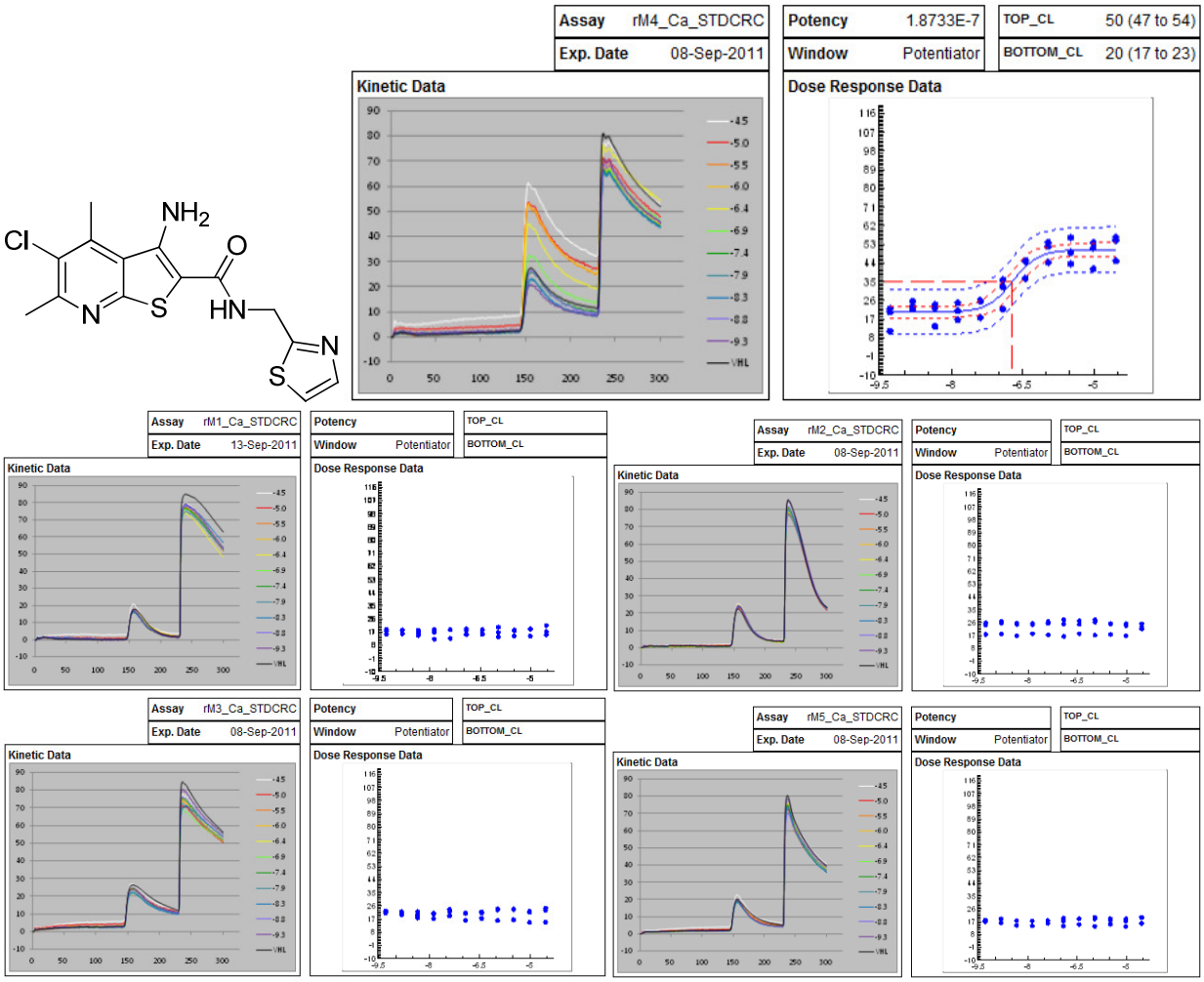
Assay rM4_Ca_STDCRC
Exp. Date 08-Sep-2011
Potency 1.8733E-7
Window Potentiator
TOP_CL 50 (47 to 54)
BOTTOM_CL 20 (17 to 23)
Kinetic Data
Dose Response Data
Cl
NH2
O
HN
N
S
N
S
Assay rM1_Ca_STDCRC
Exp. Date 13-Sep-2011
Potency
Window Potentiator
TOP_CL
BOTTOM_CL
Kinetic Data
Dose Response Data
Assay rM2_Ca_STDCRC
Exp. Date 08-Sep-2011
Potency
Window Potentiator
TOP_CL
BOTTOM_CL
Kinetic Data
Dose Response Data
Assay rM3_Ca_STDCRC
Exp. Date 08-Sep-2011
Potency
Window Potentiator
TOP_CL
BOTTOM_CL
Kinetic Data
Dose Response Data
Assay rM5_Ca_STDCRC
Exp. Date 08-Sep-2011
Potency
Window Potentiator
TOP_CL
BOTTOM_CL
Kinetic Data
Dose Response Data

VU0452129

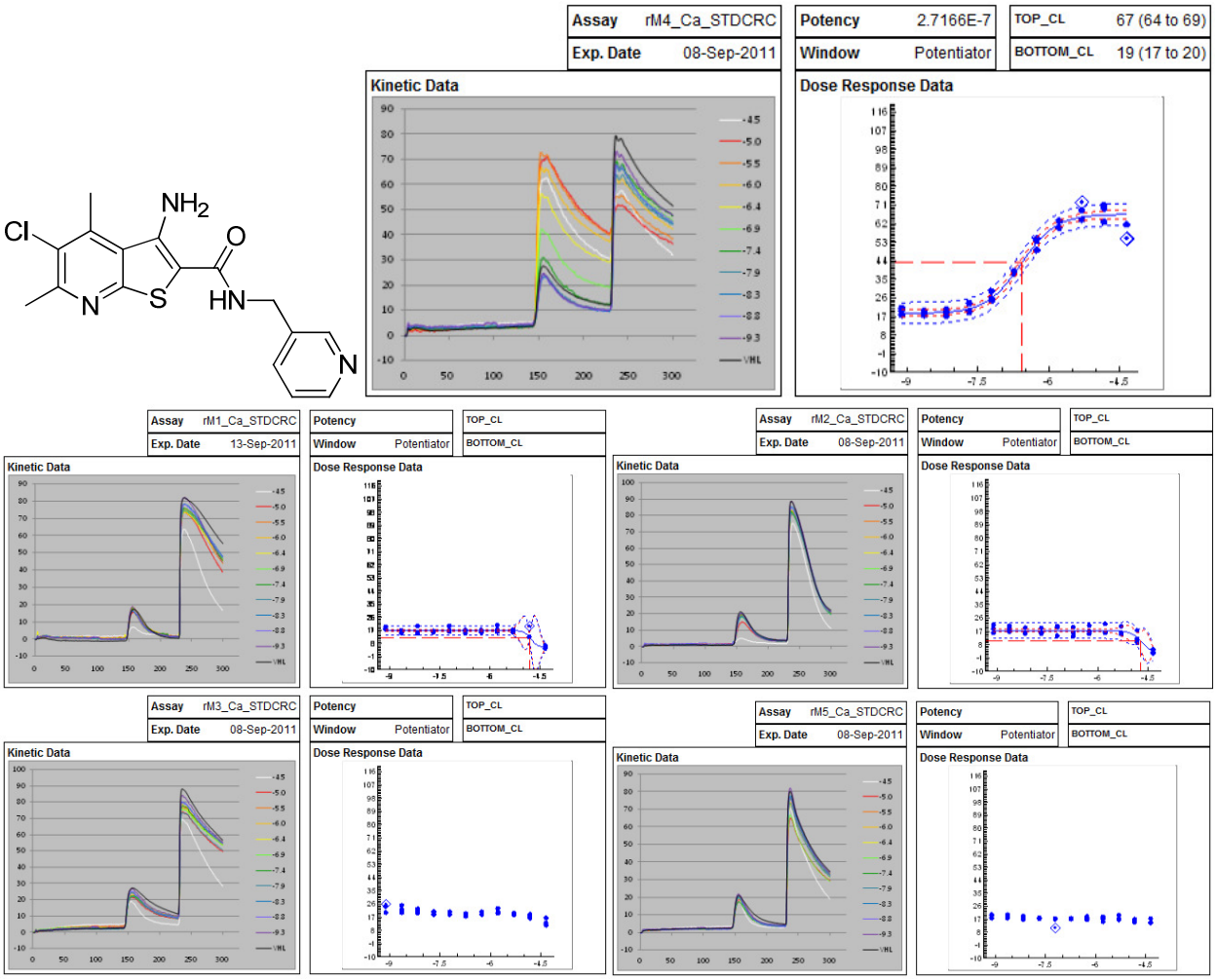
Assay rM4_Ca_STDCRC
Exp. Date 08-Sep-2011
Potency 2.7166E-7
Window Potentiator
TOP_CL 67 (64 to 69)
BOTTOM_CL 19 (17 to 20)
Kinetic Data
Dose Response Data
Cl
NH2
O
N
S
HN
N
Assay rM1_Ca_STDCRC
Exp. Date 13-Sep-2011
Potency
Window Potentiator
TOP_CL
BOTTOM_CL
Kinetic Data
Dose Response Data
Assay rM2_Ca_STDCRC
Exp. Date 08-Sep-2011
Potency
Window Potentiator
TOP_CL
BOTTOM_CL
Kinetic Data
Dose Response Data
Assay rM3_Ca_STDCRC
Exp. Date 08-Sep-2011
Potency
Window Potentiator
TOP_CL
BOTTOM_CL
Kinetic Data
Dose Response Data
Assay rM5_Ca_STDCRC
Exp. Date 08-Sep-2011
Potency
Window Potentiator
TOP_CL
BOTTOM_CL
Kinetic Data
Dose Response Data

VU0456952

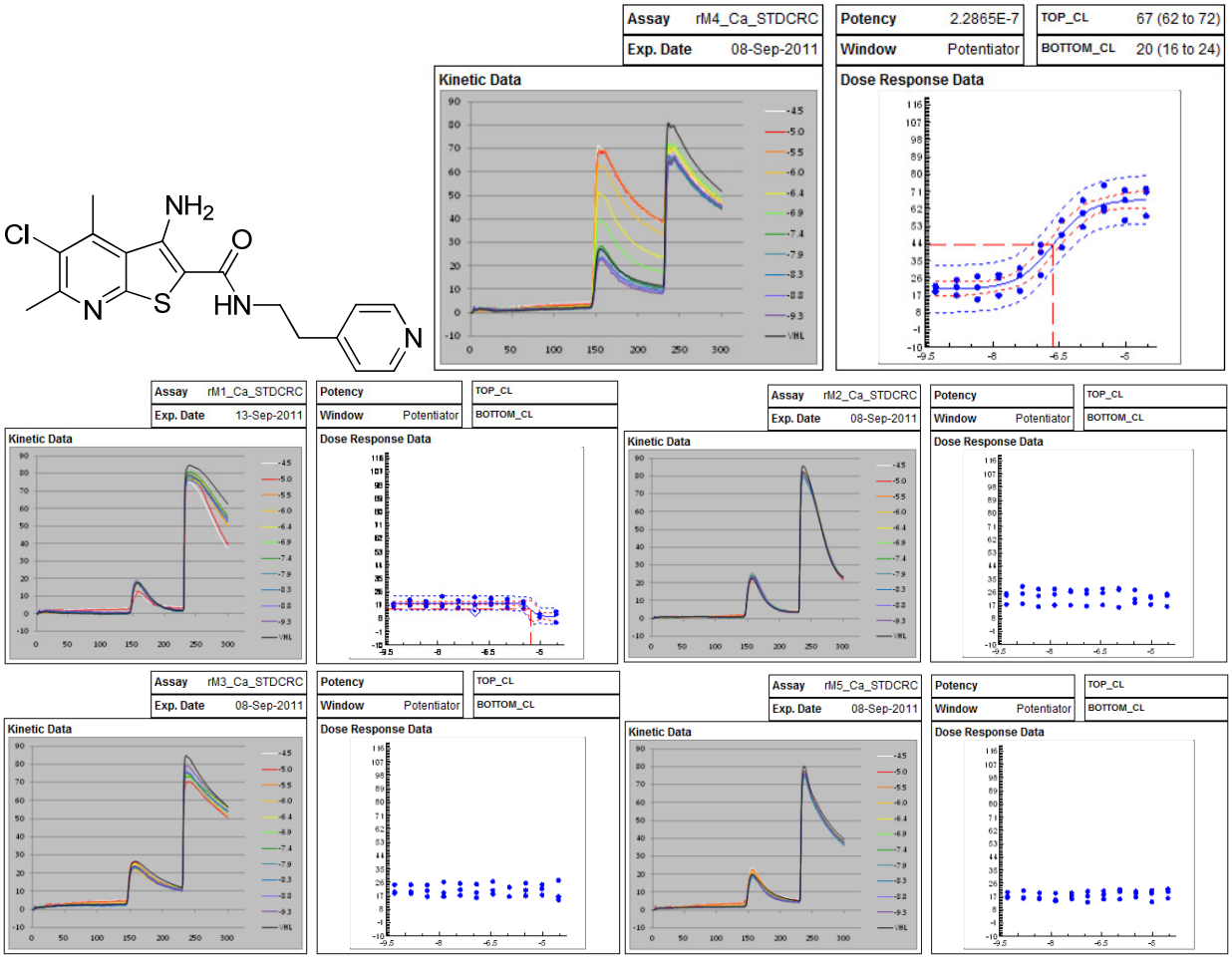
Assay rM4_Ca_STDCRC
Exp. Date 08-Sep-2011
Potency 2.2865E-7
Window Potentiator
TOP_CL 67 (62 to 72)
BOTTOM_CL 20 (16 to 24)
Kinetic Data
Dose Response Data
Cl
NH2
O
N
S
HN
N
Assay rM1_Ca_STDCRC
Exp. Date 13-Sep-2011
Potency
Window Potentiator
TOP_CL
BOTTOM_CL
Kinetic Data
Dose Response Data
Assay rM2_Ca_STDCRC
Exp. Date 08-Sep-2011
Potency
Window Potentiator
TOP_CL
BOTTOM_CL
Kinetic Data
Dose Response Data
Assay rM3_Ca_STDCRC
Exp. Date 08-Sep-2011
Potency
Window Potentiator
TOP_CL
BOTTOM_CL
Kinetic Data
Dose Response Data
Assay rM5_Ca_STDCRC
Exp. Date 08-Sep-2011
Potency
Window Potentiator
TOP_CL
BOTTOM_CL
Kinetic Data
Dose Response Data

VU0456953

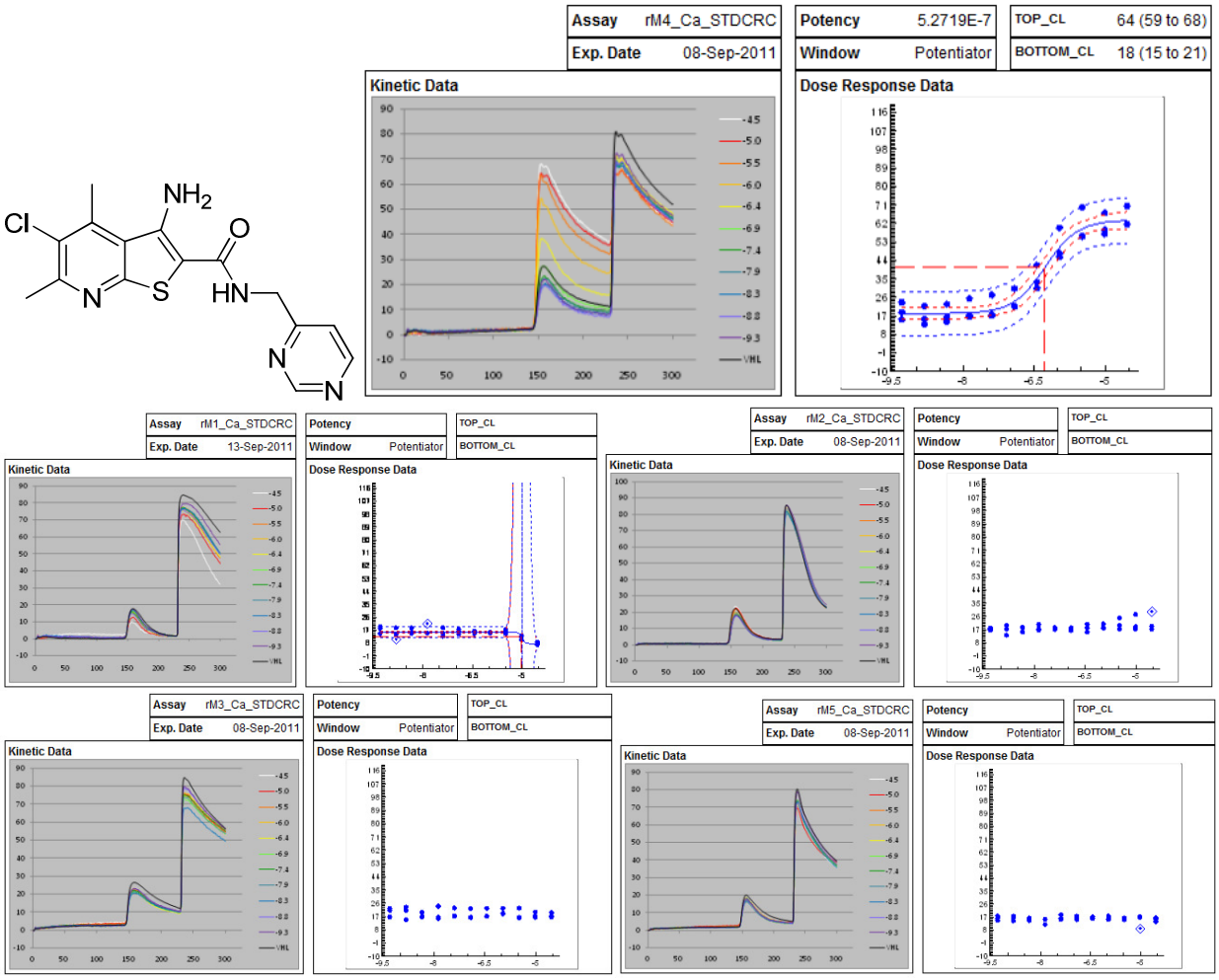
Assay rM4_Ca_STDCRC
Exp. Date 08-Sep-2011
Potency 5.2719E-7
Window Potentiator
TOP_CL 64 (59 to 68)
BOTTOM_CL 18 (15 to 21)
Kinetic Data
Dose Response Data
Cl
NH2
O
HN
N
S
N
N
Assay rM1_Ca_STDCRC
Exp. Date 13-Sep-2011
Potency
Window Potentiator
TOP_CL
BOTTOM_CL
Kinetic Data
Dose Response Data
Assay rM2_Ca_STDCRC
Exp. Date 08-Sep-2011
Potency
Window Potentiator
TOP_CL
BOTTOM_CL
Kinetic Data
Dose Response Data
Assay rM3_Ca_STDCRC
Exp. Date 08-Sep-2011
Potency
Window Potentiator
TOP_CL
BOTTOM_CL
Kinetic Data
Dose Response Data
Assay rM5_Ca_STDCRC
Exp. Date 08-Sep-2011
Potency
Window Potentiator
TOP_CL
BOTTOM_CL
Kinetic Data
Dose Response Data

REFERENCES

1. Levin, Edward D., Simon, Barbara B. Nicotinic Acetylcholine Involvement in Cognitive Function in Animals. *Psychopharmacology* 138, 217-230 (1998).

2. Hulme, E.C. Birdsall, N.J.M. & Buckley, N.J. Muscarinic Receptor Subtypes. *Annu. Rev. Pharmacol. Toxicol*. 30, 633-673 (1990).

3. Bronwen, Martin, Lopez de Maturana, Rakel, Brenne nMan, Randall, Walent, Tom, Mattson, Mark P., & Maudsley, Stuart. Class II G Protein-Coupled Receptors and Their Ligands in Neuronal Function and Protection. *Neuromolecular Med*. 7 (1-2), 3-36 (2005).

4. Conn, P.J., Christopoulos, A. & Lindsley, C.W. Allosteric modulators of GPCRs: a novel approach for the treatment of CNS disorders. *Nat Rev Drug Discov* 8, 41-54 (2009).

5. Christopoulos, Arthur & Kenakin, Terry. G Protein-Coupled Receptor Allosterism and Complexing. *Pharm Rev* 54 (2), 323-374 (2002).

6. Christopoulos, A. Allosteric binding sites on cell-surface receptors: novel targets for drug discovery. *Nat Rev Drug Discov* 1, 198-210 (2002).

7. Lanzafame, Alfred A., Sexton, Patrick M. & Christopoulos, Arthur. Interaction Studies of Multiple Binding Sites on M4 Muscarinic Acetylcholine Receptors. *Mol Pharm* 70 (2), 736 (2006).

8. Weaver, David C. Triple-Addition Assay Protocols for Detecting and Characterizing Modulators of Seven-Transmembrane Receptors. *Current Protocols in Chemical Biology* (Sep 2011).

9. Caulfield, Malcolm P. & Birdsall, Nigel J.M. International Union of Pharmacology. XVII. Classification of Muscarinic Acetylcholine Receptors. *Pharm Rev* 50 (2), 279-290 (1998).

10. Nathanson, Neil M. Molecular Properties of the Muscarinic Acetylcholine Receptor. *Ann. Rev. Neurosci* 10, 195-236 (1987).

11. Conn, P. Jeffrey, Tamminga, Carol, Schoepp, Darryle D., Lindsley, Craig. Schizophrenia Moving Beyond Monoamine Antagonists. *Molecular Interventions* 8 (2), 99-107 (2008).

12. Freedman, Robert. Schizophrenia. *New England Journal of Medicine* 349, 1738-1749 (2003).

13. Gray, John A., Roth, Bryan L. Molecular Targets for Treating Cognitive Dysfunction in Schizophrenia. *Schizophrenia Bulletin* 33 (5), 1100-1119 (2007).

14. Barak, Segev. Modeling Cholinergic Aspects of Schizophrenia: Focus on the Antimuscarinic Syndrome. *Behavioural Brain Research* 204, 335-351 (2009).
15. Heresco-Levy, U. Ermilov, M., Lchtnberg, P. Bar, G., Javitt, D.C. High-dose Glycine Added to Olanzapine and Risperidone for the Treatment of Schizophrenia. *Biol Psychiatry* 55, 165-171 (2004).

16. Moghaddam, Bita. Targeting Metabotropic Glutamate Receptors for Treatment of the Cognitive Symptoms of Schizophrenia. *Psychopharmacology* 174, 39-44 (2004).

17. Patil, Sandeep T. et al. Activation of mGlu2/3 Receptors as a New Approach to Treat Schizophrenia: A Randomized Phase 2 Clinical Trial. *Nature Medicine* 13 (9), 1102-1107 (2007).

18. Sur, Cyrille & Kinney, Gene G. Selective Targeting of Muscarinic Receptors: Novel Therapeutic Approaches for Psychotic Disorders. *Current Neuropharmacology* 3, 63-71 (2005).

19. Tamminga, Carol A. The Neurobiology of Cognition in Schizophrenia. *Journal of Clinical Psychiatry* 67, 9-13 (2006).

20. Bymaster, Frank P., McKinzie, David L., Felder, Christian C., Wess, Jurgen. Use of M1-M5 Muscarinic Receptor Knockout Mice as Novel Tools to Delineate the Physiological Roles of the Muscarinic Cholinergic System. *Neurochemical Research* 38 (3/4), 437-442 (2003).

21. Langmead, C.J., Watson, J. & Reavill, C. Muscarinic acetylcholine receptors as CNS drug targets. *Pharmacol Ther* 117, 232-43 (2008).

22. Conn, P. Jeffrey, Jones, Carrie K., Lindsley, Craig W. Subtype-Selective Allosteric Modulators of Muscarinic Receptors for the Treatment of CNS Disorders. *Trends in Pharmacological Sciences* 30 (3), 148-155.

23. Digby, Gregory J., Shirey, Jana K., Conn, P. Jeffrey. Allosteric Activators of Muscarinic Receptors as Novel Approaches for Treatment of CNS Disorders. *Molecular BioSystems* 6, 1345-1354 (2010).

24. Felder, Christian C. et al. Elucidating the Role of Muscarinic Receptors in Pyschosis. *Life Sciences* 68, 2605-2613 (2001).

25. Dean, B et al. Decreased Muscarinic 1 Receptors in the Dorsolateral Prefrontal Cortex of Subjects with Schizophrenia. *Mol Psychiatry* 7, 1083-1091 (2002).

26. Wess, Jürgen, Eglen, Richard M. & Gautam, Dinesh. Muscarinic acetylcholine receptors: mutant mice provide new insights for drug development. *Nat Rev Drug Discov* 6, 721-733 (2007).

27. Raedler, Thomas J., Knable, Michael B., et al. In Vivo Determination of Muscarinic Acetylcholine Receptor Availability in Schizophrenia. *Am J Psychiatry* 160, 118-127 (2003).

28. Bodick, N.C. et al. Effects of Xanomeline, a Selective Muscarinic Receptor Agonist, on Cognitive Function and Behavioral Symptoms in Alzheimer Disease. *Arch Neurol* 54, 465-73 (1997).

29. Sellin, A.K., Shad, M., Tamminga, C. Muscarinic Receptor Agonist Xanomeline as a Novel Treatment Approach for Schizophrenia. *Am J Psychiatry* 165 (8), 1033-1039 (2008).

30. Shekhar, Anantha, Potter, William Z. et al. Selective Muscarinic Receptor Agonist Xanomeline as a Novel Treatment Approach for Schizophrenia. *Am J Psychiatry* 165, 1033-1039 (2008).

31. Woolley, Marie L. Carter, Helen J., Gartlon, Jane E., Watson, Jeanette M. Dawson, Lee A. Attenuation of Amphetamine-Induced Activity by the Non-Selective Muscarinic Receptor Agonist, Xanomeline, is Absent in Muscarinic M4 Receptor Knockout Mice and Attenuated in Muscarinic M1 Receptor Knockout Mice. *European Journal of Pharmacology* 603, 147–149 (2009).

32. Bridges, Thomas M., LeBois, Evan P., Hopkins, Corey R., Wood, Michael R. Jones, Carrie K., Conn, P. Jeffrey & Lindsley, Craig W. The Antipsychotic Potential of Muscarinic Allosteric Modulation. *Drug News and Perspective* 23(4), 229-240 (2010).

33. Marcotte, Eric R., Pearson, Debra M., Srivastava, Lalit K. Animal Models of Schizophrenia: a critical review. *Journal of Psychiatry & Neuroscience* 26 (5), 395-410 (2001).

34. Fritts, Mary E. Mueller, Kathryne, Morris, Laurie. Amphetamine-Induced Locomotor Streotypy in Rats is Reduced by a D1 but not a D2 Antagonist. *Pharmacology Biochemistry and Behavior* 58 (4), 1015-1019 (1997).

35. Chan, W.Y. et al. Allosteric modulation of the muscarinic M4 receptor as an approach to treating schizophrenia. *Proc Natl Acad Sci U S A* 105, 10978-83 (2008).

36. Shirey, J.K. et al. An allosteric potentiator of M4 mAChR modulates hippocampal synaptic transmission. *Nat Chem Biol* 4, 42-50 (2008).

37. Brady, A.E. et al. Centrally active allosteric potentiators of the M4 muscarinic acetylcholine receptor reverse amphetamine-induced hyperlocomotor activity in rats. *J Pharmacol Exp Ther* 327, 941-53 (2008).

38. Kennedy, Phillip J., Bridges, Thomas M. et al. Synthesis and Structure Activity Relationships of Allosteric Potentiators of the M_4 Muscarinic Acetylcholine Receptor. *ChemMedChem* 4, 1600-1607 (2009).

39. Hou, Tingjun et al. ADME Evaluation in Drug Discovery. 6. Can Oral Bioavailability in Humans be Effectively Predicted by Simple Molecular Property-Based Rules? *Journal of Chem. Inf. Model* 47, 460-463 (2007).

40. Birkett, Donald J. *Pharmacokinetics Made Easy*. The McGraw-Hill Companies, Inc. New York, 2002.

41. Lu, Chuang et al. Comparison of Intrinsic Clearance in Liver Microsomes and Hepatocytes from Rats and Humans: Evaluation of Free Fraction and Uptake in Hepatocytes. Drug *Metabolism and Disposition* 34 (9), 1600-1605 (2006).

42. Guengerich, Peter F. Cytochrome P450s and Other Enzymes in Drug Metabolism and Toxicity. *The AAPS Journal* 8 (1), E101-E111 (2006).